POLYETHYLENE FUNCTIONALIZED WITH HIGHLY POLAR GROUPS

By

KATHLEEN L. OPPER

A DISSERTATION PRESENTED TO THE GRADUATE SCHOOL
OF THE UNIVERSITY OF FLORIDA IN PARTIAL FULFILLMENT
OF THE REQUIREMENTS FOR THE DEGREE OF
DOCTOR OF PHILOSOPHY

UNIVERSITY OF FLORIDA

2010

To my parents

ACKNOWLEDGMENTS

First I would like to thank my family for all of their support throughout the many years of learning. To my sister, Lynne, I thank her for her fine example. Of course I thank my parents for their watchful eye in learning from others while finding my own way.

I would also like to thank my role models, two wonderful ladies, Grandma Vaughan and Karen Ross. I owe my practical side to my Grandma from learning the true meaning of “reuse”. I thank Karen Ross for being a role model in how to be kind and thoughtful while letting me practice on her numerous lovely animals and vegetables. Growing up in the small town of New Lebanon I appreciated the endless photos and stories from almost everywhere on the planet and showing me something to strive toward.

From New Lebanon to RPI, I thank Professor James Crivello, Professor James Moore, and Professor Brian Benicewicz for making Organic Chemistry interesting with their many random facts about polymers during classes and labs. I thank Professor Julie Stenken for the encouragement in Analytical Chemistry, my first chemistry class as a new Chemistry major. For the encouragement to complete the Chemistry track, the opportunity to experience research in polymer chemistry, and the chance to visit the University of Florida I am grateful to Dr. Benicewicz.

While studying at the University of Florida I have met so many wonderful people. I thank all of my coworkers in the Butler Polymer Research Labs especially past members Dr. Ed Lehman, Dr. Garrett Oakley, Dr. Travis Baughman, Dr. Erik Berda, Dr. Stephen Ellinger, Dr. Bob Brookins, Dr. Giovanni Rojas, Dr. James Leonard, Dr. Ryan Walczak, Dr. Dan Patel, and Sam Popwell. There are so many others I had the pleasure of working with and getting to know including many international students from and

apart from UF. I thank Dr. Dilyana Markova, Katja Nilles and Robert Haschick for the pleasure of working with them. I especially would like to thank Professor Dr. Klaus Müllen and Dr. Markus Klapper for the opportunity to continue joint projects in Germany.

For founding such a unique and cooperative laboratory environment I thank Josephine Butler and the late Professor George Butler. For providing funding I thank the Army Research Office and also for the many stimulating conversations I thank Dr. Rick Beyer and Dr. Ken Caster. For helping in so many areas that I am not even aware I thank Sara Klossner and Lori Clark.

Lastly, for providing guidance throughout my graduate career I thank Professor John Reynolds and Professor Ken Wagener. Especially I thank Dr. Wagener for his constant concern about people. I will always remember the stories and lessons I have learned from him about polymers and people.

TABLE OF CONTENTS

page

LIST OF TABLES

LIST OF FIGURES

LIST OF ABBREVIATIONS

ADMET	Acyclic diene metathesis
ATMET	Acyclic triene metathesis
ATR-IR	Attenuated total reflection infrared spectroscopy
CM	Cross metathesis
DSC	Differential scanning calorimetry
EAA	poly(ethylene-*co*-acrylic acid)
EMAA	poly(ethylene-*co*-methacrylic acid)
EP	ethylene/propylene copolymer
EPDM	ethylene/propylene/diene copolymer
FT-IR	Fourier transform infrared spectroscopy
KT	Kinning Thomas
NMR	Nuclear magnetic resonance
PDI	polydispersity index
PE	polyethylene
PVPA	poly(vinyl phosphonic acid)
RCM	Ring closing metathesis
ROM	Ring opening metathesis
ROMP	Ring opening metathesis polymerization
SAXS	Small-angle X-ray scattering
SM	Self metathesis
TGA	Thermal gravimetric analysis
WAXS	Wide-angle X-ray scattering
YC	Yarusso Cooper

Abstract of Dissertation Presented to the Graduate School
of the University of Florida in Partial Fulfillment of the
Requirements for the Degree of Doctor of Philosophy

POLYETHYLENE FUNCTIONALIZED WITH HIGHLY POLAR GROUPS

By

Kathleen L. Opper

August 2010

Chair: Kenneth B. Wagener
Major: Chemistry

Polyethylene copolymers were synthesized containing highly polar and acidic functionality by a well-known metathesis mode followed by hydrogenation. Compared to the copolymers obtained by conventional polymerization techniques, the copolymers obtained and described herein have perfectly controlled primary polymer structure owing to polymerization via Acyclic Diene Metathesis (ADMET). High molecular weight polymers were attained using appropriate protecting group chemistry while precision was ensured by using Grubbs' first generation catalyst.

By applying ADMET to appropriately protected acid α,ω-diene monomers, an unsaturated copolymer is produced and then hydrogenated to yield a well defined polyethylene (PE) copolymer with functionality evenly spaced along the polymer backbone. The functional group frequency and identity are exact. Implications of the perfect polymer microstructure, supported by ^{1}H, ^{13}C, and ^{31}P nuclear magnetic resonance (NMR), and Fourier transform infrared absorbance (FT-IR), are further supported by morphological studies. With several anologous series of precision polyethylene copolymers increasing in polarity from sulfonic acid esters, to phosphonic acid ester, to phosphonic acids and finally to carboxylate ionomers, the ensuing thermal

properties by differential scanning calorimetry (DSC) and morphology by small-angle X-ray scattering (SAXS) and wide-angle X-ray scattering (WAXS) are revealed as a progression throughout. The research described herein provides a progression increasing in polarity and complexity along with fundamental outcomes allowing for further advancements in understanding more functional polymers and is significant for creating highly ordered macromolecular structures.

As an overview of metathesis Chapter 1 highlights the history of ADMET in relation to past, present, and future progress. Chapter 2 describes the synthesis of sulfonic acid esters with precise frequency and varied attachment with an aromatic spacer. Primary structure characterization confirms the precision polymer structures while additional secondary microstructure analysis by DSC shows different behavior depending upon frequency and identity. Phosphonic acid precision copolymers with varying frequency and identity, useful in studying the interplay of crystallization and hydrogen bonding, are described in Chapters 3 and 4. Chapter 5 describes the analogous synthesis of random phosphonic acid copolymers obtained by ADMET along with detailed thermal analysis, complimented by SAXS and WAXS comparisons to the simpler precise and random poly(ethylene-*co*-acryclic acid) (EAA) copolymers. Lastly Chapter 6 rounds out the polarity profile presented here through acid ionization with varying metal size. As a collective story, the research described herein provides a progression increasing in polarity and complexity along with fundamental outcomes allowing for further advancements in understanding more functional polymers.

CHAPTER 1
INTRODUCTION

Introduction to Olefin Metathesis

Olefin metathesis is a powerful synthetic technique in forming carbon-carbon bonds.[1,2] The developments in mechanism and useful catalysts collectively earned Robert H. Grubbs, Richard R. Schrock, and Yves Chauvin the 2005 Nobel prize in Chemistry.[3] Metathesis describes the interchange of atoms within molecules, and more specifically olefin metathesis describes the apparent double bond substituent interchange with the key mechanistic step of the apparent interchange proceeding through a metallocyclobutane (Figure 1-1).[1,4]

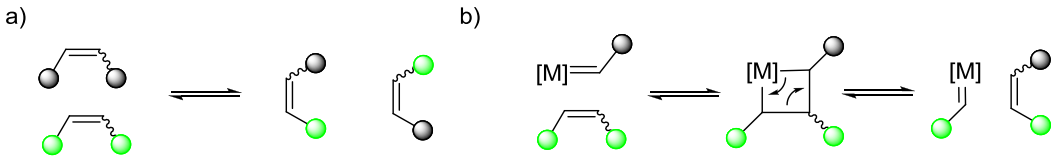

Figure 1-1. Overview of a) apparent interchange of olefin substituents b) metallocyclobutane formation and reversion

Using this mild reaction in forming carbon-carbon double bonds, more complex modes (Figure 1-2) have developed beyond the simplest olefin metathesis mode involving the cross-metathesis highlighted above.[2] Cross metathesis (CM) involves two different olefins and hetero-interchange while self metathesis (SM) involves two of the same olefins and homo-interchange as a result.[5] Furthermore, rings may be opened using ring opening metathesis (ROM)[6] with a selected opening species or closed using ring closing metathesis (RCM)[7,8] releasing ethylene. A combination of metathesis modes coupled with understanding reactivity has even allowed for metathesis polymerization modes including ring opening metathesis polymerization (ROMP)[6,9] and

Acyclic Diene Metathesis polymerization (ADMET).[10-12] ROMP relies on releasing ring strain by ring opening via a cyclic alkene monomer in an addition chain polymerization.

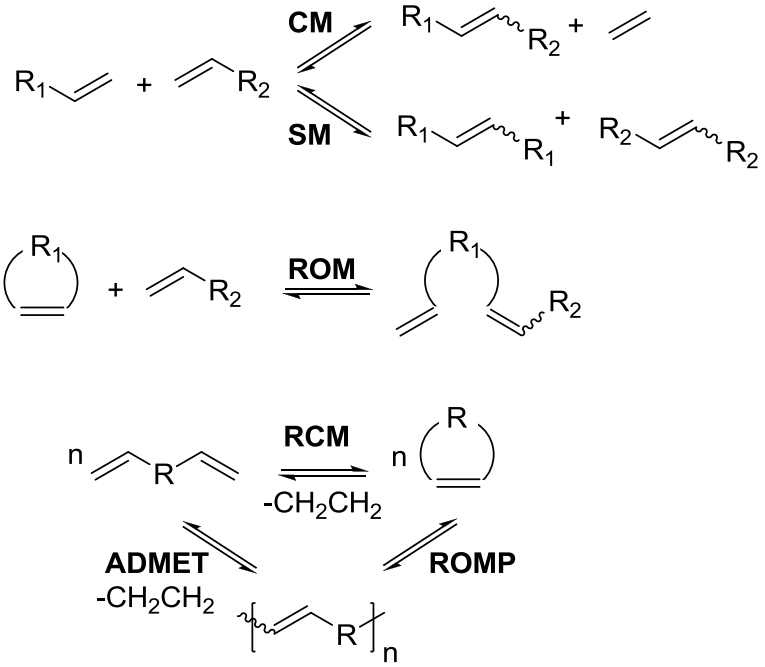

Figure 1-2. Modes of metathesis

Contrary, ADMET polymerization relies on CM with ethylene removal driving the reaction in a step-growth condensation polymerization (Figure 1-3). ADMET has more recent historical roots as this polymerization was not discovered until 1987,[10] which coincided with choosing an appropriate catalyst mixture from the vast library of available metathesis catalysts to drive the previously hypothetical reaction.

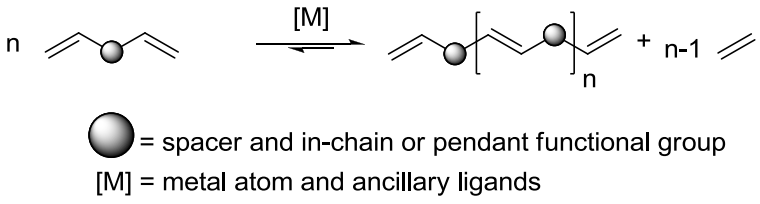

Figure 1-3. ADMET reaction

Controlling certain features of this reaction results in high molecular weight linear polymer structures with the most ADMET reaction features affecting polymerization summarized in Figure 1-3 and developed herein with an emphasis on functionalization. Olefin metathesis remains the commonality between the specific reaction modes with a history beginning in the 1950s.

Olefin Metathesis Evolution

Olefin Metathesis Discovery

Indeed catalyst and initiator developments bridging organometallic chemistry with polymer chemistry have been investigated since before the metathesis reaction with traditional multi-site initiator pursuits for stereoselective polymerization in the early 1950s by Karl Ziegler[13] in Germany and Giulio Natta[14] in Italy for which they earned the 1963 Nobel Prize in Chemistry.[15] Industrial pursuits in metathesis chemistry can be traced to reports in the 1950s and 1960s during a time when synthetic polyolefin advances centered around catalyst mixtures of high oxidation metal salts and an activating agent. Such is the case with the first patent arising in 1957 by DuPont chemist Herbert Eleuterio and the discovery of various gaseous α-olefins resulting from supported oxide catalyst MoO_3/AlO_3 propene polymerization.[16] Although a few reports also surfaced independently on exchange reactions along with ring opening polymerization using Zieglar-Natta type catalyst $MoCl_5/Et_3Al$, little mechanistic insight was offered.[17,18]

The connection that these reactions were in fact the same reaction (metathesis) became apparent in 1967 when Goodyear chemist Nissim Caulderon noted rapid polymerization of cyclic alkene monomers and disproportionation of 2-pentene using $WCl_6/EtAlCl_2/EtOH$.[19-22] Hence the term “olefin metathesis” was coined by Caulderon as

he released further articles explaining a mechanism involving a three step process with the first involving bisolefin-metal coordination.

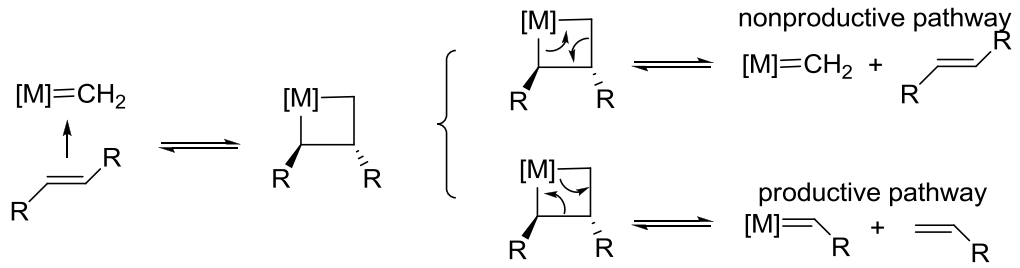

Figure 1-4. Metal carbene metallocyclobutane formation

The accepted mechanism first proposed by Yves Chauvin in 1971 begins through metallocyclobutane formation (Figure 1-4).[23,24] The mechanism debate continued and though the mechanism was not confirmed until 1975 by Thomas Katz,[25] Chauvin's proposal took time before it gained acceptance among the numerous incorrect proposals of the 1970s. Katz compared several of the other proposed mechanisms and compared the statistical distribution of different products based on starting olefin structural and electronic variations expected in the intermediate stability within the metal-carbene mechanism.[26,27]

Although not all considerations could be explained, Katz envisioned applications forthcoming along with initiator and catalyst developments. Just after Katz's mechanistic report, Robert Grubbs released support for the metal-carbene mechanism including vigorous isotopic labeling and isolation of the various metathesis pathway products.[28] Katz proceeded in developing low oxidation state electrophilic Fischer carbenes promoting ROMP but unsuccessful in promoting olefin metathesis.

Metathesis Catalyst and Initiator Evolution

However it was the developments of the 1970s by Richard Schrock, then a researcher at DuPont, toward homogenous metathesis catalysts that eventually led to the isolation of a high oxidation state nucleophilic carbenes, termed “Schrock carbenes”, including tantalum carbene complexes.[29] Schrock carbene ligands are viewed as X2 ligands with +2 charge in contrast to the neutral Fischer carbene L ligands. With tantalum catalyst activity too low, further catalyst developments utilizing tungsten[30,31] and molybdenum[32,33] followed (Figure 1-5).

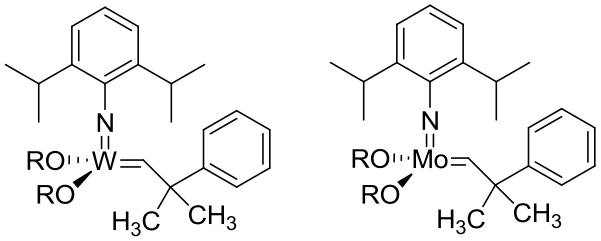

W1 **Mo1**

Figure 1-5. Schrocks’ tungsten (**W1**) and molybdenum (**Mo1**) ADMET active catalysts

The multitude of highly active early-transition metal catalysts allowed for diverse applications that were however limited by the electrophillic and oxophillic metal centers sensitive to air, moisture and functional groups. Late-transition metals remained desirable as they are less electrophilic and moving toward that direction, Schrock and coworkers eventually also created olefin metathesis active rhenium complexes.[34] From Schrock’s work, numerous achievements in small molecules and polymers were possible.

Simultaneous discoveries by Grubbs throughout the 1980s led to spectroscopically characterizable titanacyclobutanes from titanium/Lewis acid mixtures,[35-37] which brought

the understanding of olefin metathesis to a more complete level. Grubbs also found success on moving from the titanium/Lewis Acid mixtures to well-defined homogenous catalysts with rhenium and the more successful ruthenium centers such with Grubbs' first generation catalyst (**Ru1**) and second generation catalyst (**Ru2**) (Figure 1-6).[38-40]

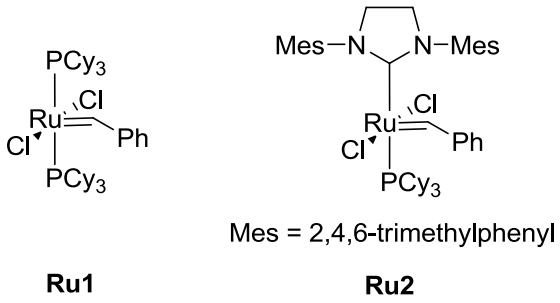

Figure 1-6. Grubbs' ruthenium catalysts, first (**Ru1**) and second (**Ru2**) generation

While ruthenium has proven to be the most successful late-transition metal in reducing air, moisture and coordinating functionality sensitivity, the first generation catalysts were less active than early-transition metal catalysts. In particular structures such as those shown in Figure 1-6 were interesting in that they exhibited features of Fischer and Schrock carbenes, but not exclusively classified as either. This allowed for a continuum between early- and late-transition metals, dependent on metal and ligand selection in altering electronics and/or sterics for particular metathesis modes.

Certainly all of these catalyst developments have established a huge library from which a number of challenging synthetic challenges in pharmaceuticals, petrochemicals, and polymers have been solved in the industrial setting where metathesis investigations began more than 50 years ago. These catalyst developments have also allowed for a multitude of developments in the more specialized ADMET polymerization reaction since the early 90s. The focus on polymerization requirements resulting from the

ADMET mechanism and a survey of the most recent developments of the evolution of ADMET since 2005 will be presented.

ADMET Features

ADMET Mechanism

Although the commonalities of the metathesis modes include an exchange of double bond substituents, ADMET polymerization is a step, condensation polymerization and thus has numerous features differentiating the polymerization from the more commonly employed ROMP chain technique.[41] The polymerization cycle proceeds through the same basic metal carbene mechanism as in CM with features optimized to enhance polymerization through productive metathesis (Figure 1-7).[42-45]

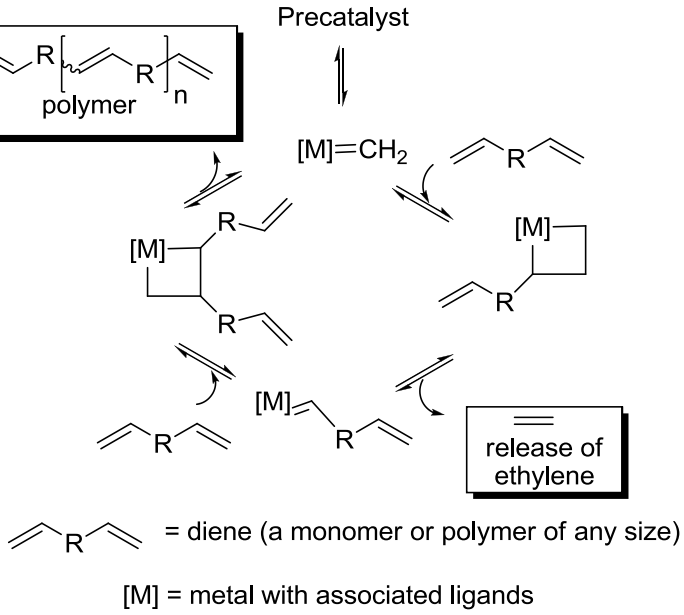

Figure 1-7. Productive ADMET polymerization cycle

The precatalyst involves a metal species with associated ligands [M], which reacts reversibly to form a metal methylidene carbene. The open coordination site allows for olefin coordination, and 2 + 2 cycloaddition forming a metallocyclobutane, which

decomposes by a 2 + 2 cycloreversion, releasing ethylene condensate and resulting in an α-substituted metal alkylidene with an open coordination site.

The metal alkylidene species may be monomer or polymer and coordination of another monomer or polymer molecule productively results in a α,β-substituted metallocyclobutane. The cycloreversion results in the release of two linearly coupled molecules and regenerates the metal methylidene carbene.

Additionally regiochemical considerations of metallocyclobutane formation are more complicated in achieving productive metathesis with this step-growth process. The regiochemical cycloreversion results in a non-productive pathway if the starting materials are simply regenerated and productive pathway if the alternate regiochemical cycloreversion results in a new olefin and new metal-carbene as was previously shown in Figure 1-4. The regiochemical requirements for productive metathesis are two-fold including metallocyclobutane sterics and metallocyclobutane reversion breaking the original bonds generating the interchange of double bond substituents. Metallocyclobutane formation can proceed forming either α,α′ substitution or α,β substitution (Figure 1-8).

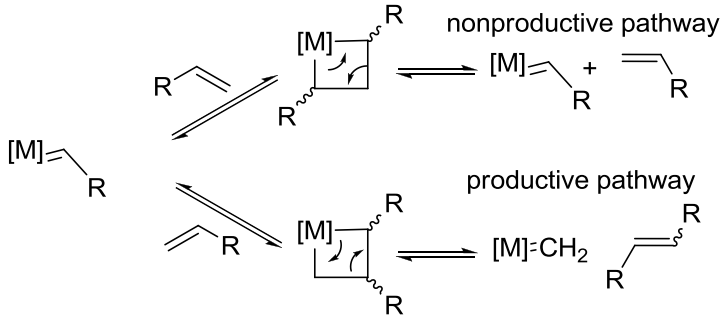

Figure 1-8. Regiochemical productive and nonproductive routes

Sterics favor α,α′ substitution but lead to non-productive metathesis and more specifically degenerate metathesis. To favor α,β substitution, the least sterically demanding monomers are generally employed — α,ω-dienes.

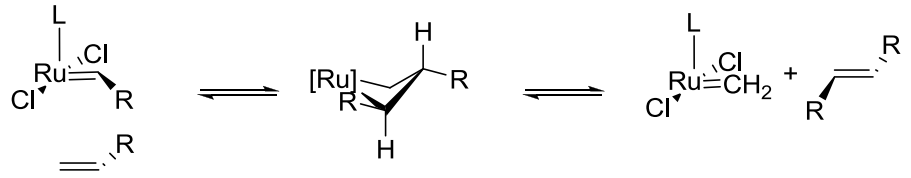

Figure 1-9. Stereochemical trans outcome rationale

The cis:trans stereochemical outcome of productive ADMET with Grubbs catalysts has implications on the overall polymer properties yet is rooted in the mechanism. With cis:trans ratios of 3:7 and 1:4 with more time, the preference of trans can be rationalized with the lesser sterically favored approach and resulting α,β-metallocyclobutane conformation (Figure 1-9).[46] The trans microstructure is a consequence of the kinetic product formed by olefin approach and resulting metallocyclobutane conformation with equatorial substituents as well as the thermodynamic equilibration to the thermodynamically preferred trans olefins.

Condensation Polymerization

As ADMET is classified as a condensation polymerization and as with most condensation polymerizations, this equilibrium process requires desired functional groups reacting in a step-wise fashion allowing for molecular weight increase proceeding step-wise from monomer, dimer, trimer and so on to high polymer.[41] This step-wise event occurs as the linearly coupled molecules are released during the metathesis catalytic cycle. To drive the equilibrium ethylene is removed from the reaction.

Mathematically the number average molecular weight, X_n (or degree of polymerization) compared to extent of reaction, p (or monomer conversion) is related by Carothers' equation (Figure 1-10).

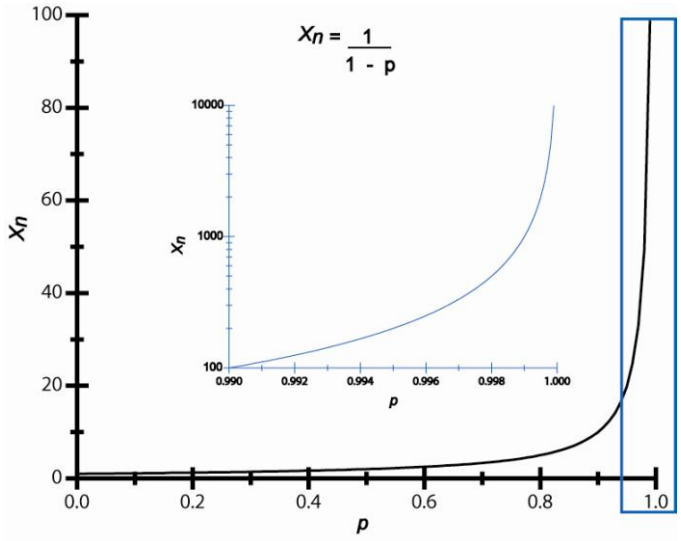

Figure 1-10. A plot of Carothers' equation with the inset highlighting high conversions needed for high molecular weight

Most visibly according to a plot comparing extent of conversion versus number average molecular weight, high conversion is needed to achieve a high molecular weight (greater than p of 0.99 or 99%). Also at high conversion, each coupling between polymer chains, reduces the number of polymer molecules in the sample significantly. This stark contrast to the situation at low conversions, which results in only a small reduction of polymer molecules, results in a low polymerization rate until high conversions are realized. Implications on catalysis include necessitating a highly active catalyst that remains active throughout the polymerization cycle.

High conversions are achieved by removing the condensate, driving the equilibrium. Using the least sterically demanding monomers, α,ω-dienes, the ethylene condensate is removed thus preventing the reverse reaction regenerating monomer.

Despite the high conversion required for high molecular weight as with typical condensation polymers, several commercially important condensation polymers are utilized successfully including polyesters and polyamides.

Molecular weight distributions in ADMET polymers are also typical of other condensation polymers. The polydispersity index (PDI) is defined as the weight average molecular weight, X_w divided by the number average molecular weight, X_n and describes the molecular weight distribution. Statistically, condensation polymers typically have PDIs approaching 2.0 as conversion (p) reaches 1 or 100%.

Considerations

Equilibrium along with regiochemical considerations allow for productive and non-productive pathways upon coordination of a disubstituted olefin in forming high polymer described previously. Other typical well-known equilibrium that occur in polycondensation chemistry have effects on ADMET polymers including cyclization and interchange.[41]

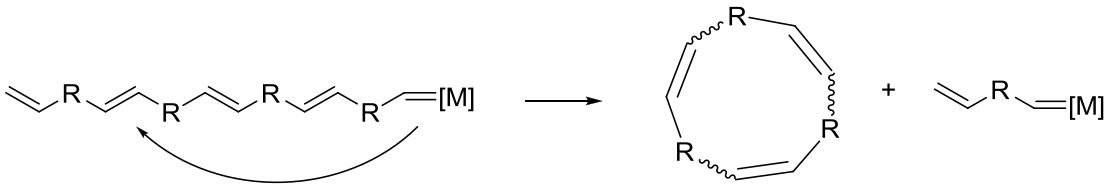

Figure 1-11. Cyclization of a linear metal alkylidene chain end by backbiting

Cyclization is favored under high dilution and occurs in metathesis chemistry by backbiting of an oligomeric or polymeric metal carbene with a double bond on the backbone of that polymer (Figure 1-11). Indeed, cyclics have been observed in ADMET polymerization.[47] With mechanism an underlying similarity in cyclic formation of ADMET polymerization and ROMP, the backbiting has actually been optimized via a **Ru2** modification to form wholly cyclic polymers.[48] Similarly RCM has seen utility in yielding

rings of more than 20 atoms.[49] To avoid cyclizations, bulk or high concentrations favoring intermolecular reactions are typical along with monomers incapable of forming favored ring sizes.

Once high molecular weight polymer is achieved interchange reactions can occur when the chain end or backbone is still active toward condensation chemistry as with polyesters, polyamides and polysulfides. This is true of internal double bonds in ADMET polymers and as with interchange reactions on condensation polymers, another pathway resulting in degenerate reactions without altering the average molecular weight. In ADMET polymer interchange can occur in a few circumstances (Figure 1-12).

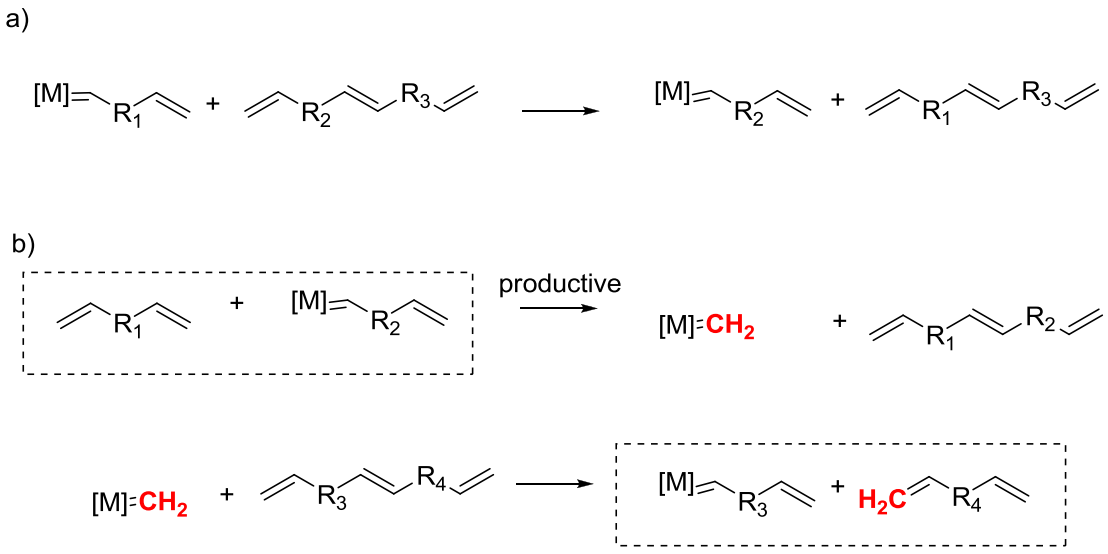

Figure 1-12. Interchange reactions of ADMET polymers

Between a metal alkylidene and polymer molecule, a different metal alkylidene is generated along with a different polymer molecule and is representative of a simple degenerate reaction. Similarly the sequence involving metal methylidene is also degenerate following reaction of a metal alkylidene with an olefin endgroup forming a metal methylidene generated as product of productive metathesis, which further reacts

with a polymer backbone, regenerating metal alkylidene and an olefin endgroup. There is no change in average molecular weight but interchange does however allow depolymerization with ethylene or random incorporation with other olefins.[50,51] For this reason, monomer purity is critical. Introduction of a monofunctional olefin will reduce the number average molecular weight with varying effects based on conversion.

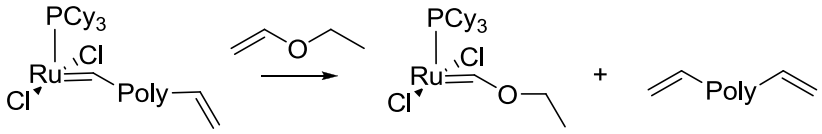

Figure 1-13. ADMET polymerization quenching

Limiting molecular weight or end-capping the polymer chains may prove beneficial to processing. In fact ADMET polymerizations are commonly quenched by addition of monofunctional ethyl vinyl ether dissolved in toluene, replacing a metal alkylidene active chain-end with a well defined termal olefin CH_2 group (Figure 1-13) while also forming a stable Fischer carbene, which is fairly metathesis inactive.[52,53] This technique has been developed in preparing various copolymers and telechelic functional polymers as will be discussed with the evolution of ADMET.

ADMET Evolution

From the discovery of ADMET using the $WCl_6/EtAlCl_2$ catalyst system in the simplest and model cases, to the most recent advances using well-defined catalysts, many advances and application areas have seen success. Along with significant progress in catalysis in the past several years, significant utility has also been pursued. The most recent active areas from the past 5 years will be described including functional polyolefins, advanced applications as well as functional polyolefins for advanced applications.

Functional Polyolefins

ADMET remains a choice polymerization technique, generating a continuum of functional polymers, which may be hydrogenated to yield analogous polyethylene (PE) copolymers, except linear with exact functional group placement (Figure 1-14). PE is commercially sought after for its cost effectiveness, production ease, and range of properties.[54,55] For these reasons, PE is produced in the greatest amounts by weight and simple manipulations of structure to improve the properties have been under investigation for the past several decades. Polymers unattainable by other techniques and exact models of commercially produced PEs by less controlled techniques have continued to be developed using ADMET polymerization.

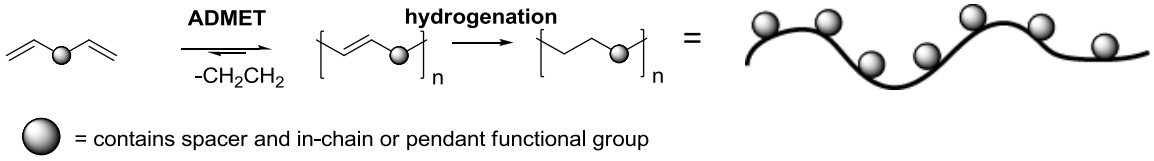

Figure 1-14. ADMET polymerization/hydrogenation route to linear precise polymers

Following pivotal work of early 2000,[11,12,56] several alkyl branched polyethylenes have been synthesized and studied since 2005 showing further dramatic effects on thermal behavior and crystallinity.[56-62] By choosing an appropriate monomer both the branch identity and frequency can systematically be changed.

With exact incorporation dependent on functional group, materials deviating from orthorhombic PE are obtained beginning with the simplest methyl group modeling ethylene-propylene copolymers.[63] PE bearing a methyl group on every 15th and 21st carbon showed a lamellar morphology with the thickness greater than the distance between methyl groups indicating an inclusion of the defect into the crystalline lattice. With more frequent introduction of methyl defects, these ethylene-propylene copolymer

mimics are rendered amorphous although low temperature annealing reveals melting endotherms as well.[64]

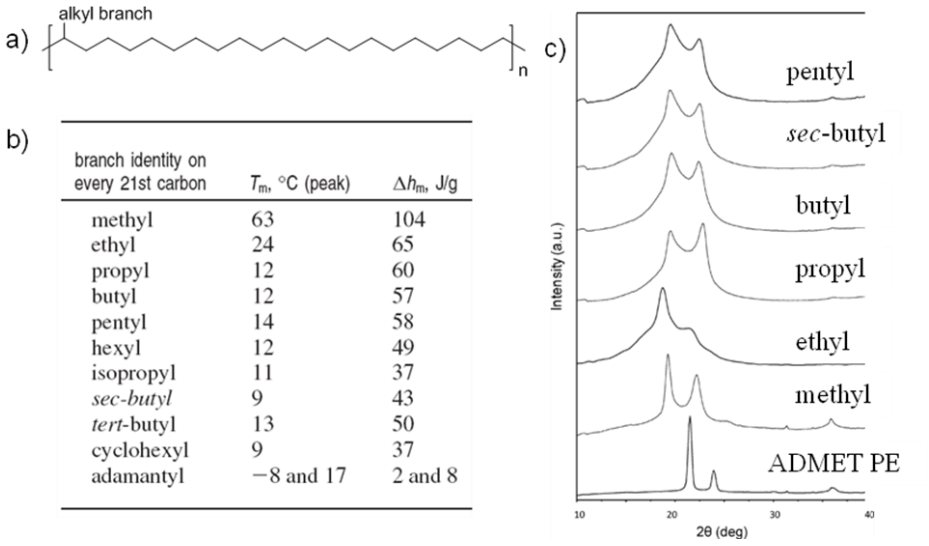

branch identity on every 21st carbon	T_m, °C (peak)	Δh_m, J/g
methyl	63	104
ethyl	24	65
propyl	12	60
butyl	12	57
pentyl	14	58
hexyl	12	49
isopropyl	11	37
sec-butyl	9	43
tert-butyl	13	50
cyclohexyl	9	37
adamantyl	−8 and 17	2 and 8

Figure 1-15. Summary of a) structure b) melting and c) crystallinity of an alkyl branched precision PE series adapted from Reference 65

In a later study comparing methyl, geminal-methyl, and ethyl groups on every 21st carbon, alternate crystal structures were proposed in accommodating the feature into the crystal structure.[57,58] To further elucidate changes in morphology including crystal structure and defect fate (included or excluded from the crystal), a series of polymers was synthesized and exhaustively characterized (Figure 1-15).[65] Inclusion of the methyl and ethyl branch was proposed and certainly the progressive convergent decrease of melting temperatures and similar degree of crystallinity of larger alkyl groups supports this finding. There is a change in crystal structure when the size is increased beyond ethyl.

Indeed these results were confirmed in a TEM study comparing the lamella thickness and thickness distribution between a precise PE containing either an ethyl or a hexyl group on every 21st carbon.[60] The 55Å thickness of the ethyl functional PE

polymer corresponds to twice the length between ethyl branches with three branches, one of which is included in the lamella. The 25-26Å thickness found for the hexyl functional PE suggests the lamella stem is composed of only one ethylene length between hexyl branches, and the hexyl branch excluded.

Significant progress has been accomplished in understanding these strictly alkyl functional and similar effort has been undertaken in more functional PE polymers. As polar group incorporation into a hydrophobic backbone has shown to improve particular properties such as impact resistance and polymer adhesion, but also as chemical barriers, the catalyst developments underlying the ADMET polymerization chemistry here give rise to nearly limitless options with regard to drawing functional groups from the period table ranging from metals[66-69] to halogens[70-72] and various ether,[73-77] ester,[78-83] acid,[84-86] and ionic[87-89] functionality.

Advanced Applications

Drawing from the progress in highly functional polymers, using fundamental ADMET polymerization chemistry combined with various other emerging polymer developments, materials have been obtained in multiple areas including architectures of telechelic,[90-93] block,[79-82] crosslinked,[94-96] and hyperbranched copolymers.[97-100] Biological applications have also been pursued and in addition numerous contributions in liquid crystalline and conjugated materials have emerged with ADMET serving as the choice polymerization technique.

Utilizing ADMET homopolymerizaiton and copolymerization, various architectures have been sought. Beyond copolymerization in synthesizing statistically random ADMET polymers, telechelic structures have been isolated by several methods including polymerizing a diolefin with a monofunctional olefin, depolymerizing an

ADMET polymer or optimizing synthetic steps (Figure 1-16).[90] In addition to varying molecular weight control, the resulting telechelic polymers were amorphous and precisely end-functional with 2 hydroxyl groups allowing for potential application as thermoplastic elastomers or hydrolysis and UV resistant polyurethanes. Progress in this area has also been realized in polyesters[79] and oligo(oxyethylene) carbosilanes.[96]

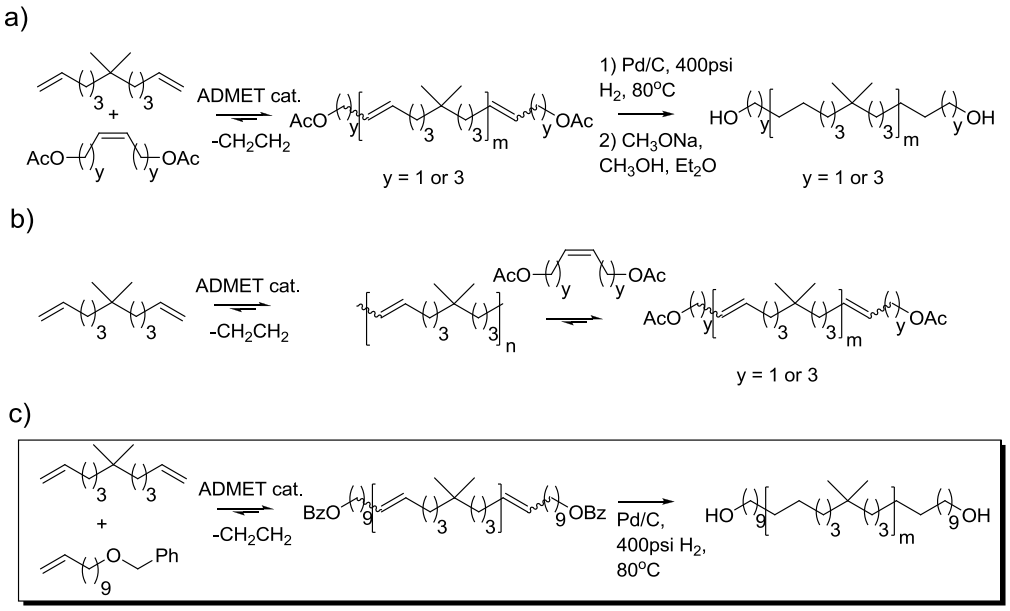

Figure 1-16. A comparison of pathways to telechelic hydrocarbon diols adapted from Reference 90

Replacing unreactive hydrocarbon with reactive silane functionality has allowed for crosslinking via chemical crosslinking and photocuring both forming thermosets.[94] Crosslinking can of course be accomplished by increasing the monomer functionality from 2 to 3 by synthesizing trienes and polymerizing by using ADMET conditions[97,98,100] or otherwise termed acyclic triene metathesis (ATMET)[99] where combining trifunctional monomers with single olefins allowed for end group and molecular weight control. Further hyperbranched pursuits have allowed for highly functional materials[97,98] while

controlled self-assembly and crosslinking stabilization of nano-objects has also been successful.[101]

With the same fundamental ADMET polymerization chemistry and considerations underlying the successes highlighted, biological advances have been developed. From the most recent years, advances have centered around obtaining suitable diene monomers from renewable resources including fatty acids,[79-82] carbohydrates,[102] amino acid dimers,[103] and even bile acid[104] while probing polymer interactions more typical to biological systems.[101,105,106] Moving toward using the well-defined ADMET polymers in delivery applications[107,108] has also seen vast progress (Figure 1-17).

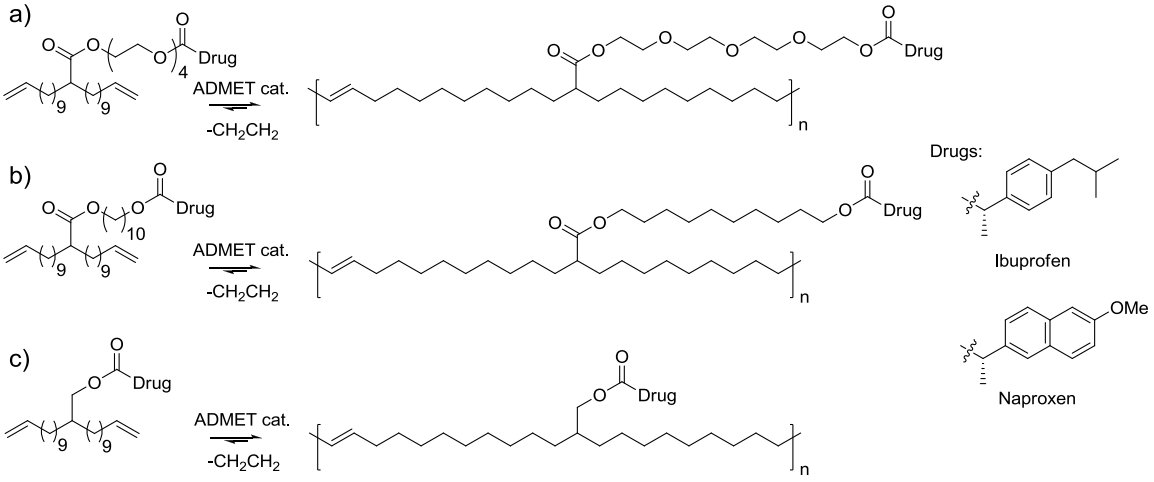

Figure 1-17. A comparison of polymer structures with variable polymer drug linkers adapted from Reference 107

Multiple areas beyond those mentioned thus far include ADMET derived liquid crystalline and conjugated systems.[109] Most recently main-chain ADMET liquid crystalline structures have been of interest in designing materials for electromechanical actuators,[110] and non linear optic in display technologies.[111-113] Further research in display technologies has been accomplished in conjugated systems. Although in the minority of conjugated materials synthetic approaches, ADMET has proven a useful

one.[114-116] An abundance of specific experimental techniques have been optimized to produce the particular desired materials. While bulk solution techniques were mentioned as the most desirable to preclude cyclization, the best techniques are those that achieve appropriate molecular weights and well-defined polymers. Often bulk techniques are not possible beyond the solid-state and instead solution techniques are employed with conjugated monomers offering the advantage of a rigid backbone incapable of cyclization.[117-120] However solid-state ADMET polymerization has been successful in poly(phenylene vinylene) (PPV) synthesis.[121] As PPV is one of the most widely studied conjugated polymers,[122,123] the synthesis has of PPV nanoparicles in aqueous emulsion has also been reported.[124] Meanwhile typical tandem ADMET-hydrogenolysis has been utilized in preparing polyfluorenes without a conjugated backbone.[125] The more traditional bulk ADMET technique has seen utility in this area yet accompanied with formation of cyclic observed from ADMET of a flexible monomer while exploring σ-π conjugation through silyl bonds in divinyl silanes.[126]

Functional Polyolefins for Advanced Applications

With complete primary polymer structure control comes several opportunities for tailoring polymers as models for more traditional polyethyelene and α-olefin copolymers and as novel structures that would be otherwise unattainable. Revisiting several commodity polymers with models has had a profound impact on studying structure-property relationships as was already mentioned. Using such polymers to investigate the hydrogen bonding of highly polar functionalized materials and the clustering phenomenon in ionomer materials has been investigated.[89]

An ionomer is defined as a polymer containing between 10-15% ionic groups and the bulk properties result from ionic interactions in discrete regions — the ionic

aggregates.[127,128] The free acid, metal-carboxylate, and polymer backbone form a physically associated material. Differences from polyelectrolytes, which contain a majority of ionic groups become apparent in the bulk ionomer morphology with the associations of ionic groups and polymer continuing to be studied. The ionic groups are pendant in contrast to ionenes where the often quaternary nitrogen is located in the chain.[129] Early types of ionic containing polymers were reported as early as 1930 with a carboxylated butadiene and acryclic acid copolymer disclosed in a 1933 French patent.[130] In an effort to find suitable crosslinking technology, work in the 1960s by DuPont chemist Richard W. Rees, simultaneous with coworker John B. Armitage,[131] led to not only the discovery of Surlyn ionomer resins in 1961, but also coined the term *ionomer*.[132,133]

With a history spanning close to 80 years and the past 40 more recognizable to the current direction, the field of ionomers has seen many advances and disputes. The vast number of ionomer materials offers an equal number of models to describe morphology disputed from the beginning.[127,128,134] Common ionomer morphology features include ionic aggregates, amorphous, and crystalline polymer. The exact aggregate structure has been proposed in the numerous models and used to explain particular experimental features.

The models have evolved from specific studies on ionomers varying in structure. With the variability in structure having effects on solubility, thermal, and viscoelastic behavior, one encompassing model becomes challenging although there have been several attempts. Detailed studies on ethylene ionomers in the late 1960s by Arthur V. Tobolsky of Princeton and William J. MacKnight of the University of Massachusettes led

to a series of articles and the first illustration of ionomer morphology by Tobolsky in 1967,[135-137] further explored by Union Carbide scientists Bonotto and Bonner in 1968.[138] Meanwhile also in 1968, DuPont scientists Longworth and Vaughan were the first to examine ion aggregation experimentally using small-angle X-ray scattering (SAXS),[139] a technique still used today. While the original interpretation of the data is no longer accepted, the SAXS ionic peak is shown in Figure 18, comparing a branched PE to a branched polyethylene methacrylic acid (PEMAA) copolymer to a neutralized PEMAA ionomer.

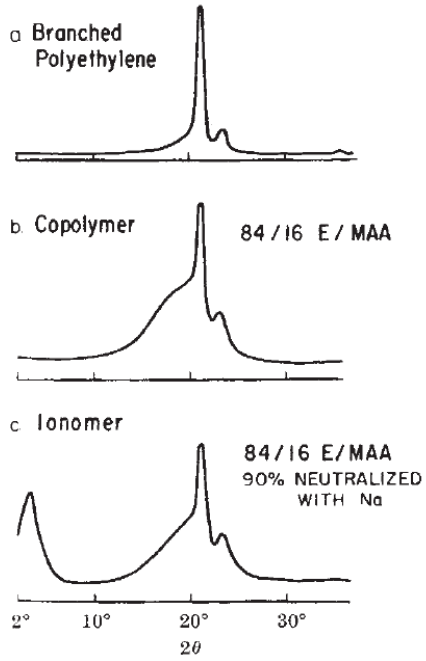

Figure 1-18. Ionic aggregation by SAXS adapted from reference 139

By 1970, Adi Eisenberg of McGill University proposed a multiplet-cluster model with the first theoretical paper.[140] Features of this model have pervaded subsequent models with efforts continuing toward a complete explanation elucidating the organization of aggregates, distribution of ions, and explanation of mechanical properties. Out of the debates, certain models became more prevalent than others.

Early attempts at correlating SAXS data led to a model correlating ~5nm Bragg spacing to ordering of *polymer chains* between ionic aggregates.[141] But this particle model did not account for increases in SAXS intensity of cesium versus lithium salts. MacKnight instead was able to correlate the ionomer peak to intraparticle interference and the upturn at small angles from ionic groups ordering around the clusters in a Core-Shell model (Figure 1-19a).[142] Several shortcomings between experimentation and this Core-Shell model led to an acceptance of interparticle interference (Figure 1-19b).

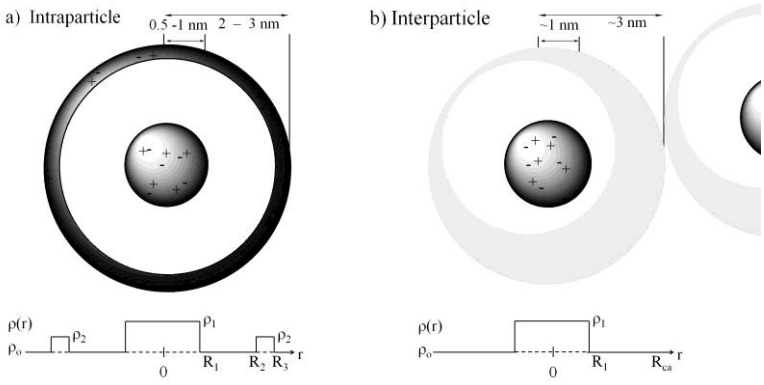

Figure 1-19. Overview of a) intraparticle and b) interparticle scattering models and corresponding electron density profiles

Yarusso and Cooper explained experimental SAXS data using hard-sphere liquid theory.[143] The YC model was fairly successful in modeling the ionomer peak while failing to reproduce the upturn at very low angles. As scattering of X-rays is divided into form factor scattering (due to the shape of the particle) and structure factor scattering (due to the arrangement of particles in space), several theories can be used to describe and calculate various parameters. Kinning and Thomas also were able to describe experimental SAXS data using hard-sphere liquid theory except using a different correlation function.[144] The KT model successfully captured both the ionomer peak and upturn. In turn, Eisenberg in cooperation with Hird and Moore attempted to correlate

mechanical behavior and SAXS by detailing the multiplet's role in lowering the bulk T_g and also forming clusters with dimensions large enough to exhibit the second T_g often observed.[145]

These debates have captured numerous ways to explain ionomer morphology with the most recent investigations moving toward direct imaging, although again not without challenges.[146-149] Precisely defined polymer structures have added a level of control in studying ionomer morphology and the interplay of ionic interactions with crystallization. Although un-ionized acids have only been found to aggregate in perfluorinated polymers, more polar and acidic sulfonic and phosphonic acid functional groups have been incorporated into polyethylene to study the interplay of size, hydrogen bonding, and crystallization.

Purpose of this Dissertation

A progression detailing the ongoing utility of ADMET in producing polyethylene copolymers with desired functionality is described. The synthetic details presented in this dissertation for the isolation of polar monomers via a two-step one pot reaction followed by polymerization, hydrogenation, and post-polymerization modifications including deprotection and ionomerization is significant for creating highly ordered macromolecular structures. Acidity and polarity are increased with ensuing microstructure and bulk property comparisons. *High molecular weight polymers were attained using appropriate protecting group chemistry while precision was ensured by using Grubbs' first generation catalyst.*

Chapter 2 describes the synthesis of sulfonic acid esters. With precise frequency and by varying the attachment, introducing an aromatic spacer rendered the ester materials amorphous. Linear ethylene copolymers containing sulfonic acid ethyl esters

precisely spaced on every 21st and 9th carbon were synthesized using metathesis polycondensation chemistry using an ester monomer versus a reduced sulfur analogue. Previously, ethylene and vinyl sulfonic acid copolymers synthesized using conventional methods were difficult to produce but now using this metathesis strategy, one semicrystalline precision copolymer and one completely amorphous copolymer were obtained. Primary structure characterization confirms the precision polymer structures. Additional secondary microstructure analysis by DSC shows a recoverable endothermic melt transition of polyethylene-like lamellae crystallites of the directly attached ester while completely amorphous behavior is observed when the ester is spaced away from the backbone with an aromatic group. Upon increasing the frequency, purely amorphous materials are obtained no matter the attachment. Efforts at complete deprotection are being followed as the initial investigation indicates that while an aromatic sulfonic acid would yield a more acidic copolymer, the directly attached ester spaced by 20 carbons will be useful in studying the interplay of crystallization and hydrogen bonding.

Indeed with the pursuit of varying acidity and hydrogen bonding capabilities in precision copolymers, Chapter 3 describes the successful synthesis of a linear ethylene copolymer containing phosphonic *acid* precisely spaced on every 21st carbon. The phosphonic acid group must be protected during polymerization to avoid catalyst poisoning; deprotection is done after the polymer is formed. Full deprotection, required to yield such precisely functionalized polyethylenes, was confirmed by solid-state NMR and infrared spectroscopy.

Implications of introducing such a highly polar group became apparent in studying the thermal behavior. Thus a family varying in architecture and frequency were synthesized with the ensuing structure and thermal behavior studied in Chapter 4. Polyethylene structures containing precisely placed phosphonic acids were synthesized varying both the frequency of acid appearance along the backbone and the architecture associated with each position. Single, geminal, and benzyl attachment schemes are described with symmetry of placement being an important feature. Altering these precision primary structures has a direct effect on secondary structure where changes in thermal behavior become obvious, particularly in terms of crystallization behavior. It is evident that strong interactions between polymer chains exist, effecting polymer crystallization and solubility depending upon both the length of methylene run-lengths between symmetrically placed acids and whether or not the acid group is protected as the ester or free to participate in hydrogen bonding, which directly influences interchain interaction.

Due to the complicated crystallization behavior observed in the various phosphonic acid architectures as a result of increasing the polarity and available interactions, further studies were devised in comparing previously studied simpler precise and random carboxylic acid copolymer analogues to the highly polar copolymers. Chapter 5 first describes the analogous synthesis of random phosphonic acid copolymers obtained by ADMET along with detailed thermal analysis, complimented by a comparison to previous SAXS and WAXS.

Finally, Chapter 6 describes the implications of increasing the polarity through ionization and varying the metal size. Preliminary WAXS as well as the future

challenges and outlook in this area highlight the utility of precise ionomers stemming from the underlying primary structure obtained via metathesis polymerization. As a collective story, the research described herein provides a progression increasing in polarity and complexity along with fundamental outcomes allowing for further advancements in understanding more functional polymers.

CHAPTER 2
SULFONIC ACID ESTERS

Introduction*

Significant progress in tailoring physical properties of polyethylene (PE) has already been achieved by incorporating both nonpolar and polar functionalities.[150] In particular, polar acidic groups can enhance PE in terms of strength and toughness, as well as barrier and transport properties, which have importance in membrane technologies.[151] Using a polar-group tolerant ruthenium catalyst such as Grubbs' first generation catalyst, which does not cause isomerization of the terminal olefin as Grubbs' second generation catalyst has proven, microstructural limitations caused by conventional polymerization techniques can be lessened with protection chemistry and a metathesis polycondensation chemistry approach — allowing for detailed crystalline, thermal and morphological investigations.[152-155]

Recently, this approach was employed in the synthesis of precision carboxylic acid functionalized polyethylene copolymers used to model conventional poly(ethylene-*co*-acrylic acid) (EAA) copolymers.[153,156] The morphology suggested by X-ray scattering includes layers of carboxylic acid groups stacked periodically in the precision structure.

This chapter focuses on PE with precisely spaced sulfonic acid ester substituents, which when hydrolyzed for example, will result in the desired highly acidic groups for particular membrane applications possibly further enhanced by a layered morphology. A reduced route is also introduced although not ultimately followed. Instead using metathesis polycondensation chemistry, the synthesis of linear precisely functionalized

* Reproduced in part with permission from: Opper, K.L..; Wagener, K.B. Macromol. Rapid Comm. **2009**, *30*, 915-919. Copyright 2009 Wiley VCH

copolymers, specifically one containing a directly attached sulfonic acid ethyl ester on every 21st and 9th carbon and one spaced away from the backbone as an aromatic sulfonic acid ethyl ester on every 21st carbon and 9th carbon is described. Although homopolymers of vinyl sulfonic acid and vinyl sulfonate have been be produced by radical polymerization, copolymer synthesis by radical chemistry is limited.[156-158] Additionally, most sulfonated polystyrene copolymers are produced by random post-polymerization sulfonation chemistry.[150, 156] Here, post-polymerization deprotection is required and efforts are described in deprotection as well as in using the alternate pentafluorophenol ester group.

Experimental

Methods

All ^{1}H NMR (300 MHz) and ^{13}C NMR (75 MHz) spectra were recorded on a Varian Associates Mercury 300 spectrometer. Chemical shifts for ^{1}H and ^{13}C NMR were referenced to residual signals from $CDCl_3$ (^{1}H = 7.27 ppm and ^{13}C= 77.23 ppm). Thin layer chromatography (TLC) was performed on EMD silica gel-coated (250 μm thickness) glass plates. Developed TLC plates were stained with iodine adsorbed on silica to produce a visible signature. Reaction progress and relative purity of crude products were monitored by TLC and ^{1}H NMR.

High-resolution mass spectral (HRMS) data were obtained on a Finnegan 4500 gas chromatograph/mass spectrometer using either the chemical ionization (CI) or electrospray ionization (ESI) mode.

Molecular weights and molecular weight distributions were determined by gel permeation chromatography (GPC), performed using a Waters Associates GPCV2000 liquid chromatography system equipped with a differential refractive index detector

(DRI) and an autosampler. These analyses were performed at 40°C using two Waters Styragel HR-5E columns (10 microns PD, 7.8 mm ID, 300 mm length) with HPLC grade THF as the mobile phase at a flow rate of 1.0 mL/minute. Injections were made at 0.05-0.07 % w/v sample concentration using a 220.5 µL injection volume. Retention times were calibrated versus narrow molecular weight polystyrene standards (Polymer Laboratories; Amherst, MA).

Infrared spectroscopy was obtained using a Perkin-Elmer Spectrum One FT-IR outfitted with a $LiTaO_3$ detector. Samples were dissolved in chloroform and cast on a KBr disc by slow solvent evaporation.

Differential scanning calorimetry (DSC) was performed using a TA Instruments Q1000 at a heating rate of 10ºC/min under nitrogen purge. Temperature calibrations were achieved using indium and freshly distilled n-octane while the enthalpy calibration was achieved using indium. All samples were prepared in hermetically sealed pans (4-7 mg/sample) and were run using an empty pan as a reference.

Materials

All materials were purchased from Aldrich and used as received, unless otherwise specified. Tetrahydrofuran (THF) was obtained from an MBraun solvent purification system. Lithium diisopropyl amide (LDA) was prepared prior to monomer synthesis. Grubbs' first generation ruthenium catalyst, bis(tricyclohexylphosphine)benzylidine ruthenium(IV)dichloride, was a gift from Materia, Inc. Wilkinson's rhodium catalyst, $RhCl(PPh_3)_3$, was purchased from Strem Chemical. Synthesis of synthon 11-bromoheneicosa-1,20-diene **(2-1)** was synthesized using a previously reported procedure.[70]

Reduced Sulfur Synthesis

Henicosa-1,20-dien-11-yl ethanethioate (2-2). In a dry three neck round bottom flask equipped with a magnetic stir bar under argon, 2.40g (21 mmol, 1.3 eq) of potassium thioacetate was added and then dissolved with 20mL dry dimethylformamide. Dropwise, 6g (16mmol, 1 eq) of bromide **2-1** was added over 15 minutes. The reaction proceeded at room temperature for 8 hours. Once conversion of bromide **2-1** was complete by TLC, the reaction was quenched with an excess of water. The aqueous reaction mixture was then extracted with hexane (3 x 50 mL), washed with brine and concentrated to a dark brown oil. A lighter brown oil was obtained after column chromatography using 4:1 hexane:ethyl acetate. From bromide **2-1**, thioate **2-2** was obtained in 67% yield. ^{1}H NMR ($CDCl_3$): δ (ppm) 1.27 (br, 24H), 1.55 (br, 4H), 2.04 (q, 4H), 3.51(p, 1H), 4.92-5.03 (m, 4H), 5.78-5.87 (m, 2H). HRMS calcd for $C_{23}H_{42}OS$ $[M+H]^+$ (*m/z*), 367.3066; found, 367.3056. Anal. Calcd for $C_{23}H_{48}OS$: C, 75.34; H 11.55; O, 4.36; S, 8.75 found: C, 75.35; H, 11.68

Henicosa-1,20-diene-11-thiol (2-3). Thioate **2-2** was added over 15 minutes, dropwise to a stirred slurry of 0.7g (11 mmol, 2 eq) lithium aluminum hydride in 20mL dry tetrahydrofuran at 0°C under argon. After the addition, the solution was allowed to warm to room temperature over 1 hour while stirring. The reaction was quenched with deionized water (10 mL), 15% (w/v) NaOH (10 mL), and more water (50 mL). The solution stirred until cool and the reaction mixture appeared as a white slurry. The precipitate was filtered, facilitated by adding diethyl ether. The crude mixture was stirred over magnesium sulfate for 20 minutes. The solution was filtered and concentrated to a yellow oil with no further purification neccessary. From thioate **2-2**, thiol **2-3** was obtained in 72% yield. ^{1}H NMR ($CDCl_3$): δ (ppm) 1.29-1.50 (br, 26H), 1.55-1.63 (br, 2H),

2.05 (q, 4H), 4.92-5.03 (m, 4H), 5.76-5.89 (m, 2H). HRMS: calcd for $C_{21}H_{40}S$ [M+] (*m/z*), 324.2845; found, 324.2845

Directly Attached Sulfonic Acid Ester Synthesis

Ethyl tricosa-1,22-diene-12-sulfonate (2-4). In a flame dried 3-necked flask equipped with a magnetic stir bar, 2.5mL (20 mmol, 1 eq) of ethyl methane sulfonate and 4.4mL (20 mmol, 1 eq) of 11-bromoundecene were stirred in 20 mL of dry THF under argon. After bringing the solution to -78°C, 0.9 eq of LDA was added dropwise over 30 minutes and stirred for 30 additional minutes. The solution was then warmed to 0°C and stirred for 1 to 2 hours until mono-alkylation was observed and alkenyl bromide disappeared by TLC. After bringing the solution back to -78°C, 0.9 eq of 11-bromoundecene was added slowly and allowed to dissolve. With the solution at -78°C, 0.9 eq of LDA was added dropwise over 30 minutes and stirred for 30 additional minutes. The solution was then warmed to 0°C and stirred for 2 to 3 hours until the conversion from mono-alkylation to diene product was no longer observed. The reaction was quenched by adding ice cold water. This mixture was then extracted (3 x 50 mL) with diethyl ether, dried over magnesium sulfate and concentrated to a colorless oil. Column chromatography, using 1:19 diethyl ether:hexane as the eluent, afforded dialkylation product **2-1** in 30% recovered yield. ^{1}H NMR ($CDCl_3$): δ (ppm) 1.29 (br, 32H), 1.41 (t, 3H), 2.05 (q, 4H), 2.98 (p, 1H), 4.28 (q, 2H), 4.92-5.03 (m, 4H), 5.75-5.81 (m, 2H). ^{13}C NMR ($CDCl_3$): δ (ppm) 15.47, 26.83, 29.14, 29.15, 29.33, 29.52, 29.65, 29.70, 61.45, 65.47, 114.35, 139.41. HRMS calcd for $C_{25}H_{48}O_3S$ $[M\text{-}C_2H_5]^-$ (*m/z*), 399.2901; found, 399.2917. Anal. Calcd for $C_{25}H_{48}O_3S$: C, 70.04; H 11.29; O, 11.20; S, 7.48 found: C, 69.99; H, 11.33

Ethyl undeca-1,10-diene-6-sulfonate (2-4a). ^{1}H NMR ($CDCl_3$): δ (ppm) 1.39 (t, 3H), 1.56 (m, 4H), 1.65 (m, 2H), 2.05 (m, 2H), 2.12 (q, 4H), 2.98 (p, 1H), 4.28 (q, 2H), 4.97-5.06 (m, 4H), 5.72-5.83 (m, 2H). ^{13}C NMR ($CDCl_3$): δ (ppm) 15.41, 25.94, 28.52, 33.62, 61.11, 65.58, 115.49, 137.92. HRMS calcd for $C_{13}H_{24}O_3S$ $[M+H]^+$ (*m/z*), 261.1519; found, 261.1527. Anal. Calcd for $C_{13}H_{24}O_3S$: C, 59.96; H 9.29; O, 18.43; S, 12.31 found: C, 59.96; H, 9.40

Homopolymerization conditions

In a flame dried 50 mL round bottom flask, an exact amount of monomer was weighed. Using a 400:1 monomer:catalyst ratio (0.25 mol%), Grubbs' first generation catalyst was added and mixed into the monomer while under a blanket of argon. A magnetic stir bar was placed into the mixture while a schlenk adapter was fitted to the round bottom. After sealing the flask under argon it was moved to a high vacuum line. The mixture was stirred and slowly exposed to vacuum over an hour at room temperature. After stirring for an hour at room temperature under eventual high vacuum (10^{-3} torr), the flask was lowered into a prewarmed 50ºC oil bath for an appropriate number of days allowing removal of ethylene bubbling through viscous polymer. Polymers were quenched by dissolution of polymer in an 1:10 ethyl vinyl ether:toluene solution under argon. Upon precipitation into an appropriate solvent, the polymers were isolated.

Polymerization of Ethyl tricosa-1,22-diene-12-sulfonate (2-5). ^{1}H NMR ($CDCl_3$): δ (ppm) 1.29 (br, 32H), 1.41 (br, 3H), 1.96 (br, 4H), 2.97 (p, 1H), 4.29 (q, 2H), 5.39 (br, 2H). ^{13}C NMR ($CDCl_3$): δ (ppm) 15.47, 26.85, 27.46, 29.16, 29.42, 29.57,

29.65, 29.71, 29.74, 29.91, 30.01, 32.84, 61.46, 65.49, 130.56. GPC data (THF vs. polystyrene standards): M_w = 63900 g/mol; P.D.I. (M_w/M_n) = 1.8

Polymerization of Ethyl undeca-1,10-diene-6-sulfonate (2-5a). ^{1}H NMR ($CDCl_3$): δ (ppm) 1.40 (t, 3H), 1.51 (m, 4H), 1.67 (m, 2H), 1.90 (m, 2H) 2.05 (m, 4H), 2.98 (p, 1H), 4.29 (q, 2H), 5.41 (m, 2H). ^{13}C NMR ($CDCl_3$): δ (ppm) 15.47, 26.60, 26.72, 27.26, 28.62, 29.67, 32.52, 61.17, 65.68, 129.80, 130.33. GPC data (THF vs. polystyrene standards): M_w = 22700 g/mol; P.D.I. (M_w/M_n) = 2.1

Hydrogenation conditions

A solution of unsaturated polymer was dissolved in toluene and degassed by bubbling a nitrogen purge through the stirred solution for an hour. Wilkinson's catalyst [$RhCl(PPh_3)_3$] was added to the solution along with a magnetic stir bar, and the glass sleeve was sealed in a Parr reactor equipped with a pressure gauge. The reactor was filled to 700 psi hydrogen gas and purge three times while stirring, filled to 500 psi hydrogen, and stirred for an appropriate number of days. After degassing the solution, the crude solution was isolated, precipitated into an appropriate solvent.

Hydrogenation to yield copolymer (2-6). ^{1}H NMR ($CDCl_3$): δ (ppm) 1.29 (br, 41H), 1.41 (br, 3H), 2.97 (p, 1H), 4.29 (q, 2H). ^{13}C NMR ($CDCl_3$): δ (ppm) 15.45, 26.82, 29.13, 29.55, 29.72, 29.78, 29.85, 29.94, 61.44, 65.48

Hydrogenation to yield copolymer (2-6a). ^{1}H NMR ($CDCl_3$): δ (ppm) 1.38 (br, 12H), 1.40 (t, 3H), 1.69 (m, 2H), 1.90 (m, 2H), 2.98 (p, 1H), 4.29 (q, 2H) ^{13}C NMR ($CDCl_3$): δ (ppm) 15.41, 25.94, 28.52, 33.62, 61.11, 65.58

Aromatic Spaced Sulfonic Acid Ester Synthesis

Ethyl 4-(tricosa-1,22-dien-12-yl)benzenesulfonate (2-7). Column chromatography using 1: 19 diethyl ether:hexane as the eluent, afforded dialkylation

product 2-4 in 35% recovered yield. ^{1}H NMR ($CDCl_3$): δ (ppm) 1.07-1.37 (br, 32H), 1.30 (t, 3H), 1.53-1.65 (m, 4H), 1.97-2.05 (m, 4H), 2.59 (sp, 1H), 4.12 (q, 2H) 4.88-5.00 (m, 4H), 5.72-5.85 (m, 2H), 7.29-7.32 (d, 2H), 7.80-7.83 (d, 2H). ^{13}C NMR ($CDCl_3$): δ (ppm) 14.86, 27.62, 29.05, 29.22, 29.57, 29.64, 29.74, 33.90, 36.77, 46.35, 66.81, 114.24, 127.96, 128.57, 133.85, 139.21, 153.35. HRMS calcd for $C_{31}H_{52}O_3S$ $[M+H]^+$ (*m/z*), 505.3710; found, 505.3719. Anal. Calcd for $C_{31}H_{52}O_3S$: C, 73.76; H 10.38; O, 9.51; S, 6.35 found: C, 73.75; H, 10.37

Ethyl 4-(undeca-1,10-dien-6-yl)benzenesulfonate (2-7a). ^{1}H NMR ($CDCl_3$): δ (ppm) 1.17 (m, 4H), 1.30 (t, 3H), 1.53-1.65 (m, 4H), 1.95-2.03 (m, 4H), 2.60 (sp, 1H), 4.13 (q, 2H) 4.87-4.98 (m, 4H), 5.65-5.78 (m, 2H), 7.27-7.33 (d, 2H), 7.82-7.83 (d, 2H). ^{13}C NMR ($CDCl_3$): δ (ppm) 14.91, 26.91, 33.81, 36.14, 46.18, 66.95, 114.80, 128.08, 128.62, 134.03, 138.61, 152.94. HRMS calcd for $C_{13}H_{24}O_3S$ $[M+H]^+$ (*m/z*), 337.1832; found, 337.1818. Anal. Calcd for $C_{31}H_{52}O_3S$: C, 67.82; H 8.39; O, 14.26; S, 9.35 found: C, 68.01; H, 8.46

Polymerization of Ethyl 4-(tricosa-1,22-dien-12-yl)benzenesulfonate (2-8). ^{1}H NMR ($CDCl_3$): δ (ppm) 1.06-1.37 (br, 32H), 1.32 (t, 3H), 1.51-1.69 (m, 4H), 1.95 (br, 4H), 2.58 (sp, 1H), 4.11-4.18 (q, 2H) 5.33-5.38 (m, 2H), 7.29-7.32 (d, 2H), 7.81-7.84 (d, 2H). ^{13}C NMR ($CDCl_3$): δ (ppm) 14.96, 27.42, 27.73, 29.38, 29.50, 29.70, 29.78, 29.87, 29.97, 32.80, 36.88, 46.46, 66.93, 128.03, 128.66, 130.07, 130.53, 133.86, 153.47. GPC data (THF vs. polystyrene standards): M_w = 62626 g/mol; P.D.I. (M_w/M_n) = 1.95

Polymerization of Ethyl 4-(undeca-1,10-dien-6-yl)benzenesulfonate (2-8a). ^{1}H NMR ($CDCl_3$): δ (ppm) 1.15 (br, 4H), 1.34 (t, 3H), 1.48-1.62 (m, 2H), 1.88 (br, 2H), 2.58 (br, 1H), 4.16 (q, 2H), 5.24-5.33 (m, 2H), 7.27-7.30 (d, 2H), 7.79-7.83 (d, 2H). ^{13}C NMR

($CDCl_3$): δ (ppm) 14.98, 18.09, 27.32, 27.74, 30.55, 32.70, 36.39, 45.58, 46.26, 67.00, 125.61, 128.08, 128.65, 128.74, 129.83, 130.32, 130.78, 134.01, 152.95. GPC data (THF vs. polystyrene standards): M_w = 8000 g/mol; P.D.I. (M_w/M_n) = 1.50

Hydrogenation to yield copolymer (2-9). ^{1}H NMR ($CDCl_3$): δ (ppm) 1.24 (br, 36H), 1.32 (t, 3H), 1.51-1.69 (m, 4H), 2.58 (sp, 1H), 4.11-4.18 (q, 2H), 7.29-7.32 (d, 2H), 7.81-7.84 (d, 2H). ^{13}C NMR ($CDCl_3$): δ (ppm) 14.97, 27.74, 29.73, 29.84, 29.87, 29.93, 36.88, 46.45, 66.97, 128.03, 128.66, 133.74, 153.50

Hydrogenation to yield copolymer (2-9a). ^{1}H NMR ($CDCl_3$): δ (ppm) 1.13 (br, 12H), 1.31 (t, 3H), 1.60 (m, 4H), 2.54 (br, 1H), 4.15 (q, 2H), 7.27-7.31 (d, 2H), 7.79-7.83 (d, 2H). ^{13}C NMR ($CDCl_3$): δ (ppm) 14.97, 27.75, 29.74, 29.82, 29.87, 29.93, 36.88, 46.45, 66.99, 128.04, 128.66, 133.73, 153.51

General Protection Synthesis

Perfluorophenyl methanesulfonate (2-10). To a dry 3-neck flask equipped with a stirbar, septa, stopper and gas inlet adapter dry methylene chloride (35mL) was added under an argon atmorphere. Pentfluorophenol (3.5g, 19mmol) was added by syringe and weighing by subtraction. Distilled triethylamine was then added by syringe (4.88mL, 35mmol). The mixture was then cooled to 0°C in an ice bath. Mesyl chloride (1.32mL, 17mmol) was added via syringe and stirred for 3 hours at 0°C. Upon partial addition a white precipitate formed and proceeded to form throughout the reaction. The reaction was allowed to warm to room temperature and stirred overnight. Any unreacted mesyl chloride was quenched with water. The mixture was then extracted in methylene chloride (3 x 50mL). The methylene chloride was then washed with 1M HCl (100mL). Upon concentration, the crude material was stored at 10°C. With some decomposition noticed, column chromatography afforded 2.95g or 66% purified yield. ^{1}H NMR ($CDCl_3$):

δ (ppm) 3.37 (s, 3H). ^{13}C NMR ($CDCl_3$): δ (ppm) 39.59, 136.58, 138.94, 140.72, 142.34, 144.16. HRMS calcd for $C_7H_3F_5O_3S$, [M+] (*m/z*), 261.9723; found, 261.9709

Results and Discussion

Copolymers of ethylene containing precisely spaced sulfonic acid ester groups have not been synthesized previously. Their synthesis opens the way to observe distinct morphologies, such as one containing layers, which may contribute to unique ionomer membrane properties once hydrolyzed. The copolymers presented here offer two molecular architectures to begin investigating this possibility.

Previous work on precision carboxylic acid functionalized polyolefins exhibited the need for protecting group chemistry to attain high molecular weights using metathesis polycondensation chemistry.[153,159] To circumvent similar hindered catalysis, first a reduced sulfur route was followed (Figure 2-1).

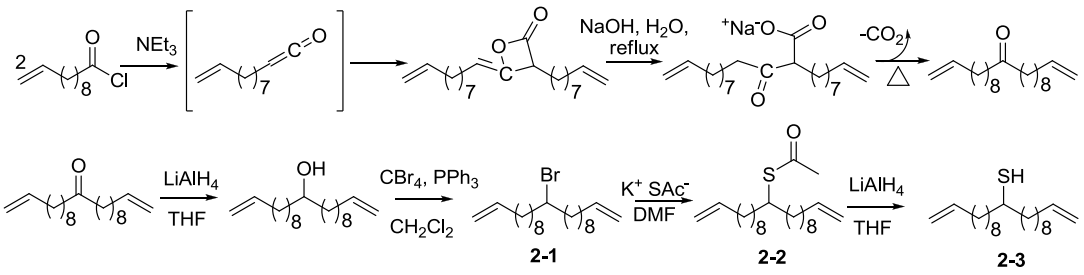

Figure 2-1. Reduced sulfur monomer synthesis

The bromide precursor, prepared from literature precendents,[70] was transformed to the thioate by a nucleophilic displacement with potassium thioacetate to form thioate monomer **2-2**. The thioate diene **2-2** was synthesized as a reduced-protected sulfonic acid. If obtained, the hydrogenated thioate polymer is the sulfur analogue to poly(vinyl acetate). Just as poly(vinyl alcohol) is prepared from poly(vinyl acetate), the thiol was expected from a similar reaction on-polymer (tested on the monomer to produce **2-3**).

The sulfonic acid would follow from oxidation of the thiol on polymer. However, Grubbs' 1st generation catalyst (**Ru1**) only produced oligomers with a degree of polymerization of approximately 5 (GPC relative M_w of 2,300 g/mol). If polymer was produced, reduction/hydrolysis and oxidation would need to be quantitative to preserve the precision placement. Otherwise, there would be randomly incorporated thioate and thiol defects.

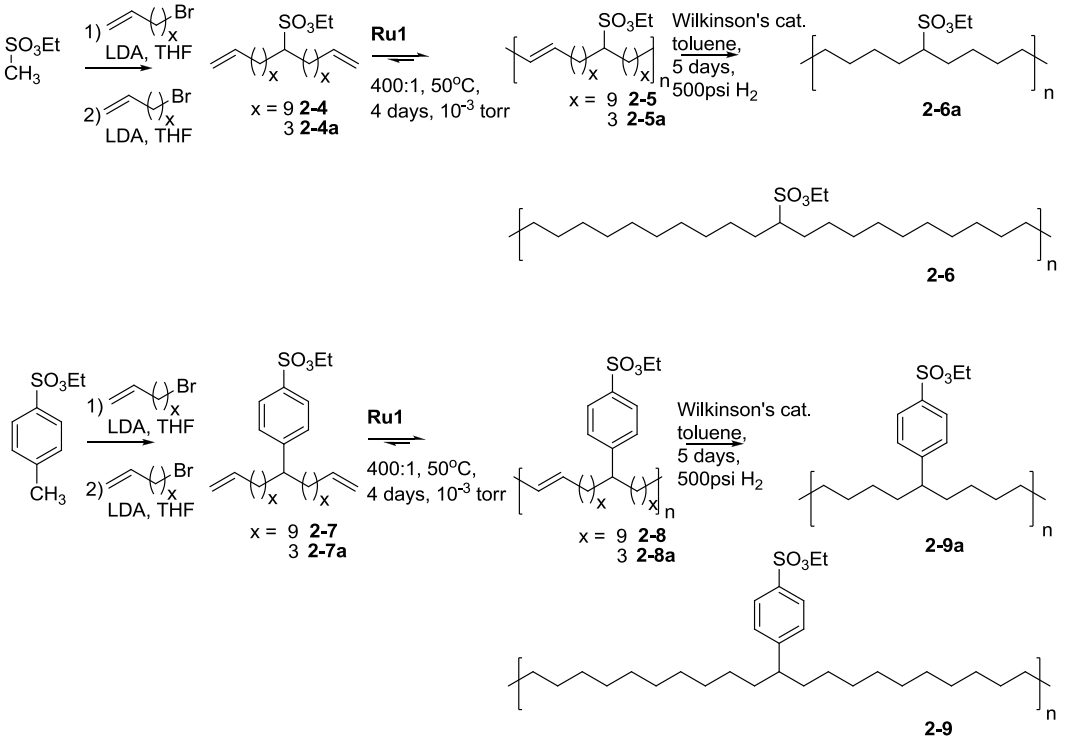

Figure 2-2. Synthesis of ethylene-*co*-ethyl vinyl sulfonic acid ester copolymers **2-6** and **2-6a** aromatic copolymers **2-9** and **2-9a**

However, success was met by incorporating the oxidized sulfonic acid ethyl ester into the monomer prior to polymerization (Figure 2-2). Establishing the exact structural repeat into the single monomer allows for successful metathesis polycondensation and isolation of the final ethylene-*co*-vinyl sulfonic acid ethyl ester copolymer as an example.

Beginning with ethyl methane sulfonate, alpha di-alkylation using a modified lithiation procedure yields monomers **2-4** and **2-4a** in a two-step, one-pot reaction.[160-162]

Although imidazolyl, phenoxy, neopentyl or isopropyl groups are often used to circumvent elimination reactions,[162-164] it was found that the ethyl group remains intact during monomer synthesis. As a prime example monomer **2-4** polymerizes readily with the mild polymerization conditions of 50ºC under high vacuum (10^{-3} torr) removing ethylene, to produce copolymer **2-5** with a relative M_n of 36,000 and PDI of 1.8. These results indicate that the ethyl group is a sufficient step-growth polymerization protecting group. Upon exhaustive catalytic hydrogenation using Wilkinson's catalyst, the linear ethylene-*co*-vinyl sulfonic acid ethyl ester copolymer **2-6** having a sulfonic acid ethyl ester precisely spaced on every 21st carbon is obtained. The same approach yielding higher frequency directly attached sulfonic acid esters as well as aromatic copolymers was utilized beginning with ethyl p-toluenesulfonate to yield monomers **2-7(a)**, unsaturated copolymers **2-8(a)**, and final aromatic copolymers **2-9(a)**.

Evidence of the primary structural control and linearity achieved by metathesis polycondensation is clearly seen in the ^{13}C NMR again using copolymer **2-6** as the prime example (Figure 2-3). The symmetry of the monomer is directly transferred into the polymer repeat unit. As such, there are seven magnetically different carbon atoms in the polymer spectrum: the ethyl CH_2 and CH_3; methine; α-, β-, and γ- methylenes; and the remaining unresolved backbone carbons. The absence of olefin signal indicates complete saturation.

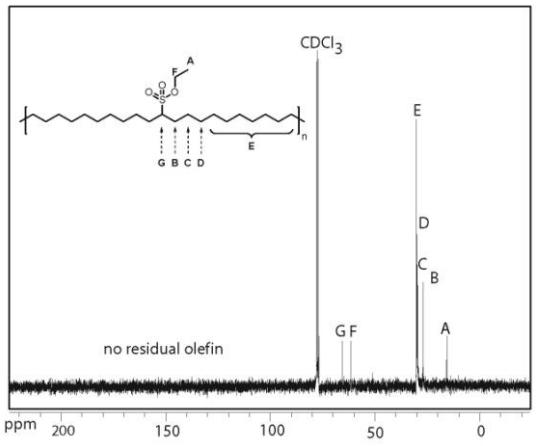

Figure 2-3. ^{13}C spectrum of ethylene-*co*-ethyl vinyl sulfonic acid ester copolymer **2-6** in $CDCl_3$

Fourier transform infrared spectroscopy (FT-IR) confirms complete saturation of copolymer **2-6** by the additional absence of residual olefin C-H wag that would appear at 967 cm^{-1} (Figure 2-4). Typical PE absorbances remain and include CH_2 scissoring at 1466 cm^{-1} (a), CH_2 rocking at 720 cm^{-1} (g), and unorganized C-C crystalline stretching at 799 cm^{-1} (f).

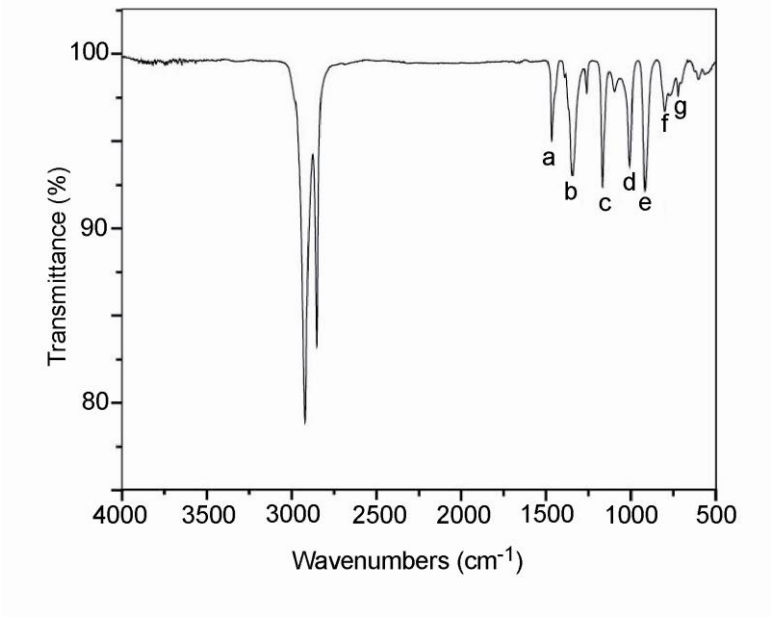

Figure 2-4. IR spectrum of ethylene-*co*-ethyl vinyl sulfonic acid ester copolymer **2**-**6** film.

In addition, the asymmetric O=S=O stretch is observed at 1343 cm^{-1} (b), while the symmetric O=S=O stretch is observed at 1167 cm^{-1} (c). The remaining vibrations indicated in Figure 2 are S-O-C stretches at 1006 cm^{-1} (d) and 916 cm^{-1} (e).

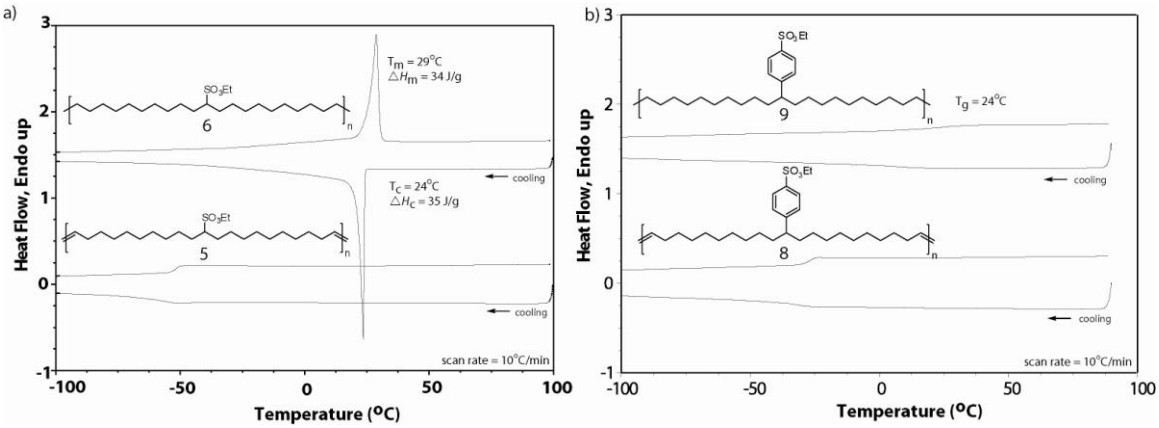

Figure 2-5. Representation of (left) DSC of unsaturated copolymer **2-5** and saturated ethylene-*co*-ethyl vinyl sulfonic acid ester copolymer **2-6**; (right) DSC of unsaturated copolymer **2-8** and saturated copolymer **2-9** (arbitrary vertical offsets for clarity)

The crystalline behavior of **2-6** suggested by FT-IR measurements was then examined using differential scanning calorimetry (DSC). Thermograms of both the unsaturated copolymer **2-5** and saturated copolymer **2-6** are shown in Figure 2-5 alongside copolymers **2-8** and **2-9**. Copolymer **2-5** exhibits completely amorphous behavior with a T_g of -52 ºC, while full saturation yields semicrystalline copolymer **2-6** indicating the intervening 20 methylenes between groups are now able to crystallize. Copolymer **2-6** exhibits a recoverable endothermic melt transition of these polyethylene-like crystallites at an onset of 25 ºC (ΔH_m = 34 J/g) and peak T_m of 29 ºC. Exothermic recrystallization is observed at a very sharp onset of 24 ºC (ΔH_c = 35 J/g) and peak T_c of 24 ºC. The secondary microstructural behavior analyzed by DSC corresponds well with previous work on PE copolymers with similar precisely spaced functionalities, including ethylene-*co*-acrylates and ethylene-*co*-acetates.[165]

However, when compared to the phenyl spaced copolymers, both unsaturated copolymer **2-8** and saturated copolymer **2-9** exhibit completely amorphous behavior with glass transitions at -27 ºC (ΔC_p = 0.08 J/(gºC)) and 24 ºC (ΔC_p = 0.07 J/(gºC)) respectively. In this case, removing the double bond through exhaustive hydrogenation does not allow for crystallization during the time-scale of the standard experiment. These results were confirmed by additional annealing experiments but no crystallization was observed. By simply introducing an aromatic spacer in copolymer **2-9** as compared to copolymer **2-6**, completely different thermal behavior is observed.

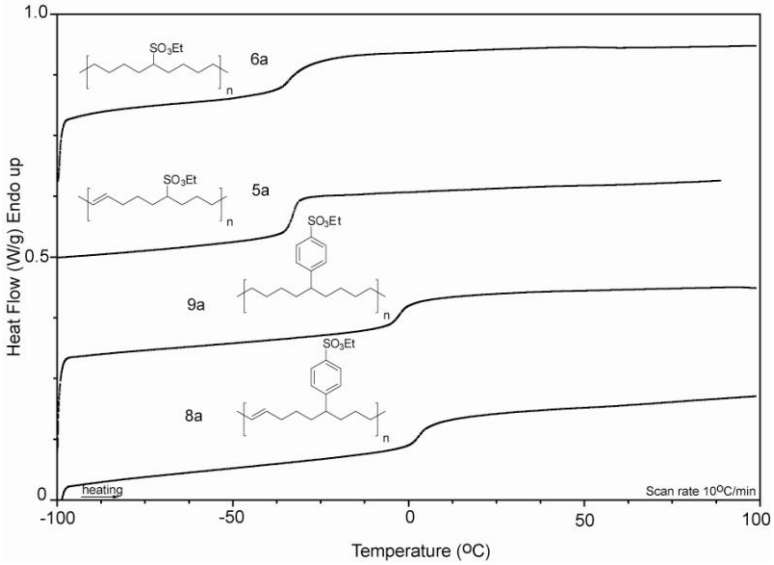

Figure 2-6. DSC of amorphous copolymers saturated **2-6a** and **2-9a** as well as unsaturated **2-5a** and **2-8a** (arbitrary vertical offsets for clarity)

Amorphous materials were also obtained upon increasing the functional group frequency (Figure 2-6). The T_g of the directly attached sulfonic acid esters do not differ much between unsaturated **2-5a** and **2-6a** while there is slight increase in T_g upon introducing the aromatic spacer in copolymers **2-8a** and **2-9a**. More energy is required to free the chain motion and undergo the glass transition in aromatic spaced polymers due to a higher concentration of associating aromatic groups. But the similar T_g

between the copolymers presented in Figure 2-6 indicates that once below a certain runlength, the methylene segments take a similar amount of energy to free the chain mobility. Also below a certain runlength, the PE segments are not long enough to crystallize in the presence of the bulky ester groups. Interestingly with the long 20 carbon methylene runlength of copolymer **2-9**, rather than crystallize, the aromatic spacer also served to preclude crystallization as well as reduce chain mobility with a higher T_g.

Freeing the acid remains the real interest in these materials. Various attempts at hydrolysis on the monomer were attempted including simple acid or base hydrolysis. Additionally, the monomer was treated with the strong trimethylsilyl bromide electrophile in an effort to silate the ester. However, no reaction was observed and only the starting materials were isolated. Efforts to increase the lability of the ester group were then undertaken and small molecule test reactions were successful (Figure 2-7).

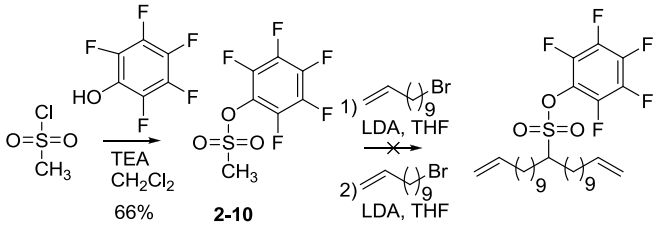

Figure 2-7. Preparation of active esters

This synthesis was met with some success in the isolation of a protected mesyl acid. However, while **2-10** could be purified, premature deprotection was observed by TLC and by ^{19}F NMR. Even upon alkylation attempted alkylation of carefully stored molecule **2-10**, no alkylated product was observed but free pentafluorophenol was observed by TLC. The protecting group was too labile under reasonable conditions and in undergoing alkylation.

Conclusions

This simple alkylation-metathesis strategy, successful in obtaining the semicrystalline ethylene-co-vinyl sulfonic acid ethyl ester copolymer and amorphous aromatic version, offers added diversity to various other highly acidic structures depending on monomer starting material choices. Amorphous materials were also obtained by increasing the functional group frequency below a methylene run-length that PE segments can crystallize. Although attempts at complete deprotection of the ethyl protecting group were unsuccessful a library of hemi-acetal esters, and amides remain. However, even in the ester copolymers the architecture plays a role in determining the final behavior of the precision polymer. This point will be developed in the remaining chapters.

CHAPTER 3
SIMPLE PHOSPHONIC ACID

Introduction*

Incorporating polar functionality into PE follows the underlying theme of introducing highly interactive groups and broadens the possibilities of altering both microstructure and morphology, thus targeting properties for specific applications.[166,167] Phosphonic acid based functionalization in polyolefins has gained increasing attention due to the range of properties attainable, rendering these materials useful for applications such as chemical separation, ion exchange, and ion conductive membranes;[168,169] flame retardants;[170] as well as biomaterials suitable for cell adhesion,[171] bone integration,[172] and dental cements.[173-174] Specifically, due to its importance in a number of these applications, poly(vinylphosphonic acid) PVPA has been the focus of detailed investigations of homopolymerization mechanisms and resulting microstructures.[175-176] While vinyl phosphonic acid polymers have been examined rather extensively, copolymers of ethylene and vinylphosphonic acid have received less attention: they have proven to be difficult to make.

Ethylene based copolymers containing a variety of functional groups can be made via metathesis polymerization,[177-178] and recently the full investigation on examining ethylene based polymers containing precisely placed acid groups began.[78] Beyond the first examples of random and low molecular weight acid polyethylenes, preparation of a series of the precision poly(ethylene-*co*-acrylic acid) (EAA) copolymers was reported, where for the first time structural precision allowed for a layered morphology.[179] The

* Reproduced in part with permission from: Opper, K.L..; Fassbender, B. Brunklaus, G., Spiess, H.W., Wagener, K.B. Macromolecules **2009**, *42*, 4407-4409. Copyright 2009 American Chemical Society

preparation of a precision phosphonic acid copolymer, an analog of the carboxylic acid materials mentioned above, placing the phosphonic acid functional group on every 21st carbon of a strictly linear polyethylene backbone is further described here.

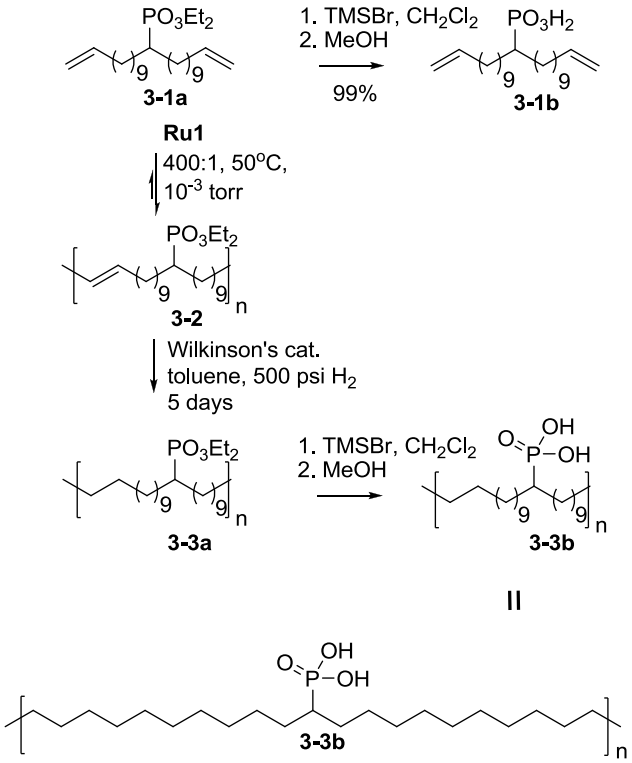

Figure 3-1. Synthetic scheme of precisely functionalized polyethylene with phosphonic acid on every 21st carbon

The copolymer was synthesized by metathesis polycondensation chemistry of an appropriately protected α,ω–diene monomer with precision ensured by utilizing Grubbs' first generation catalyst, followed by complete saturation and quantitative deprotection (Figure 3-1). Compared to the typical oxidative phosphorylation reactions on polyethylene,[180-181] this method offers complete control of the microstructure, which will lead to a systematic understanding of how microstructure and resulting morphology dictate particular properties.

Experimental

Methods

All ^{1}H (300 MHz) and ^{13}C (75 MHz) solution NMR spectra were recorded on a Varian Associates Mercury 300 spectrometer. Chemical shifts for ^{1}H and ^{13}C NMR were referenced to residual signals from $CDCl_3$ (^{1}H = 7.27 ppm and ^{13}C= 77.23 ppm). Thin layer chromatography (TLC) was performed on EMD silica gel-coated (250 μm thickness) glass plates. Developed TLC plates were stained with iodine adsorbed on silica to produce a visible signature. Reaction progress and relative purity of crude products were monitored by TLC and ^{1}H NMR.

Molecular weights and molecular weight distributions were determined by gel permeation chromatography (GPC) using a Waters Associates GPCV2000 liquid chromatography system equipped with a differential refractive index detector (DRI) and an autosampler. These analyses were performed at 40°C using two Waters Styragel HR-5E columns (10 microns PD, 7.8 mm ID, 300 mm length) with HPLC grade THF as the mobile phase at a flow rate of 1.0 mL/minute. Injections were made at 0.05-0.07 % w/v sample concentration using a 220.5 μL injection volume. Retention times were calibrated versus narrow molecular weight polystyrene standards (Polymer Laboratories; Amherst, MA).

Infrared spectra were obtained on a Perkin-Elmer Spectrum One FT-IR equipped with a $LiTaO_3$ detector. Samples were dissolved in chloroform and cast on a KBr disc by slow solvent evaporation. Due to rather poor solubility, the spectrum of the deprotected polymer was obtained by means of an ATR accessory.

Proton solid-state NMR spectra were recorded at 700.1 MHz (Bruker Avance spectrometer) using a magic-angle spinning (MAS) rate of 30 kHz. The ^{13}C CPMAS and

^{31}P MAS NMR spectra were obtained on a Bruker DSX 500 spectromter operating at 125.8 MHz (^{13}C) and 202.5 MHz (^{31}P), respectively, and a MAS rate of 15 kHz. All spectra were recorded at room temperature.

Materials

All materials were purchased from Aldrich and used as received, unless noted otherwise. Tetrahydrofuran (THF) was obtained from a MBraun solvent purification system. Lithium diisopropyl amide (LDA) was prepared prior to monomer synthesis. Grubbs' first generation ruthenium catalyst, bis(tricyclohexylphosphine)benzylidine ruthenium(IV)dichloride, was a generous gift from Materia, Inc. Wilkinson's rhodium catalyst, $RhCl(PPh_3)_3$, was purchased from Strem Chemical.

Synthesis

Diethyl tricosa-1,22-dien-12-ylphosphonate (3-1a). In a flame dried 3-necked flask equipped with a magnetic stir bar, 2.2 mL (15 mmol, 1 eq) of diethyl methane phosphonate and 3.3 mL (15 mmol, 1 eq) of 11-bromoundecene were stirred in15 mL of dry THF under argon. After bringing the solution to -78°C, 0.9 eq of LDA was added dropwise over 30 minutes and stirred for 30 additional minutes. The solution was then warmed to 0°C and stirred for 1 to 2 hours until mono-alkylation was observed and alkenyl bromide disappeared by TLC. After bringing the solution back to -78°C, 0.9 eq of 11-bromoundecene was added slowly and allowed to dissolve. With the solution at -78°C, 0.9 eq of LDA was added dropwise over 30 minutes and stirred for 30 additional minutes. The solution was then warmed to 0°C and stirred for 2 to 3 hours until the conversion from mono-alkylation to diene product was no longer observed. The reaction was quenched by adding ice cold water. This mixture was then extracted (3 x 50 mL) with diethyl ether, dried over magnesium sulfate and concentrated to a colorless oil.

Column chromatography, using 2:1 ethyl acetate:hexane as the eluent, afforded dialkylation product **3-1** in 43% recovered yield. ^{1}H NMR ($CDCl_3$): δ (ppm) 1.26-1.36 (br, 38H), 1.63-1.69 (m, 4H), 1.98-2.06 (q, 4H), 4.07 (p, 4H), 4.89-5.00 (m, 4H), 5.73-5.86 (m, 2H). ^{13}C NMR ($CDCl_3$): δ (ppm) 16.72 ($^{3}J_{CP}$ 5.9Hz), 27.79 ($^{2}J_{CP}$ 9.3Hz), 28.39($^{3}J_{CP}$ 3.6Hz), 29.13, 29.33, 29.63, 29.67, 29.75, 29.91, 34.01, 36.14 ($^{1}J_{CP}$ 138Hz), 61.46 ($^{2}J_{CP}$ 6.8Hz), 114.86, 138.59; ^{31}P NMR ($CDCl_3$, PPh_3 reference): δ (ppm) 34.70. Anal. Calcd for $C_{27}H_{53}O_3P$: C, 71.01; H 11.70; O, 10.51; P, 6.78 found: C, 70.96; H, 11.72. HRMS Calcd for $C_{27}H_{53}O_3P$ [$(M+H)^{+}$] (*m/z*), 457.3805; found, 457.3783. The polymerization, hydrogenation, and characterization are described in the text.

Tricosa-1,22-dien-12-ylphosphonic acid (3-1b). Into a 2-neck round bottom flask 207 mg of **3-1a** was weighed. Then the flask was equipped with a stir bar, gas inlet adapter and septa. After flushing the flask with argon, 10 mL of dry dichloromethane was added via syringe followed by 0.6 mL (4.5 mmol,10 eq) bromotrimethylsilane added dropwise by syringe under a continuous flow of argon. After stirring with a constant flow of argon for 24 hours, the residual reactants were removed under vacuum prior to adding 20 mL of methanol (not anhydrous). The reaction was allowed to stir with a constant flow of argon for another 24 hours. Upon removal of residual methanol and trimethylsilyl species, the 182 mg of acid was obtained in quantitative yield (99%) without any purification necessary. ^{1}H NMR ($CDCl_3$): δ (ppm) 1.26-1.36 (br, 32H), 1.63-1.69 (m, 4H), 1.98-2.06 (q, 4H), 4.89-5.00 (m, 4H), 5.73-5.86 (m, 2H). ^{13}C NMR ($CDCl_3$): δ (ppm) 27.79 ($^{2}J_{CP}$ 9.3Hz), 28.39($^{3}J_{CP}$ 3.6Hz), 29.13, 29.33, 29.63, 29.67, 29.75, 29.91, 34.01, 36.24 ($^{1}J_{CP}$ 138Hz), 114.86, 138.59. ^{31}P NMR ($CDCl_3$, PPh_3 reference): δ = 40.39 Anal. Calcd for $C_{23}H_{45}O_3P$: C, 68.96; H 11.32; O, 11.98; P, 7.73

found: C, 68.75; H, 11.27. HRMS Calcd for $C_{23}H_{45}O_3P$ [$(M+H)^+$] (*m/z*), 401.3179; found, 401.3135

Deprotection of hydrogenated copolymer to yield acid copolymer (3-3b). Using the same method as the small molecule monomer, the polymer was deprotected. Following methanolysis, the polymer was precipitated from the sides of the flask with acetone. The precipitated polymer was rinsed through an osmotic filter with acetone and dried at 50˚C for 24 hours. Characterization of this polymer is described in the main text.

Results and Discussion

Key to success in this synthetic strategy is the preparation of a diene monomer with the functional group of interest (in this case, the phosphonic acid) symmetrically disposed within. This symmetry is carried into the repeat unit, thereby leading to unequivocal structural precision. Also key to success is devising suitable protection chemistry, sufficient to avoid poisoning of the rhuthenium catalysts yet capable of being completely removed after the polymer chemistry is done. This chemical balancing act is a major challenge, one that has been met in the case of these polymers.

Figure 3-1 provides a view of the protection and polymer chemistry used to synthesize the first precision ethylene/vinyl phosphonic acid copolymers reported to date. The monomer was synthesized using the alpha di-alkylation approach described previously,[182] incorporating the polymer repeat unit into the single symmetrical α,ω-diene **3-1a.** The ethyl groups present in the starting material served as protecting groups throughout monomer synthesis, purification, and metathesis polycondensation chemistry. Complete deprotection was first demonstrated on the monomer (prior to polymerization) as a model study of this chemistry. Quantitative deprotection was observed using the bromotrimethylsilane approach to form a silated ester in situ, which

was then cleaved in aqueous methanol to the free acid **3-1b** with no further purification necessary after removal of residual reactants.[183] There is no question that the protection group can be removed quantitatively using this approach (Figure 3-2).

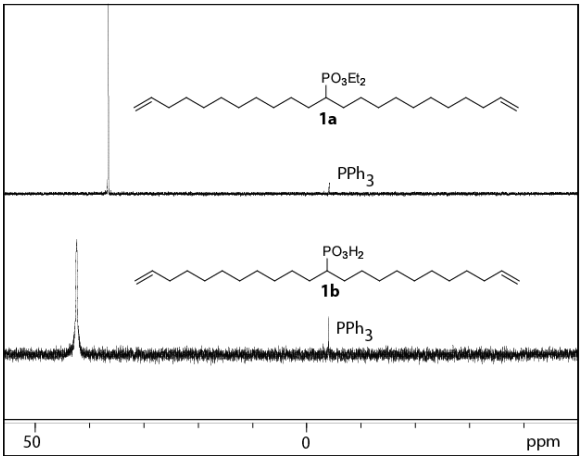

Figure 3-2. ^{31}P NMR spectrum of ester **3-1a** compared to acid **3-1b** in $CDCl_3$ referenced to PPh_3

Copolymer **3-2** was obtained after polymerization of protected monomer **3-1a** using Grubbs' first generation catalyst under the mild conditions of 50ºC and high vacuum. Exhaustive catalytic hydrogenation using Wilkinson's catalyst and 500 psi hydrogen gas yielded the linear ethylene-*co*-vinyl phosphonic acid diethyl ester copolymer **3-3a** with a phosphonic acid ester on every 21st PE backbone carbon. The relative M_n of 19,500 and PDI of 1.7 (determined by GPC versus polystyrene standards) indicate a successful strategy in forming the protected version of the target precision copolymer.

The ^{1}H, ^{13}C and ^{31}P solution NMR of **3-3a** (the protected version of the target copolymer) clearly demonstrate the pristine chemical microstructure (Figure 3-3). The ^{1}H NMR spectrum shown on top contains the methyl endgroup at 0.88 ppm; incident backbone olefin (d), γ methylene (c), and methyl groups (h) centered at a broad 1.25

ppm; α-protons (a) centered at 1.69 ppm; methine protons (f) at 1.96 ppm; and downfield-shifted ethyl ester methylene (g) broadened pentet resonance centered at 4.08 ppm.

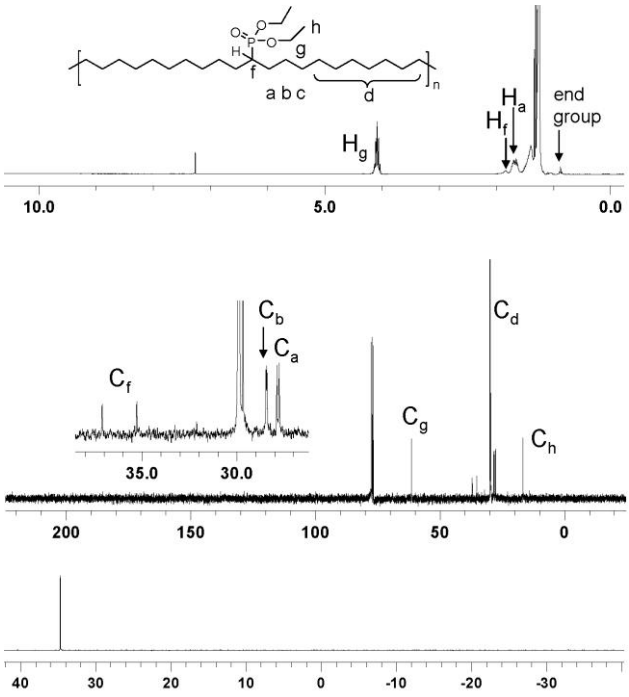

Figure 3-3. Solution NMR in $CDCl_3$ of ester copolymer 3-3a; from the top ^{1}H, ^{13}C, and ^{31}P spectra

The ^{1}H, ^{13}C and ^{31}P solution NMR of **3-3a** (the protected version of the target copolymer) clearly demonstrate the pristine chemical microstructure (Figure 3-3). The ^{1}H NMR spectrum shown on top contains the methyl endgroup at 0.88 ppm; incident backbone olefin (d), γ methylene (c), and methyl groups (h) centered at a broad 1.25 ppm; α-protons (a) centered at 1.69 ppm; methine protons (f) at 1.96 ppm; and downfield-shifted ethyl ester methylene (g) broadened pentet resonance centered at 4.08 ppm. Selected proton integration, specifically ester methylene and the methyl end group, are comparable to the GPC M_n measurement. In addition, the controlled precise

microstructure is directly transferred from the symmetrical monomer to the saturated copolymer repeat unit with seven distinct ^{13}C NMR resonances additionally showing coupling to ^{31}P. The ^{13}C NMR spectrum of **3-3a**, shown in the middle, contains major resonances include the ethyl group CH_2 doublet at 62.45 ppm, $^{2}J_{CP}$ 6.9 Hz (g), CH_3 doublet at 16.73 ppm, $^{3}J_{CP}$ 5.9 Hz (h), methine (f), α- (a), β- (b), and γ- (c) methylenes, and the remaining unresolved backbone carbons (centered at 29.84 ppm). Coupling between phosphorous and the methine (doublet at 36.20 ppm, $^{1}J_{CP}$ 137 Hz), α-methylene (doublet at 27.83 ppm, $^{2}J_{CP}$ 9.2 Hz), and β-methylene (doublet at 28.44 ppm, $^{3}J_{CP}$ 3.5 Hz) carbon atoms splits the resonances into doublets as shown in the inset, while the γ-methylene remains uncoupled on the shoulder of the unresolved backbone carbons at 29.68 ppm. Additionally, the 100% naturally abundant ester ^{31}P is shown as a sharp singlet at 34.81 ppm in the bottom spectrum.

Deprotection is the final step in the synthesis scheme, and though such chemistry would appear to be a facile part of the general scheme, it can be quite challenging. In this case, deprotection using the conditions applied to the monomer (as a model study) is highly effective: as noted below, deprotection of copolymer **3-3a** is quantitative to yield the precision phosphonic acid copolymer **3-3b**.

Copolymer **3-3b** is an extremely tough material, with interchain interaction between the precisely placed phosphonic acid groups apparently being highly effective. It also is quite insoluble in a variety of typical polar organic solvents and solvent mixtures. Consequently, solid state proton, carbon, and phosphorus NMR was used to firmly delineate the repeat unit structure (Figure 3-4). The ^{1}H MAS NMR spectrum of **3-3b** exhibits two peaks at 10.2 ppm and 1.4 ppm corresponding to acidic protons and

aliphatic protons respectively. Similarly to PVPA, the latter resonance is attributed to the polymer backbone while the peak at 10.2 ppm clearly reflects partially immobilized hydrogen-bonded protons of the $PO(OH)_2$ unit.[179]

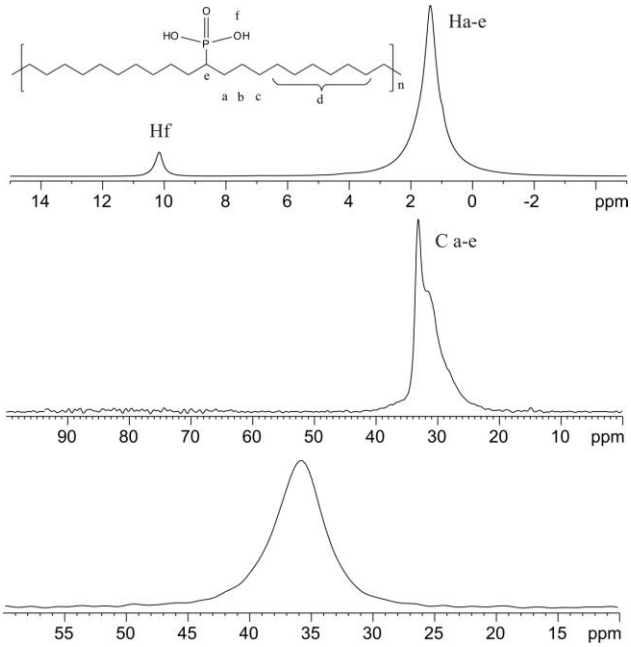

Figure 3-4. Solid-state NMR of the phosphonic acid copolymer **3-3b**; from the top ^{1}H, ^{13}C, and ^{31}P spectra

Notably, the corresponding ^{13}C-CP MAS NMR spectrum is rather complex. The sharp peak at 33.2 ppm, corresponds to the all-trans conformation in the crystalline regions of PE,[184] which is also present in the corresponding precise polymer with CH_3 groups on every 21st carbon.[185] Broadened resonances around 37 ppm, 31.7 ppm and 28.8 ppm, are assigned to the CH group, and the CH_2 groups of the polymer backbone adjacent to the phosphonic acid group, respectively. Moreover the CH_2-units in the non-crystalline regions of the system will give rise to a broad peak around 29-32 ppm.[184,185] Recently, the nature of defects in such precisely defined polyolefins and their dynamics was elucidated by ^{2}H- ^{13}C-solid state NMR.[185] In the analogous system with CD_3 instead of $PO(OH)_2$ groups, the chain defects are highly mobile close to the melting point.

Whereas in the systems studied here, hydrogen bonding apparently precludes such chain mobility. No peak was found at about 65 ppm (OCH_2 unit), hence indicating successful deprotection of the former ester group. This is further supported by the ^{31}P MAS NMR spectrum that shows *one* fairly sharp resonance at 36.0 ppm (FWHH = 887 Hz) typically found for phosphonic acid containing polymers.[179] In addition, no indication of anhydride formation is found.[4]

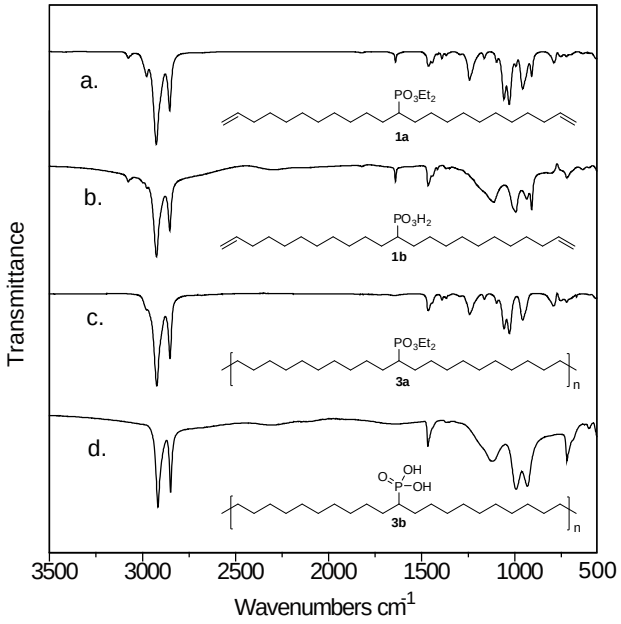

Figure 3-5. Infrared spectra of a) protected monomer **3-1a** b) deprotected monomer **3-1b** c) protected copolymer **3-3a** and d) deprotected copolymer **3-3b**. Samples a, b, and c prepared by $CHCl_3$ solution cast onto KBr discs; spectrum d obtained via ATR

Quantitative deprotection was also examined using IR spectroscopy (Figure 3-5). Ester monomer **3-1a** reveals a characteristic ester P=O stretching vibration at 1243cm^{-1} (Figure 3-5a) that shifts and broadens to lower frequency at 1143cm^{-1} in the corresponding acid compound **3-1b** (Figure 3-5b). Monomer **3-1a** also shows further P-O-C ester absorbances at 957cm^{-1}, 1029cm^{-1}, and 1163cm^{-1}, while the acid **3-1b** exhibits the P-OH absorbances of 939cm^{-1} and 1004cm^{-1}. The additional P-O-H

absorbance at ~3000cm^{-1} is more apparent as a broadening of the methylene stretching vibrations at 2998cm^{-1} and 2800cm^{-1}. Upon polymerization and hydrogenation to yield ester copolymer **3-3a** (Figure 3-5c), the absorbances attributed to ester functionality match those in the ester monomer **3-1a,** as expected. Notably after hydrolysis, peaks due to the former ester functionality are removed and replaced by absorbances characteristic of the acid (Figure 3-5d). In addition the olefin out-of-plane C-H wag at 967cm^{-1} is no longer present indicating the backbone hydrogenation was complete. These results confirm complete deprotection evidenced by solid-state NMR and support the overall synthesis of precisely defined poly(ethylene-co-vinylphosphonic acid) containing a phosphonic acid on every 21st carbon.

Conclusions

Solid-state NMR and FT-IR spectroscopic techniques clearly demonstrate the successful synthesis of polyethylene possessing precisely spaced phosphonic acid groups and support the unprecedented structural control in acid-containing polylolefins by the metathesis polycondensation method. All esters were hydrolyzed freeing the phosphonic acid group to participate in hydrogen bonding. The solubility was thus reduced and precluded typical solution characterization.

However several interesting outcomes have surfaced including: 1) the test reactions on ester monomer quantitatively yielded acid monomer, 2) the subsequent ester monomer polymerization, hydrogenation, and deprotection led to isolation of a precision polymer structure analogous to previous work on precise EAA copolymers, 3) the strong interchain interactions upon hydrolysis led to isolation of an insoluble polymer, and 4) the solid-state NMR spectra and FT-IR comparison on the insoluble polymer supports quantitative ester hydrolysis and proves polymer deprotection. Prior

work on precision EAA copolymers containing a carboxylic acid on every 21st carbon showed this level of structural control leads to a new morphology.[179] Due to the interplay of precise primary structure and hydrogen bonded chain immobilization indicated by solid-state NMR, the next chapters will describe these investigations.

CHAPTER 4
MORE COMPLEX PHOSPHONIC ACIDS

Introduction*

The wide range of chemical and physical properties make polyolefins, specifically polyethylene, the highest volume commercial synthetic polymer produced today[186] and the reason to investigate introducing even more highly polar groups than the sulfonic esters and single phosphonic acid presented thus far. The number of commercial applications can be increased by varying the architecture and functionality, thereby enhancing the chemical and physical properties of the otherwise unreactive hydrocarbon backbone.[187-190] Functionalization of polyolefins is typically achieved using polymerization techniques having common pathways of comonomer incorporation or post-polymerization modifications.[188,191-193] There are advantages and disadvantages to each approach. Although polymer composition is easily tunable using comonomer incorporation, monomer reactivity and catalyst activity represent possible challenges. Modifying an existing polymer may result in chain breakage, crosslinking, and unknown amounts of functionality incorporation.

It has been shown throughout the first chapters that polymers containing exact placement of functional groups can be obtained using the step-growth metathesis polycondensation technique, ADMET.[194-196] This approach has been utilized to synthesize strictly linear and otherwise challenging polyethylene (PE) copolymers. After incorporating several traditional ethylene/vinyl repeat units into a single symmetrical α,ω-diene monomer, polymerization via metathesis polycondensation followed by

* Reproduced in part with permission from: Opper, K.L..; Markova, D.M.; Klapper, M.; Muellen, K.; Wagener, K.B. Macromolecules **2010**, *43*, 3690-3698. Copyright 2009 American Chemical Society

hydrogenation yields a precisely functionalized PE copolymer. This technique not only allows for the precise and tunable incorporation of functional groups but also results in unique polymer structures and morphologies.[197,198]

To further study PE crystallization in the presence of interactive hydrogen bonding groups,[199-201] a family of polyethylenes functionalized with phosphonic acids has been synthesized. Phosphonic acid-containing polymers already have multiple applications as membranes for ion transport, exchange, or barriers,[202-206] as well as biomaterials for dental cements, bone integration or cell adhesion.[207-209] Accordingly, creating a well-defined family of precisely functionalized phosphonic acid-containing polymer architectures, discussed herein, potentially increases the range of applications for such polymers,[210] as recently it was shown that order and crystallinity can dramatically improve the proton mobility by generating defined proton pathways.[211] This study comprises a systematic investigation relating primary and secondary structure of these polymers in the presence of resilient, highly-interactive phosphonic acid groups.

Experimental

Methods

All ^{1}H (300 MHz) and ^{13}C (75 MHz) solution NMR spectra were recorded on a Varian Associates Mercury 300 spectrometer. Chemical shifts for ^{1}H and ^{13}C NMR were referenced to residual signals from $CDCl_3$ (^{1}H = 7.27 ppm and ^{13}C= 77.23 ppm). Thin layer chromatography (TLC) was performed on EMD silica gel-coated (250 μm thickness) glass plates. Developed TLC plates were stained with iodine adsorbed on silica to produce a visible signature. Reaction progress and relative purity of crude products were monitored by TLC and ^{1}H NMR.

Molecular weights and molecular weight distributions were determined by gel permeation chromatography (GPC) using a Waters Associates GPCV2000 liquid chromatography system equipped with a differential refractive index detector (DRI) and an autosampler. These analyses were performed at 40°C using two Waters Styragel HR-5E columns (10 microns PD, 7.8 mm ID, 300 mm length) with HPLC grade THF as the mobile phase at a flow rate of 1.0 mL/minute. Injections were made at 0.05-0.07% w/v sample concentration using a 220.5 µL injection volume. Retention times were calibrated versus narrow molecular weight polystyrene standards (Polymer Laboratories; Amherst, MA).

Infrared spectra were obtained on a Perkin-Elmer Spectrum One FT-IR equipped with a $LiTaO_3$ detector. Samples were dissolved in chloroform and cast on a KBr disc by slow solvent evaporation. Due to rather poor solubility, the spectrum of the deprotected polymer was obtained by means of an ATR accessory.

Thermogravimetric analysis (TGA) was performed using a TA Instruments Q5000 using high resolution dynamic resolution under nitrogen atmosphere. Differential scanning calorimetry (DSC) was performed using a TA Instruments Q1000 at a heating rate of 10ºC/min under nitrogen purge. Temperature calibrations were achieved using indium and freshly distilled n-octane while the enthalpy calibration was achieved using indium. All samples were prepared in hermetically sealed pans (4-7 mg/sample) and were run using an empty pan as a reference.

Materials

All materials were purchased from Aldrich and used as received, unless noted otherwise. Tetrahydrofuran (THF) was obtained from an MBraun solvent purification system. Lithium diisopropyl amide (LDA) was prepared prior to monomer synthesis.

Grubbs' first generation ruthenium catalyst, bis(tricyclohexylphosphine)benzylidine ruthenium(IV)dichloride, was a generous gift from Materia, Inc. Wilkinson's rhodium catalyst, $RhCl(PPh_3)_3$, was purchased from Strem Chemical.

Synthesis

General synthesis of monomer containing single directly attached phosphonic acid ester

The synthesis was previously reported with the exception of appropriate alkenyl halide synthon choice for each monomer.[212] In a flame dried 3-necked flask equipped with a magnetic stir bar, 2.2 mL (15 mmol, 1 eq) of diethyl methane phosphonate and 3.3 mL (15 mmol, 1 eq) of 11-bromoundecene were stirred in15 mL of dry THF under argon. After bringing the solution to -78°C, 0.9 eq of LDA was added dropwise over 30 minutes and stirred for 30 additional minutes. The solution was then warmed to 0°C and stirred for 1 to 2 hours until mono-alkylation was observed and alkenyl bromide disappeared by TLC. After bringing the solution back to -78°C, 0.9 eq of 11-bromoundecene was added slowly and allowed to dissolve. With the solution at -78°C, 0.9 eq of LDA was added dropwise over 30 minutes and stirred for 30 additional minutes. The solution was then warmed to 0°C and stirred for 2 to 3 hours until the conversion from mono-alkylation to diene product was no longer observed. The reaction was quenched by adding ice cold water. This mixture was then extracted (3 x 50 mL) with diethyl ether, dried over magnesium sulfate and concentrated to a colorless oil. Column chromatography, using 2:1 ethyl acetate:hexane as the eluent, afforded dialkylation product **1** in 43% recovered yield.

Diethyl undeca-1,10-dien-6-ylphosphonate (4-1). Column chromatography, using 3:1 ethyl acetate:hexane as the eluent, afforded dialkylation product **4-1** in 56%

recovered yield. ^{1}H NMR ($CDCl_3$): δ (ppm) 1.30 (t, 6H), 1.49 (br, 6H), 1.64-1.75 (br, 4H), 2.03 (q, 4H), 4.07 (p, 4H), 4.92-5.03 (m, 4H), 5.72-5.85 (m, 2H). ^{13}C NMR ($CDCl_3$): δ (ppm) 16.74 ($^{3}J_{CP}$ 5.8Hz), 27.08 ($^{2}J_{CP}$ 9.1Hz), 27.97, 28.02, 33.98, 36.10 ($^{1}J_{CP}$ 138Hz), 61.51 ($^{2}J_{CP}$ 6.9Hz), 114.91, 138.65. ^{31}P NMR ($CDCl_3$, PPh_3 reference): δ (ppm) 33.99; Anal. Calcd for $C_{15}H_{29}O_3P$: C, 62.48; H 10.14; O, 16.65; P, 10.74 Found: C, 61.98; H, 10.36. HRMS Calcd for $C_{15}H_{29}O_3P$ [$(M+H)^+$] (*m/z*), 289.1927; found, 289.1942

Diethyl heptadeca-1,16-dien-9-ylphosphonate (4-2). Column chromatography, using 5:2 ethyl acetate:hexane as the eluent, afforded dialkylation product **4-2** in 50% recovered yield. ^{1}H NMR ($CDCl_3$): δ (ppm) 1.30 (t, 6H), 1.39 (br, 21H), 1.62-1.69 (br, 4H), 2.02 (q, 4H), 4.08 (p, 4H), 4.90-5.00 (m, 4H), 5.73-5.86 (m, 2H). ^{13}C NMR ($CDCl_3$): δ (ppm) 16.74 ($^{3}J_{CP}$ 5.9Hz), 27.77 ($^{2}J_{CP}$ 9.3Hz), 28.43 ($^{3}J_{CP}$ 5.9Hz), 29.08, 29.13, 29.77, 33.98, 36.20 ($^{1}J_{CP}$ 138Hz), 114.39, 139.31. ^{31}P NMR ($CDCl_3$, PPh_3 reference): δ (ppm) 34.56; Anal. Calcd for $C_{21}H_{41}O_3P$: C, 67.71; H 11.09; O, 12.88; P, 8.31 Found: C, 67.75; H, 11.20. HRMS Calcd for $C_{21}H_{41}O_3P$ [$(M+H)^+$] (*m/z*), 373.2866; found, 373.2903

Diethyl tricosa-1,22-dien-12-ylphosphonate (4-3). Column chromatography, using 2:1 ethyl acetate:hexane as the eluent, afforded dialkylation product **4-3** in 43% recovered yield. ^{1}H NMR ($CDCl_3$): δ (ppm) 1.26-1.36 (br, 38H), 1.63-1.69 (m, 4H), 1.98-2.06 (q, 4H), 4.07 (p, 4H), 4.89-5.00 (m, 4H), 5.73-5.86 (m, 2H). ^{13}C NMR ($CDCl_3$): δ (ppm) 16.72 ($^{3}J_{CP}$ 5.9Hz), 27.79 ($^{2}J_{CP}$ 9.3Hz), 28.39($^{3}J_{CP}$ 3.6Hz), 29.13, 29.33, 29.63, 29.67, 29.75, 29.91, 34.01, 36.14 ($^{1}J_{CP}$ 138Hz), 61.46 ($^{2}J_{CP}$ 6.8Hz), 114.86, 138.59. ^{31}P NMR ($CDCl_3$, PPh_3 reference): δ (ppm) 34.70; Anal. Calcd for $C_{27}H_{53}O_3P$: C, 71.01; H 11.70; O, 10.51; P, 6.78 Found: C, 70.96; H, 11.72. HRMS Calcd for $C_{27}H_{53}O_3P$ [$(M+H)^+$] (*m/z*), 457.3805; found, 457.3783

General synthesis of monomer containing geminal substituted phosphonic acid esters

Again the appropriate alkenyl halide synthon was used for each monomer. In a flame dried 3-necked flask equipped with a magnetic stir bar, 75 mL of DMF was stirred at 0ºC under a constant argon flow. Using a powder funnel under continued constant argon flow, 2.4g of 60% NaH powder (100 mmol, 5 eq) was added to the flask. Upon resealing the flask, 5 mL (20.2 mmol, 1 eq) tetraethyl methylenediphosphonate was added dropwise over 30 minutes. After an additional hour stirring at 0ºC, 9.7mL (44.4mmol, 2.2 eq) of 11-bromoundecene was added dropwise over 30 minutes. The reaction was allowed to warm to room temperature over 4 hours and then allowed to stir at room temperature overnight. Reaction progress was monitored by TLC noting the disappearance of starting materials. The reaction was quenched at 0ºC by first diluting the mixture with hexane 75 mL and then adding 750 mL of deionized water. The reaction mixture was then extracted (3 x 75 mL) hexane. After washing the hexane with water, the crude mixture was concentrated to a light yellow oil.

Tetraethyl heptadeca-1,16-diene-9,9-diyldiphosphonate (4-4). Column chromatography, using 20:1 ethyl acetate:methanol as the eluent, afforded dialkylation product **4-4** in 24% recovered yield. ^{1}H NMR ($CDCl_3$): δ (ppm) 1.32 (br, 24H), 1.50 (br, 4H), 1.88 (m, 4H), 2.04 (q, 4H), 4.17 (p, 8H), 4.92-5.02 (m, 4H), 5.75-5.88 (m, 2H). ^{13}C NMR ($CDCl_3$): δ (ppm) 16.73 (t), 24.42 (t), 29.07, 29.12, 30.29 (t), 34.00 45.99 (t, $^{1}J_{CP}$ 123Hz), 62.55(t), 114.41, 139.39. ^{31}P NMR ($CDCl_3$, PPh_3 reference): δ (ppm) 26.72; Anal. Calcd for $C_{25}H_{50}O_6P_2$: C, 59.04; H 9.91; O, 18.87; P, 12.18 Found: C, 59.03; H, 9.92. HRMS Calcd for $C_{25}H_{50}O_6P_2$ [$(M+H)^+$] (*m/z*), 509.3102; found, 509.3116

Tetraethyl tricosa-1,22-diene-12,12-diyldiphosphonate (4-5). Column chromatography, using 50:1 ethyl acetate:methanol as the eluent, afforded dialkylation product **4-5** in 28% recovered yield. ^{1}H NMR ($CDCl_3$): δ (ppm) 1.27(br, 40H), 1.88 (m, 4H), 2.05 (q, 4H), 4.16 (p, 8H), 4.91-5.02 (m, 4H), 5.74-5.88 (m, 2H). ^{13}C NMR ($CDCl_3$): δ = 16.68 (t), 24.40 (t), 29.14, 29.34, 29.53, 29.65, 29.75, 30.23 (t), 30.57, 45.96 (t, $^{1}J_{CP}$ 123Hz), 62.46 (t), 114.28, 139.41. ^{31}P NMR ($CDCl_3$, PPh_3 reference): δ (ppm) 26.74; Anal. Calcd for $C_{31}H_{62}O_6P_2$: C, 62.81; H 10.54; O, 16.19; P, 10.45 Found: C, 62.21; H, 10.67. HRMS Calcd for $C_{31}H_{62}O_6P_2$ [$(M+H)^+$] (*m/z*), 593.4094; found, 593.4049

General synthesis of monomer containing benzyl substituted phosphonic acid ester

The phosphonic acid ester was prepared in 3 steps detailed from alkylation of alcohol with the appropriate alkenyl halide synthon, to bromide, to phosphonic acid ester.

3,5-Bis(10-undecenyloxy)phenyl)benzyl alcohol. In a 200 mL round bottom flask equipped with a magnetic stir bar, 2.8g (20 mmol, 1 eq) of 3,5-dihydroxybenzyl alcohol was dissolved in 80 mL acetonitrile. To this mixture, 6.91g (50 mmol, 2.5 eq) of K_2CO_3 and 0.83g (5mmol, 0.25 mmol) KI were added. After partial dissolution due to insolubility at room temperature, 7.72 mL (46 mmol, 2.3 eq) of 11-bromoundecene was then added and a reflux condenser attached. After refluxing at 100ºC for 24 hrs under argon, the reaction was allowed to cool to room temperature. After filtering residual K_2CO_3 and KI and adding deionized water, the mixture was extracted with (3 x 50 mL) ethyl acetate. Upon concentrating the crude mixture to an oil, the crude product was passed through a plug of silica. Using 1:1 hexane:dichloromethane, excess alkenyl

bromide was removed. Switching to 1:1 hexane:ethyl acetate led to isolation of product concentrated as a yellowish oil in 82% yield. ^{1}H NMR ($CDCl_3$): δ (ppm) 1.27 (br, 24H), 1.68 (m, 4H), 1.95 (m, 4H), 3.83 (m, 4H), 4.51 (d, 2H), 5.02-5.15 (m, 4H), 5.82-5.97 (m, 2H), 6.46 (m, 1H), 6.53 (d, 2H). ^{13}C NMR ($CDCl_3$): δ (ppm) 25.97, 29.27, 33.77, 65.31, 68.02, 100.54, 104.94, 114.14, 139.17, 143.16, 160.50

(3,5-Bis(pent-4-enyloxy)phenyl) benzyl alcohol. ^{1}H NMR ($CDCl_3$): δ (ppm) 1.75-1.95 (m, 8H), 2.27 (q, 4H), 3.98 (m, 4H), 4.64 (d, 2H), 5.01-5.13 (m, 4H), 5.80-5.96 (m, 2H), 6.46 (m, 1H), 6.53 (d, 2H). ^{13}C NMR ($CDCl_3$): δ (ppm) 28.44, 30.11, 65.4, 67.27, 100.65, 105.15, 115.21, 137.80, 143.27, 160.46

(3,5-Bis(10-undecenyloxy)phenyl) benzyl bromide. In a 200 mL round bottom flask equipped with a magnetic stir bar, the benzyl alcohol derivative obtained was dissolved in 40 mL THF. Under a blanket of argon, 1.5 eq CBr_4 was added. Upon cooling to 0ºC, 1.5 eq triphenyl phosphine was added. After warming the mixture to room temperature, progress was monitored by TLC. After stirring overnight the reaction was quenched by precipitating the triphenyl phosphine oxides in pentane, filtering off the solids and concentrating the remaining solution. Purification via column chromatography using a 1:1 hexane:dichloromethane solvent system allowed for product isolation in 67% yield as a yellowish oil. ^{1}H NMR ($CDCl_3$): δ (ppm) 1.35 (br, 24H), 1.74 (m, 4H), 2.03 (m, 4H), 3.90 (br, 4H), 4.38 (s, 2H), 5.01-5.13 (m, 4H), 5.80-5.96 (m, 2H), 6.36 (m, 1H), 6.51 (d, 2H). ^{13}C NMR ($CDCl_3$): δ (ppm) 25.99, 29.14, 33.75, 68.10, 101.36, 107.39, 114.11, 139.20, 139.45, 160.37

(3,5-Bis(pent-4-enyloxy)phenyl) benzyl bromide. ^{1}H NMR ($CDCl_3$): δ (ppm) 1.46 (br, 8H), 1.80 (p, 4H), 2.08 (m, 4H), 3.96 (t, 4H), 4.43 (s, 2H), 4.94-5.08 (m, 4H),

5.77-5.93 (m, 2H), 6.40 (m, 1H), 6.54 (d, 2H). ^{13}C NMR ($CDCl_3$): δ (ppm) 28.27, 30.11, 33.70, 67.16, 101.42, 107.38, 115.20, 137.67, 139.54, 160.27

Diethyl 3,5-bis(10-undecenyloxy)phenyl) benzyl phosphonate (4-7). In 50 mL round bottom flask equipped with a magnetic stir bar, the benzyl bromide was added with 1.3 eq of triethyl phosphite. After refluxing the solution for 72 hours, the residual triethyl phosphite was removed under vacuum and the phosphonate was obtained in quantitative yield with no further purification necessary. ^{1}H NMR ($CDCl_3$): δ (ppm) 1.26 (br, 30H), 1.67 (p, 4H), 1.98 (m, 4H), 2.92 (d, 2H), 3.82 (t, 4H), 3.95 (m, 4H), 4.94-5.06 (m, 4H), 5.76-5.92 (m, 2H), 6.38 (q, 1H), 6.45-6.47 (t, 2H). ^{13}C NMR ($CDCl_3$): δ (ppm) 16.79, 26.42, 29.73, 33.87, 33.99 ($^{1}J_{CP}$ = 137 Hz), 34.15, 62.53, 68.47, 100.51, 108.80, 114.46, 133.79, 139.59, 160.72. ^{31}P NMR ($CDCl_3$, PPh_3 reference): δ (ppm) 25.49; Anal. Calcd for $C_{33}H_{57}O_3P$: C, 70.18; H 10.17; O, 14.16; P, 5.48 Found: C, 68.06; H, 9.93. HRMS Calcd for $C_{33}H_{57}O_3P$ [$(M+H)^+$] (*m/z*), 565.4022; found, 565.4022

Diethyl 3,5-bis(oct-7-enyloxy)benzylphosphonate (4-6) ^{1}H NMR ($CDCl_3$): δ (ppm) 1.26-1.31 (t, 6H), 1.42 (br, 12H), 1.78 (m, 4H), 2.06 (m, 4H), 3.05-3.14 (d, 2H), 3.91-3.97 (t, 4H), 3.99-4.11 (m, 4H), 4.94-5.06 (m, 4H), 5.76-5.92 (m, 2H), 6.35-6.37 (q, 1H), 6.45-6.47 (t, 2H). ^{13}C NMR ($CDCl_3$): δ (ppm) 16.55, 26.03, 28.97, 29.34, 33.84, 34.16 ($^{1}J_{CP}$ = 137 Hz), 62.53, 68.07, 100.23, 108.41, 114.43, 133.59, 139.11, 160.38; ^{31}P NMR ($CDCl_3$, PPh_3 reference): δ (ppm) 25.78; Anal. Calcd for $C_{27}H_{45}O_3P$: C, 67.47; H 9.44; O, 16.64; P, 6.44 Found: C, 66.26; H, 9.51. HRMS Calcd for $C_{27}H_{45}O_3P$ [$(M+H)^+$] (*m/z*), 481.3077; found, 481.3097

General homopolymerization conditions

In a flame dried 50 mL round bottom flask, an exact amount of monomer was weighed. Using a 400:1 monomer:catalyst ratio (0.25 mol%), Grubbs' first generation catalyst was added and mixed into the monomer while under a blanket of argon. A magnetic stir bar was placed into the mixture while a schlenk adapter was fitted to the round bottom. After sealing the flask under argon it was moved to a high vacuum line. The mixture was stirred and slowly exposed to vacuum over an hour at room temperature. After stirring for an hour at room temperature under eventual high vacuum (10^{-3} torr), the flask was lowered into a prewarmed 50ºC oil bath for an appropriate number of days allowing removal of ethylene bubbling through viscous polymer. Polymers were quenched by dissolution of polymer in an 1:10 ethyl vinyl ether:toluene solution under argon. Upon precipitation into an appropriate solvent, the polymers were isolated.

Polymerization of diethyl undeca-1,10-dien-6-ylphosphonate (4-8). After 5 days of polymerization of 0.548g monomer **4-1** with 400:1 Grubbs first generation catalyst, unsaturated polymer **4-8** was obtained. ^{1}H NMR ($CDCl_3$): δ (ppm) 1.30 (t, 6H), 1.44 (br, 4H), 1.64-1.69 (br, 4H), 1.96 (br, 4H), 4.07 (p, 4H), 5.38 (m, 2H). ^{13}C NMR ($CDCl_3$): δ (ppm) 16.75 ($^{3}J_{CP}$ 5.7Hz), 27.08 ($^{2}J_{CP}$ 9.1Hz), 27.88, 28.37, 29.95, 32.90, 36.10 ($^{1}J_{CP}$ 137Hz), 61.51 ($^{2}J_{CP}$ 6.8Hz), 129.89, 130.37. ^{31}P NMR ($CDCl_3$, PPh_3 reference): δ (ppm) 34.42. GPC data (THF vs. polystyrene standards): M_w = 14100 g/mol; P.D.I. (M_w/M_n) = 1.75

Polymerization of diethyl heptadeca-1,16-dien-9-ylphosphonate (4-9). After 6 days of polymerization of 0.973g monomer **4-2** with 400:1 Grubbs first generation

catalyst, unsaturated polymer **4-9** was obtained. ^{1}H NMR ($CDCl_3$): δ (ppm) 1.27-1.39 (br, 23H), 1.65 (br, 4H), 1.95 (br, 4H), 4.06 (p, 4H), 5.37 (m, 2H). ^{13}C NMR ($CDCl_3$): δ (ppm) 16.74 ($^{3}J_{CP}$ 5.7Hz), 27.84 ($^{2}J_{CP}$ 9.1Hz), 27.88, 28.46, 29.25, 29.87, 32.81, 36.10 ($^{1}J_{CP}$ 137Hz), 61.49 ($^{2}J_{CP}$ 6.8Hz), 130.50, 130.05. ^{31}P NMR ($CDCl_3$, PPh_3 reference): δ (ppm) 34.52. GPC data (THF vs. polystyrene standards): M_w = 33800 g/mol; P.D.I. (M_w/M_n) = 1.68

Polymerization of diethyl tricosa-1,22-dien-12-ylphosphonate (4-10). After 6 days of polymerization of 0.860g monomer **4-3** with 400:1 Grubbs first generation catalyst, unsaturated polymer **4-10** was obtained. ^{1}H NMR ($CDCl_3$): δ (ppm) 1.27-1.40 (br, 35H), 1.67-1.72 (m, 4H), 1.97 (br, 4H), 4.09 (m, 4H), 5.38 (m, 2H). ^{13}C NMR ($CDCl_3$): δ (ppm) 16.73 ($^{3}J_{CP}$ 5.8Hz), 27.80 ($^{2}J_{CP}$ 9.3Hz), 28.44($^{3}J_{CP}$ 3.6Hz), 29.43, 29.56, 29.68, 29.82, 29.95, 32.84, 36.20 ($^{1}J_{CP}$ 136Hz), 61.46 ($^{2}J_{CP}$ 6.9Hz), 130.07, 130.53. ^{31}P NMR ($CDCl_3$, PPh_3 reference): δ (ppm) 34.85. GPC data (THF vs. polystyrene standards): M_w = 28700 g/mol; P.D.I. (M_w/M_n) = 1.82

Polymerization of tetraethyl heptadeca-1,16-diene-9,9-diyldiphosphonate (4-11). After 6 days of polymerization of 0.880g monomer **4-4** with 400:1 Grubbs first generation catalyst, an additional portion of catalyst was added. After the polymerization was quenched after an additional 6 days, unsaturated polymer **4-11** was obtained. ^{1}H NMR ($CDCl_3$): δ (ppm) 1.32 (br, 24H), 1.48 (br, 4H), 1.84-1.95 (br, 8H), 4.17 (p, 8H), 5.38 (m, 2H). ^{13}C NMR ($CDCl_3$): δ (ppm) 16.72 (t), 24.43 (t), 27.46, 29.22, 29.32, 29.95, 30.53, 32.85, 46.00 (t, $^{1}J_{CP}$ 123Hz), 62.52 (t), 130.05, 130.52. ^{31}P NMR ($CDCl_3$, PPh_3 reference): δ (ppm) 26.67. GPC data (THF vs. polystyrene standards): M_w = 10500 g/mol; P.D.I. (M_w/M_n) = 1.78

Polymerization of tetraethyl tricosa-1,22-diene-12,12-diyldiphosphonate (4-12). After 5 days of polymerization of 1.00g monomer **4-5** with 400:1 Grubbs first generation catalyst, unsaturated polymer **4-12** was obtained. ^{1}H NMR ($CDCl_3$): δ (ppm) 1.27-1.34(br, 36H), 1.48 (br, 4H), 1.94 (br, 8H), 4.16 (p, 8H), 5.38 (m, 2H). ^{13}C NMR ($CDCl_3$): δ (ppm) 16.68 (t), 24.43 (t), 27.46, 29.48, 29.59, 29.65, 29.75, 30.28 (t), 30.61, 32.86, 45.97 (t, $^{1}J_{CP}$ 123Hz), 62.46 (t), 130.06, 130.51. ^{31}P NMR ($CDCl_3$, PPh_3 reference): δ (ppm) 30.75. GPC data (THF vs. polystyrene standards): M_w = 28900 g/mol; P.D.I. (M_w/M_n) = 1.68

Polymerization of diethyl 3,5-bis(oct-7-enyloxy)benzylphosphonate (4-13). After 5 days of polymerization of 1.02g monomer **6** with 400:1 Grubbs first generation catalyst, unsaturated polymer **4-13** was obtained. ^{1}H NMR ($CDCl_3$): δ (ppm) 1.26-1.31 (t, 6H), 1.28 (br, 12H), 1.78 (m, 4H), 2.03 (br, 4H), 3.08 (d, 2H), 3.93 (t, 4H), 3.99-4.11 (m, 4H), 5.42 (m, 2H), 6.35-6.37 (m, 1H), 6.45-6.47 (t, 2H). ^{13}C NMR ($CDCl_3$): δ (ppm) 16.40, 25.95, 27.18, 28.94, 29.09, 29.25, 29.57, 29.70, 32.53, 34.03 ($^{1}J_{CP}$ = 138 Hz), 62.10, 67.99, 100.10, 108.30, 129.84, 130.31, 133.42, 160.25. ^{31}P NMR ($CDCl_3$, PPh_3 reference): δ (ppm) 25.79. GPC data (THF vs. polystyrene standards): M_w = 14700 g/mol; P.D.I. (M_w/M_n) = 2.30

Polymerization of diethyl 3,5-bis(10-undecenyloxy)phenyl) benzyl phosphonate (4-14). After 5 days of polymerization of 0.550g monomer **4-7** with 400:1 Grubbs first generation catalyst, unsaturated polymer **4-14** was obtained. ^{1}H NMR ($CDCl_3$): δ (ppm) 1.24-1.43 (br, 30H), 1.75 (m, 4H), 1.98 (m, 4H), 2.92 (d, 2H), 3.91 (br, 4H), 4.03 (m, 4H), 5.39 (m, 2H), 6.34 (br, 1H), 6.44 (br, 2H). ^{13}C NMR ($CDCl_3$): δ (ppm) 16.79, 26.42, 29.73, 32.27, 34.15 ($^{1}J_{CP}$ = 137 Hz), 62.53, 68.47, 100.51, 108.80,

114.46, 133.79, 139.59, 160.72. ^{31}P NMR ($CDCl_3$, PPh_3 reference): δ (ppm) 25.93. GPC data (THF vs. polystyrene standards): M_w = 15000 g/mol; P.D.I. (M_w/M_n) = 2.07

General hydrogenation conditions

A solution of unsaturated polymer was dissolved in toluene and degassed by bubbling a nitrogen purge through the stirred solution for an hour. Wilkinson's catalyst [$RhCl(PPh_3)_3$] was added to the solution along with a magnetic stir bar, and the glass sleeve was sealed in a Parr reactor equipped with a pressure gauge. The reactor was filled to 700 psi hydrogen gas and purge three times while stirring, filled to 700 psi hydrogen, and stirred for an appropriate number of days. After degassing the solution, the crude solution was isolated, precipitated into an appropriate solvent.

Hydrogenation of polymerized diethyl undeca-1,10-dien-6-ylphosphonate (4-15). After 5 days saturated polymer **4-15** was obtained. ^{1}H NMR ($CDCl_3$): δ (ppm) 1.26-1.39 (br, 19H), 1.64-1.69 (br, 4H), 4.07 (m, 4H). ^{13}C NMR ($CDCl_3$): δ (ppm) 16.70 ($^3J_{CP}$ 5.7Hz), 27.84 ($^2J_{CP}$ 9.1Hz), 28.54, 29.72, 30.00, 36.10 ($^1J_{CP}$ 137Hz), 61.55 ($^2J_{CP}$ 6.8Hz). ^{31}P NMR ($CDCl_3$, PPh_3 reference): δ (ppm) 34.76. GPC data (THF vs. polystyrene standards): M_w = 17100 g/mol; P.D.I. (M_w/M_n) = 1.61

Hydrogenation of polymerized diethyl heptadeca-1,16-dien-9-ylphosphonate (4-16). After 6 days, saturated polymer **4-16** was obtained.^{1}H NMR ($CDCl_3$): δ (ppm) 1.27-1.39 (br, 31H), 1.65 (br, 4H), 4.06 (m, 4H).^{13}C NMR ($CDCl_3$): δ (ppm) 16.74 ($^3J_{CP}$ 5.7Hz), 27.84 ($^2J_{CP}$ 9.1Hz), 27.88, 28.46, 29.25, 29.87, 32.81, 36.10 ($^1J_{CP}$ 137Hz), 61.49 ($^2J_{CP}$ 6.8Hz), 130.50, 130.05. ^{31}P NMR ($CDCl_3$, PPh_3 reference): δ (ppm) 34.52. GPC data (THF vs. polystyrene standards): M_w = 40400 g/mol; P.D.I. (M_w/M_n) = 1.71

Hydrogenation of polymerized diethyl tricosa-1,22-dien-12-ylphosphonate (4-17). After 6 days, saturated polymer **4-17** was obtained. ^{1}H NMR ($CDCl_3$): δ (ppm) 1.27-1.44 (br, 43H), 1.62-1.84 (m, 4H), 4.10 (m, 4H). ^{13}C NMR ($CDCl_3$): δ (ppm) 16.73 ($^{3}J_{CP}$ 5.8Hz), 27.82 ($^{2}J_{CP}$ 9.3Hz), 28.44($^{3}J_{CP}$ 3.6Hz), 29.69, 29.89, 29.95, 36.20 ($^{1}J_{CP}$ 136Hz), 61.46 ($^{2}J_{CP}$ 6.9Hz). ^{31}P NMR ($CDCl_3$, PPh_3 reference): δ (ppm) 34.71. GPC data (THF vs. polystyrene standards): M_w = 34500 g/mol; P.D.I. (M_w/M_n) = 1.93

Hydrogenation of polymerized tetraethyl heptadeca-1,16-diene-9,9-diyldiphosphonate (4-18). After 6 days, saturated polymer **4-18** was obtained. ^{1}H NMR ($CDCl_3$): δ (ppm) 1.32 (br, 24H), 1.48 (br, 4H), 1.84-1.95 (br, 8H), 4.17 (p, 8H), 5.38 (m, 2H). ^{13}C NMR ($CDCl_3$): δ (ppm) 16.72 (t), 24.43 (t), 27.46, 29.22, 29.32, 29.95, 30.53, 32.85, 46.00 (t, $^{1}J_{CP}$ 123Hz), 62.52 (t), 130.05, 130.52. ^{31}P NMR ($CDCl_3$, PPh_3 reference): δ (ppm) 26.67. GPC data (THF vs. polystyrene standards): M_w = 11400 g/mol; P.D.I. (M_w/M_n) = 1.82

Hydrogenation of polymerized tetraethyl tricosa-1,22-diene-12,12-diyldiphosphonate (4-19). After 5 days, saturated polymer **4-19** was obtained. ^{1}H NMR ($CDCl_3$): δ (ppm) 1.25-1.34 (br, 44H), 1.48 (br, 4H), 1.85 (br, 4H), 4.16 (p, 8H); ^{13}C NMR ($CDCl_3$): δ (ppm) 16.67 (t), 24.41 (t), 29.58, 29.88, 29.95, 30.18 (t), 30.60, 32.12, 45.97 (t, $^{1}J_{CP}$ 123Hz), 62.47 (t). ^{31}P NMR ($CDCl_3$, PPh_3 reference): δ (ppm) 30.74; GPC data (THF vs. polystyrene standards): M_w = 33400 g/mol; P.D.I. (M_w/M_n) = 1.71

Hydrogenation of polymerized diethyl 3,5-bis(oct-7-enyloxy)benzylphosphonate (4-20). After 5 days, saturated polymer **4-20** was obtained. ^{1}H NMR ($CDCl_3$): δ (ppm) 1.26-1.31 (br, 26H), 1.78 (m, 4H), 3.08 (d, 2H), 3.93 (t, 4H), 3.99-4.11 (m, 4H), 6.35-6.37 (m, 1H), 6.45-6.47 (t, 2H). ^{13}C NMR ($CDCl_3$): δ (ppm) 16.40, 26.30, 29.51, 29.93,

34.03 ($^{1}J_{CP}$ = 138 Hz), 62.35, 68.28, 100.35, 108.52, 133.42, 160.25. ^{31}P NMR ($CDCl_3$, PPh_3 reference): δ (ppm) 26.09. GPC data (THF vs. polystyrene standards): M_w = 20600 g/mol; P.D.I. (M_w/M_n) = 1.94

Hydrogenation of polymerized diethyl 3,5-bis(10-undecenyloxy)phenyl) benzyl phosphonate (4-21). After 5 days, saturated polymer **4-21** was obtained. ^{1}H NMR ($CDCl_3$): δ (ppm) 1.25-1.44 (br, 34H), 1.77 (m, 4H), 2.92 (d, 2H), 3.91 (br, 4H), 4.03 (m, 4H), 6.34 (br, 1H), 6.44 (br, 2H). ^{13}C NMR ($CDCl_3$): δ (ppm) 16.65, 22.93, 26.30, 29.51, 29.67, 29.83, 29.98, 32.15, 34.26 ($^{1}J_{CP}$ = 138 Hz), 62.37, 68.27, 100.34, 108.53, 133.62, 160.49. ^{31}P NMR ($CDCl_3$, PPh_3 reference): δ (ppm) 25.77. GPC data (THF vs. polystyrene standards): M_w = 16400 g/mol; P.D.I. (M_w/M_n) = 2.23

General hydrolysis procedure

Into a 2-necked Schlenk round bottom flask polymer ester was transferred dissolved in dry dichloromethane. Then the flask was equipped with a stir bar, and septa. After flushing the flask with argon, 10 eq bromotrimethylsilane added dropwise by syringe under a continuous flow of argon. After stirring with a constant flow of argon for 24 hours, the residual reactants were removed under vacuum prior to adding 20 mL of methanol (not anhydrous). The reaction was allowed to stir with a constant flow of argon for another 24 hours. Upon removal of residual methanol and trimethylsilyl species, acid polymer was obtained in quantitative yield (99%) without any purification necessary. Following methanolysis, the polymer was precipitated from the sides of the flask with acetone. The precipitated polymer was rinsed through an osmotic filter with acetone and dried at 50˚C for 24 hours.

Results and Discussion

Synthesis

Structure control begins with the synthesis of 7 monomers, the attachment of protected phosphonic acid groups being varied between protected single acids (**4-1 – 4-3**), protected geminal acids (**4-4** and **4-5**), and protected benzyl acids (**4-6** and **4-7**). Methylene spacing between these symmetrically placed protected phosphonic acid groups is determined using appropriate alkenyl synthons (Figure 4-1).

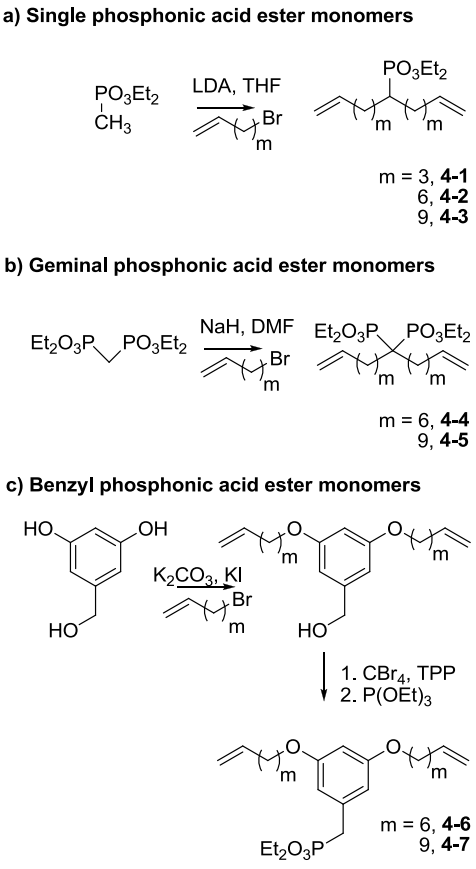

Figure 4-1. Efficient monomer syntheses

Singly attached phosphonic acid ester monomers were synthesized by a two-step, one-pot alkylation reaction.[218] Geminal phosphonic acid ester monomers were prepared using a hydride base for the alkylation, and benzyl phosphonic acid ester

monomers were introduced via an etheral benzene linkage. Specifically, after alkylation chemistry to prepare the diene benzyl alcohol, bromination using an Appel reaction followed by an Arbuzov reaction yielded the monomers **4-6** and **4-7**.

Figure 4-2 shows the step-growth metathesis polycondensation technique using protected singly attached phosphonic acid monomers **4-1 – 4-3**. Polymerization yields unsaturated polymers **4-8** – **4-10**, which upon saturation with hydrogen yields precisely spaced phosphonic acid ester polymers **4-15** – **4-17**. Quantitative deprotection (reaction iii)[212,213] yielded precisely functionalized phosphonic acid polymers **4-22** – **4-24** with the spacing between acids containing exactly 8, 14 or 20 methylenes. Polymers **4-22** – **4-24** were isolated as insoluble highly-interactive polymers after evaporating the methanol and washing with acetone.

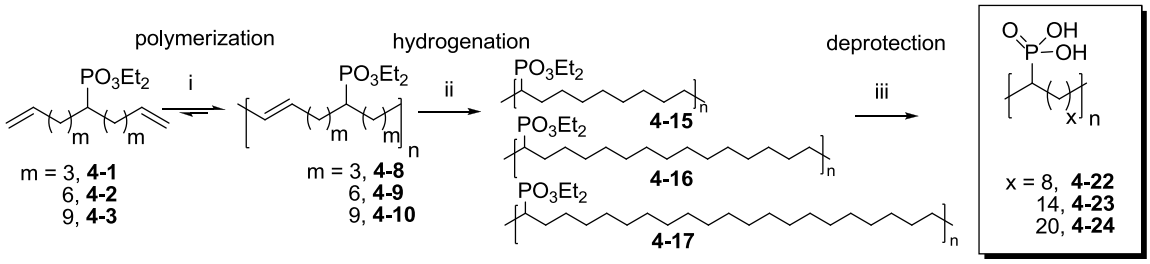

Figure 4-2. Phosphonic ester and acid polymer family: i. 0.25 mol% $(Ph_3P)_2Cl_2Ru{=}CHPh$, 50ºC, 10^{-3} mmHg; ii. $RhCl(PPh_3)_3$, H_2 (40bar), toluene; iii. 1)TMSBr, CH_2Cl_2, 24 hrs 2) MeOH, 24 hrs

The methodology used to alter the architecture of such precision phosphonic acid polymers is shown in Figure 4-3, where geminal acids are introduced as well as benzyl acids. Polymerization of protected geminal monomers **4-4** and **4-5** containing twice the functionality content yielded geminal phosphonic acid ester polymers **4-11** and **4-12**, which upon hydrogenation affords polymers **4-18** and **4-19**. Upon deprotection, precision geminal phosphonic acid polymers **4-25** and **4-26** are obtained as insoluble

polymers. Protected hydrogenated to yield **4-20** and **4-21**, and subsequently deprotected to generate insoluble precision benzyl phosphonic acid polymers **4-27** and **4-28**.

As such, solution characterization techniques were utilized on the soluble phosphonic acid ester polymers in supporting primary structure, including functionality content. Additional bulk techniques were utilized in probing acid polymer structure.

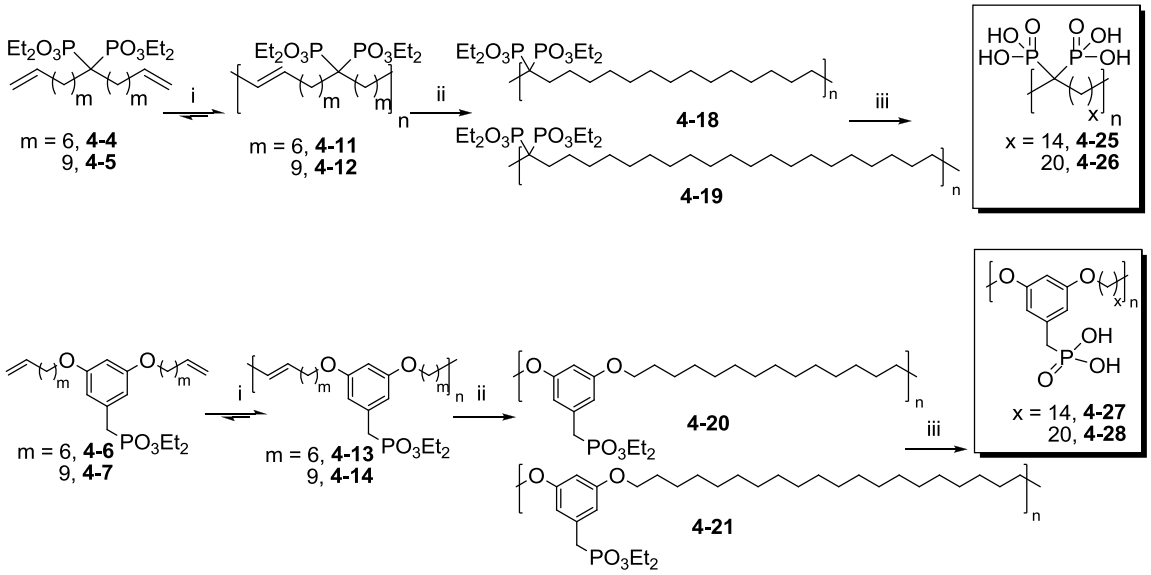

Figure 4-3. Phosphonic ester and acid variations in functionality and architecture: i. 0.25 mol% $(Ph_3P)_2Cl_2Ru{=}CHPh$, 50ºC, 10^{-3} mmHg; ii. $RhCl(PPh_3)_3$, H_2 (40bar), toluene; iii. 1)TMSBr, CH_2Cl_2, 24 hrs 2) MeOH, 24 hrs

Structure

Table 4-1 shows molecular weight and polydispersity data for the soluble, protected phosphonic acid *ester* polymers. Throughout, monomodal traces were obtained with polydispersity indices (PDIs) of about 2 consistent with the step-growth polymerization technique with the slight variations due to competing reactions. In general, protected single phosphonic acid ester polymers have higher molecular weights with degrees of polymerizations (DPs) of about 50, while an increase in

functionality (either as geminal or etheral groups) apparently leads to catalyst deactivation. The exception within single phosphonic acid ester polymers include **4-16** and **4-17** with **4-17** exhibiting a lower DP attributed to inhibition of ethylene removal. However sufficient molecular weights for property comparison were obtained after an iterative addition of 0.25 mol% catalyst halfway through the polymerization.[214] In the extreme case when geminal and benzyl monomers containing 3 methylene units underwent polymerization attempts (not shown), only oligomers were obtained. High concentration of functional groups relative to olefin led to the oligomerization under typically ideal bulk polymerization conditions. Following the path of lowering the concentration using solvent was not followed as this would theoretically increase the formation of cyclic structures specifically pre-formed into the structure by geminal substitution and the Thorpe-Ingold effect.

Table 4-1. Soluble phosphonic ester molecular weight and molecular weight distribution data

	GPC Data[a]		
Polymer	M_n	M_w	PDI
4-15	10.6	17.1	1.61
4-16	23.6	40.4	1.68
4-17	17.9	34.5	1.93
4-18	6.2	11.4	1.82
4-19	19.5	33.3	1.71
4-20	10.6	20.6	1.94
4-21	7.3	16.4	2.23

[a]In kg/mol obtained in THF relative to PS standards

Representative soluble, protected phosphonic acid ester polymer ^{1}H NMR spectra confirm molecular weight via CH_3 end-group integration, hydrogenation shown by the

absence of olefin signal at ~4.5 ppm and correct phosphonic acid ester functionality content (Figure 3).

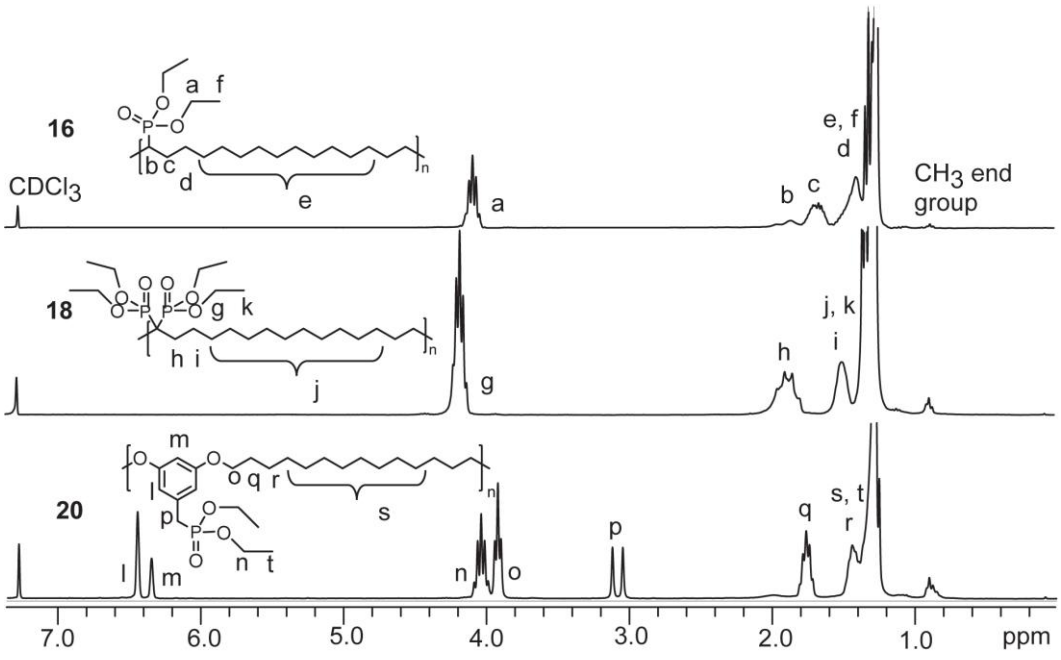

Figure 4-4. Solution ^{1}H NMR spectra in $CDCl_3$ of soluble ester polymers **4-16**, **4-18**, and **4-20**

The spectrum of single phosphonic acid ester polymer **4-16** shows the clean polymer structure including methine (b), α- (c), β- (d) and unresolved backbone methylene (e) protons along with the ethyl ester CH_2 (a) and CH_3 (f). The spectrum of geminal ester polymer **4-18** contains α-protons coupled to the two phosphorous atoms (h), β- (i) and unresolved backbone methylene (j) protons along with the ethyl ester CH_2 (g) and CH_3 (k). The spectrum of benzyl ester polymer **4-20** contains benzene protons (l) and (m); etheral oxygen backbone α- (o), β- (q), γ- (r) and unresolved (s) protons; benzyl protons (p); and ethyl ester CH_2 (n) and CH_3 (t). Additionally, all ^{31}P NMR spectra showing a single resonance indicated phosphonic acid esters remained intact prior to hydrolysis.

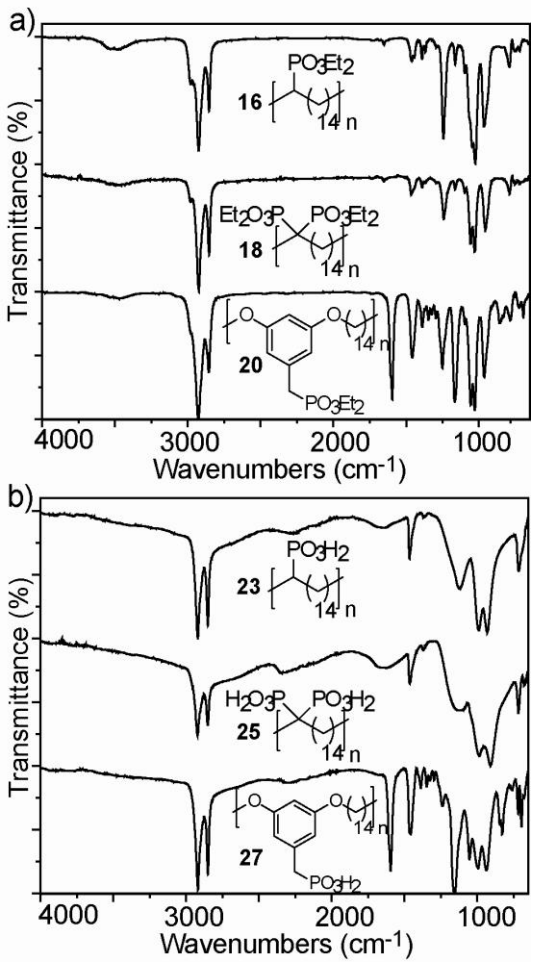

Figure 4-5. IR spectra comparing the 14-methylene spaced polymers with a) FT-IR of ester polymers and b) ATR-IR of acid polymers

Functional group identity (protected ester compared to deprotected acid) was further probed using FT-IR and ATR-IR (Figure 4-5). The most interesting absorbances result from the functional group comparing the ester polymers (**4-16**, **4-18**, and **4-20**) to acid polymers (**4-17**, **4-19**, and **4-21**) within the representative 14-methylene spaced polymers (see supporting information for all polymers). The protected single phosphonic acid ester polymer **4-16** contains absorbances including P=O stretching vibrations at 1243cm^{-1} and P-O-C aborbances at 955, 1026 and 1164cm^{-1} with the geminal (**4-18**) and benzyl (**4-20**) ester polymers displaying similar motions. Benzyl ester polymer **4-20** is complicated by 1,3,5-trisubstituted benzene ring motions: strong benzene in-plane C-

H bending band at 1054cm^{-1}, weak symmetric C-O-C stretch at 1040cm^{-1}, strong etheral C-O-C strong asymmetric stretch at 1247cm^{-1}. Other benzene motions include C=C ring stretches at 1456, and 1603cm^{-1}, along with weaker out-of-plane C-H bending bands at 780 and 851cm^{-1}. Within the representative acid polymers (**4-17**, **4-19** and **4-21**), the P=O stretch broadens to lower frequency at about 1143 cm^{-1} and P-OH stretches are observed at ~939 and ~1004cm^{-1}.

Thermal Properties

The primary structures of all polymers are exact and precisely defined, stemming from the features of metathesis polycondensation chemistry. Trends in secondary structure variation with respect to decomposition and crystallinity become apparent in the thermal properties probed by TGA and DSC.

TGA data is particularly valuable relating the profile shape and decomposition to the acid polymer functionality amount as titration of insoluble materials was not feasible. The TGAs of all protected phosphonic acid polymers show a two-step decomposition profile, attributed to ester and backbone decomposition, yet dependent on the exact identity of either single, geminal or benzyl acid ester polymers (Figure 4-6). Each single, geminal or benzyl acid ester polymer profile differs drastically from the corresponding deprotected acid polymer profiles (Figure 4-7).

Shown in Figure 4-6, the protected single phosphonic acid ester polymers and geminal ester polymers **4-16 – 4-19** first decompose at roughly 300ºC from the loss of ethylene from the ethyl esters.[215] The ether linkage effects benzyl ester polymers **4-20** and **4-21** as the first decomposition is much greater than the ester content. Due to the complexity of decomposition in all of these functional polymers, this first mass loss does not exactly correlate as observed in simpler precision halogen substituted structures.[216]

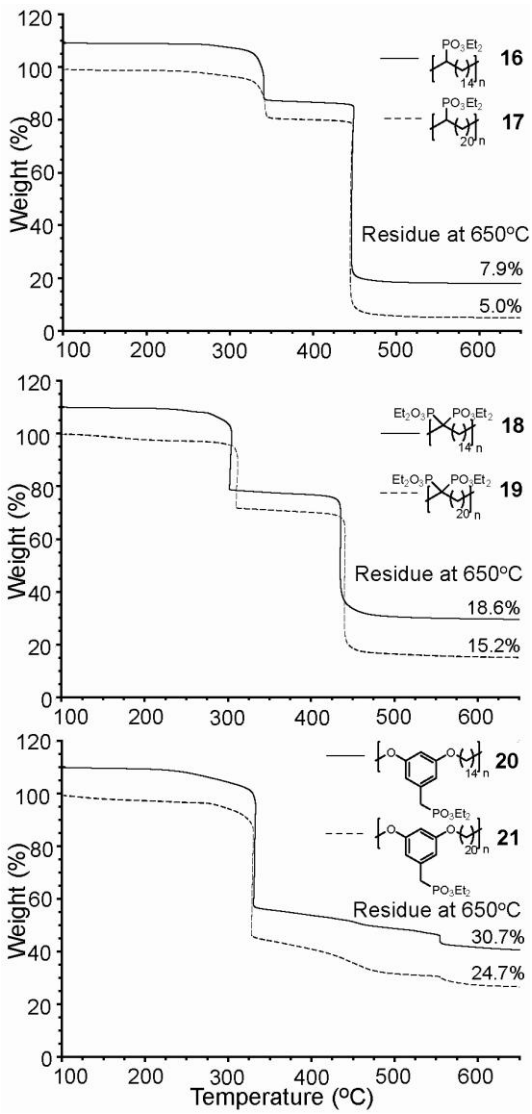

Figure 4-6. Thermogravimetric analysis comparing phosphonic acid ester polymers containing 14 and 20 methylenes

However, when comparing all of the ester polymers **4-16** – **4-21**, the residue remaining is highest in polymers containing the most functionality, i.e. polymers possessing more frequent functional groups with 14 methylenes have more residue than those with 20 methylenes, polymers having geminal attachment have more residue than those with single attachment, and polymers having benzyl attachment have the most residue due to the ether linked benzyl ester. The mass % loss of the step

decompositions does not quantitatively correlate to any assumed ethyl, ethoxide, or phosphonate cleavage. The remaining residue also does not correlate exactly to specific decomposition products but the general shape of the decomposition profile correlates to the functionalization.

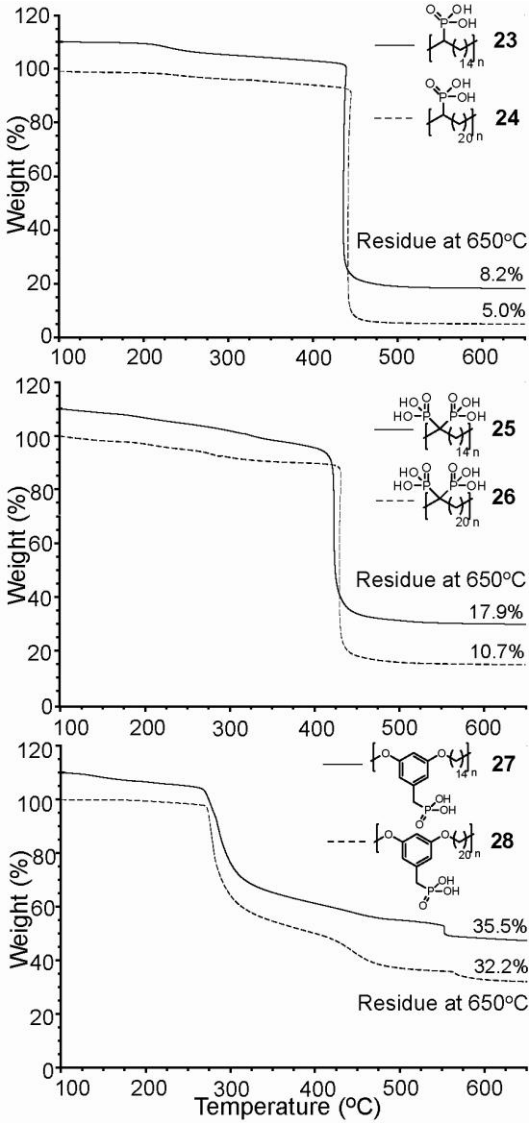

Figure 4-7. Thermogravimetric analysis comparing phosphonic acid polymers containing 14 and 20 methylenes

Within the deprotected acid polymers shown in Figure 4-7, the decomposition profile shape corresponds to a broad undefined loss of functionality coupled to loss of

water (presumably through anhydride formation), followed by a sharper one-step decomposition resulting from polymer backbone decomposition. In all cases, there are no similarities in acid decomposition profile shape to ester profile shape. Quantitatively, the functionality content by mass % loss again did not match exactly particular expected acid fragments. However, the trend relating the highest residues remaining to the most functional polymers is upheld.

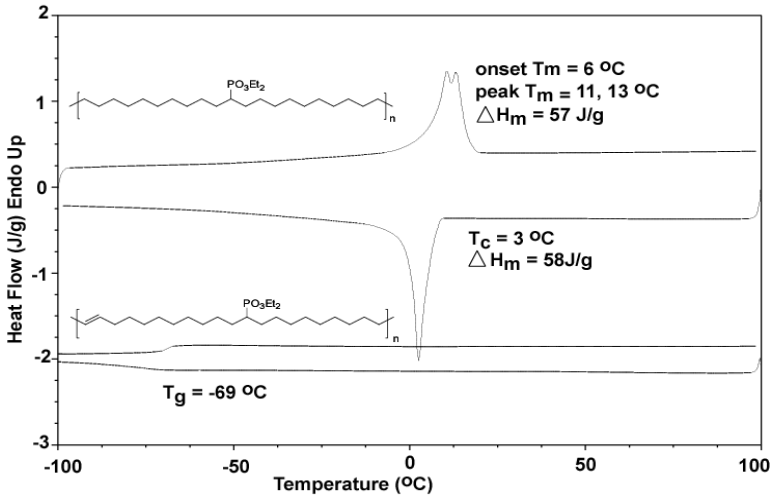

Figure 4-8. DSC of unsaturated and saturated ester copolymer detailing the crystallization due to methylene runlength

While the TGA profiles appear similar between specific simple, geminal and benzyl esters and acids, DSC reveals differences in the crystallization behavior throughout the complete protected ester and deprotected acid families (Table 4-2). Amorphous ester polymers are obtained for those spaced with 8 and 14 methylenes (polymers **4-15**, **4-16**, **4-18**, and **4-20)** with glass transitions ranging from -62 to -24°C. Semicrystalline ester polymers are obtained once the functionality is spaced by 20 methylenes (polymers **4-17**, **4-19**, and **4-21)** with crystallization being attributed to the 20-methylene run-length (Figure 4-8).

Upon hydrolysis to the acid family, amorphous and semicrystalline trends are upheld yet with transitions at higher temperatures. The glass transition temperatures of the amorphous polymers increase by more than 50°C, ranging from 32 to 45°C. The thermal behavior of semicrystalline polymers is complicated by the strongly interacting phosphonic acid functional groups, which causes the melting temperature to increase (Table 4-2) and also affects the crystallization time-scale.

Table 4-2. Summary of DSC thermal analysis

esters[a]	T_g[b] (^oC)	T_m[c] (^oC)	ΔH_m (J/g)	**acids**[a]	T_g[b] (^oC)	T_m[c] (^oC)	ΔH_m (J/g)
4-15	-57	-	-	**4-22**	44	-	-
4-16	-61	-	-	**4-23**	45	-	-
4-17	-	11, 13	55	**4-24**[d]	-	50, 67	24, 19
4-18	-42	-	-	**4-25**	32	-	-
4-19	-48	47	30	**4-26**[d]	-	87	120
4-20	-25	-	-	**4-27**	43	-	-
4-21	-	2	47	**4-28**[d]	-	46	42

[a] second heat shown at 10^{o}C/min, except where noted otherwise

[b] C_p (J/g^{o}C) were between 0.07 and 0.12

[c] peak melting temperature

[d] first heat at 10^{o}C/min after annealing at room temperature 72 hours

In a previous random phosphonic acid-modified polyethylene polymer study containing lower incorporation levels (2.8, 1.8 and 0.8 acids per 100 carbon atoms) than the precision 20-methylene spaced polymers (5 acids per 100 carbons), crystallization kinetics were significantly affected and found to be strongly influenced by annealing and the thermal history.[199] It was also observed that when phosphonic acid frequency was increased to 7.4 acids per 100 carbons, similar to 14-methylene spaced polymers, no crystallization was observed. In the precision single, geminal and benzyl phosphonic

acid polymer family presented here, a similar behavior is observed when the run-length is reduced below 20 methylenes. As noted by MacKnight, incorporating acid groups more frequently, increasing the overall acid content, results in amorphous polymers from this inability to cocrystallize with short polyethylene segments due to increased hydrogen bonding and decreased diffusional motion.

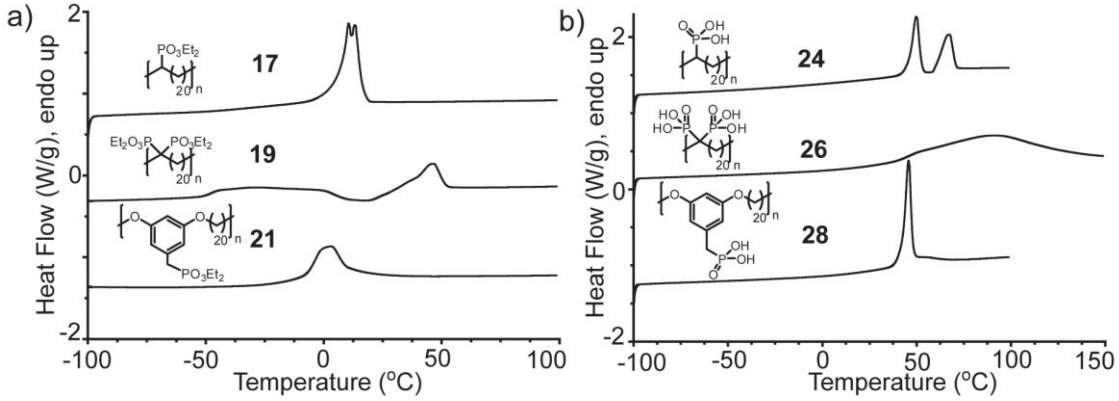

Figure 4-9. DSC thermograms of a) semicrystalline ester polymers, second heat shown b) semicrystalline acid polymers, first heat after 72 hours annealing at room temperature shown (arbitrary vertical offsets for clarity)

Indeed, an amorphous polymer is obtained when the acid content is effectively doubled with more frequent singly attached groups along the backbone (see Figure 4-2, polymers **4-22** and **4-24**). But when the architecture is altered from singly attached polymer **4-24** with twice the acid content via geminal attachment (**4-26**) or with benzyl attachment (**4-28**), the 20-methylene run-length still ensures crystallization. While typical reversible thermograms are obtained for the ester polymers (Figure 4-9a), for the acid polymers containing a run-length of 20 methylenes (Figure 4-9b), a typical experiment after erasing thermal history results in no recrystallization in the subsequent cooling cycle and thus no melting until 72 hours have passed. After 72 hours or longer, a reproducible endotherm is observed on the first heating cycle, indicating that an equilibrium structure has been achieved (Figure 4-10).

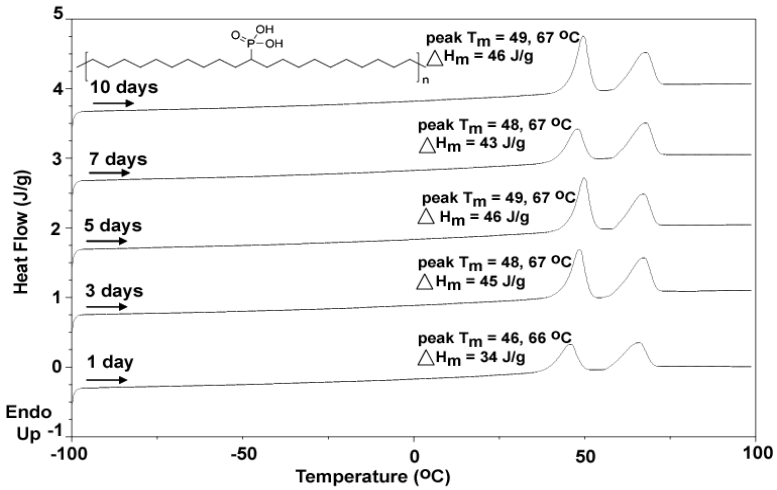

Figure 4-10. DSC first scan melting behavior after associated time scale annealing at room temperature (arbitrary vertical offsets for clarity)

The acid endotherms shown in Figure 4-9b were acquired after erasing thermal history, slow cooling, annealing at room temperature for 72 hours and heating at 10°C/min. Comparing Figure 4-9a and Figure 4-9b, the acid polymer **4-24** melts at higher temperature with well-resolved endotherms compared to the ester polymer **4-17**. Although the precise geminal ester polymer **4-19** shows more complex behavior upon heating, with a glass transition leading to cold crystallization prior to melting, a broad single endotherm is exhibited by the geminal acid polymer **4-26**. Geminal ester polymer **4-19** and geminal acid polymer **4-26** both have endotherms higher than the single and benzyl polymers. Perhaps this is due to an organized structure lending from geminal enhancement of chain folding. Also noteworthy, even though the acid content is doubled, crystallinity is retained yet less perfect as indicated by the broadened melting endotherm. In addition, acid polymer **4-28** again melts at a higher temperature compared to the ester polymer **4-21**.

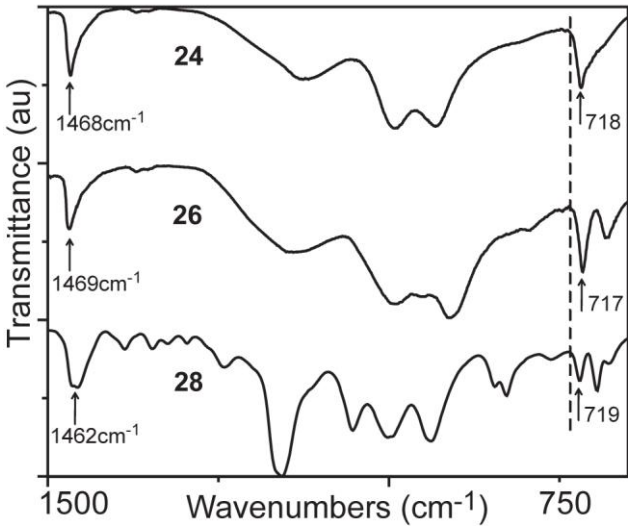

Figure 4-11. ATR-IR spectra expansion of 20-methylene spaced semicrystalline acid polymers

Backbone variations associated with crystallinity between single, geminal and benzyl acid polymers with the same thermal history as the DSC samples (prior to heating) were further investigated by ATR-IR (Figure 4-11). Singlets at ~718cm^{-1} are apparent in all 20-methylene spaced acid polymers in contrast to the typical orthorhombic PE doublet that arises from long trans CH_2 sequences rocking at 719cm^{-1} and sequences of 5 or more CH_2 rocking at 730cm^{-1}.[217,218] Singlets at 1468cm^{-1} are also apparent in all 20 methylene spaced acid polymers in contrast to the typical orthorhombic PE doublet associated with methylene bending at ~1460cm^{-1}. The singlet peaks present in all spectra suggests similar structural features, yet disorganized compared to orthorhombic PE.[219] With the exact identity of the unit cell remaining unknown from these data, the dependency on run-length in these highly interactive polymers has been shown and supports reversible interactions versus chemical crosslinking. Additional rigorous thermal treatments in inducing P-O-P bond formation

were unsuccessful and not apparent by IR. Thus efforts at determining the crystallinity and morphology in free acids will be further developed in the next chapter.

Conclusions

Precision protected phosphonic acid ester and deprotected phosphonic acid polymer families were synthesized with varying frequency and architecture. The highly-interactive acid primary structures have implications on secondary structure probed by thermal behavior. Commonalities in thermal behavior between esters and acids are found in polymers possessing 14 and 20 methylenes between attachment points. The precision acid polymers containing 20 methylenes display PE endotherms strongly dependent on annealing. Additionally, this run-length of 20 methylenes ensures reproducible endotherms attributed to melting, even in polymer structures containing geminal acid groups or a benzyl acid group. Compared to the layered morphology observed previously with dimerized carboxylic acid groups,[197] the resilient, highly-interactive phosphonic acid hydrogen bonds appear to display higher ordered structures concomitant with PE crystallization, lending toward model studies and materials design in particular applications. Further analysis by scattering and diffraction will delineate these crystallinity differences in the next chapter and give a more accurate quantification of crystallinity than simple comparison to the heat of fusion of purely orthorhombic PE.

CHAPTER 5
SEMICRYSTALLINE ACID COPOLYMER MORPHOLOGY

Introduction

With seminal advancements in both nonpolar and polar precision polyolefins in the past few years comes further progress in determining the interactive functional groups effect on structure-property relationships. Branch size plays a role in determining the crystalline unit cell. In a series of precision polymers containing branches increasing in size, once the size exceeds methyl and ethyl, which can be incorporated into the crystalline regions, the branch is excluded to the amorphous region indicating a particular ordering stemming from ADMET chemistry.[65] Indeed upon introducing interactive branches such as carboxylic acids, a unique ordering was observed in both the SAXS and WAXS of semicrystalline acid copolymers.[84] More recently increasing the interactions further with phosphonic acids has affected the crystallization behavior.[86] A progression of increasing polarity is thus followed throughout this chapter within synthesis, thermal behavior, and X-ray scattering.

Experimental

Methods

Differential scanning calorimetry (DSC) was performed using a TA Instruments Q1000 at a heating rate of 10ºC/min under nitrogen purge. Temperature calibrations were achieved using indium and freshly distilled n-octane while the enthalpy calibration was achieved using indium. All samples were prepared in hermetically sealed pans (4-7 mg/sample) and were run using an empty pan as a reference.

Materials

All chemicals were purchased from Sigma-Aldrich and used as received unless noted otherwise. The synthesis of polymers **5-1 – 5-11** were previously reported while the synthesis of the remaining polymers is described here.

Polymerization to yield geminal carboxylic acid copolymer (5-12). Polymer was obtained as unsaturated, protected precursor. Upon hydrogenation simultaneous with deprotection, precipitation into hexane and drying at 80°C overnight, polymer **5-12** was obtained as a tan powder. ^{1}H NMR (dioxane-d_8): δ (ppm) (ppm) 1.07- 1.65 (br, 40H), ^{13}C NMR (THF-d_8): δ (ppm) (ppm) 28.60, 30.69, 30.85, 33.57, 46.32, 177.29. GPC data (THF vs. polystyrene standards) on hemiacetal precursor: M_w = 21000 g/mol; P.D.I. (M_w/M_n) = 1.8

General copolymerization conditions. In a flame dried 50 mL round bottom flask, an exact amount of the smaller spaced monomer was weighed followed by 1,9-decadiene, which was calculated to result in similar random functionality percentage as homopolymers. After mixing the two monomers thoroughly using a magnetic stir, using a 400:1 monomer:catalyst ratio, Grubbs' first generation catalyst was added and mixed into the monomers while under a blanket of argon. A Schlenk adapter was then fitted to the round bottom. After sealing the flask under argon it was moved to a high vacuum line. The mixture was stirred and slowly exposed to vacuum over an hour at room temperature. After stirring for an hour at room temperature under eventual high vacuum (10^{-3} torr), the flask was lowered into a prewarmed 50ºC oil bath for an appropriate number of days allowing removal of ethylene bubbling through viscous polymer. Copolymers were quenched by dissolution of polymer in an 1:10 ethyl vinyl

ether:toluene solution under argon. Upon precipitation into an appropriate solvent, the copolymers were isolated

Copolymerization yielding randomized single phosphonic acid (5-13). ^{1}H NMR ($CDCl_3$): δ (ppm) 1.28-1.48 (br, 8H), 1.67-1.72 (m, 4H), 1.97 (br, 4H), 4.09 (m, 2H), 5.38 (m, 2H). ^{13}C NMR ($CDCl_3$): δ (ppm) 16.73 ($^{3}J_{CP}$ 5.8Hz), 27.79 ($^{2}J_{CP}$ 9.3Hz), 29.29, 29.84, 32.82, 36.20 ($^{1}J_{CP}$ 136Hz), 61.46 ($^{2}J_{CP}$ 6.9Hz), 130.07, 130.53. ^{31}P NMR ($CDCl_3$, PPh_3 reference): δ (ppm) 34.26. GPC data (THF vs. polystyrene standards): M_w = 24215 g/mol; P.D.I. (M_w/M_n) = 1.64 Upon hydrogenation, subsequent deprotection, and drying at 80°C overnight, polymer **5-13** was obtained as a grey powder.

Copolymerization yielding randomized geminal phosphonic acid (5-14). ^{1}H NMR ($CDCl_3$): δ (ppm) 1.27-1.34(br, 10H), 1.55 (br, 4H), 1.94 (br, 6H), 4.16 (p, 4H), 5.38 (m, 2H). ^{13}C NMR ($CDCl_3$): δ (ppm) 16.68 (t), 24.46 (t), 27.53, 29.25, 29.32, 29.43, 29.85, 32.83, 33.39, 33.54, 45.87 (t, $^{1}J_{CP}$ 123Hz), 62.52 (t), 130.36, 130.52. ^{31}P NMR ($CDCl_3$, PPh_3 reference): δ (ppm) 30.55. GPC data (THF vs. polystyrene standards): M_w = 10101 g/mol; P.D.I. (M_w/M_n) = 1.47 Upon hydrogenation, subsequent deprotection, and drying at 80°C overnight, polymer **5-14** was obtained as a grey powder.

Results and Discussion

Synthesis of Acid Analogues

Comparable structures between carboxylic and phosphonic acid containing polymers have been previously reported with some analogous pieces missing within the family (Table 5-1). To complete the analogous series, additional polymers were synthesized first.

A geminal carboxylic acid copolymer was synthesized using previously reported monomer synthesis although never followed to polymer (Figure 5-1). The monomer synthesis proceeds through alkylation of diethyl malonate.

Table 5-1. Comparison of carboxylic acids to more polar phosphonic acid copolymers

Carboxylic acid copolymers	Phosphonic acid copolymers
Precise amorphous:	
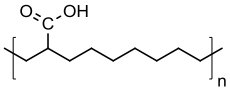 **5-1**	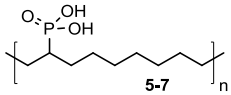 **5-7**
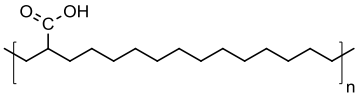 **5-2**	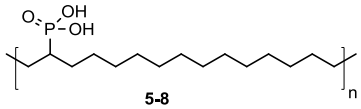 **5-8**
	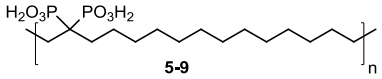 **5-9**
Precise semicrystalline:	
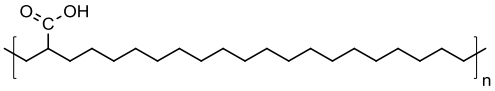 **5-3**	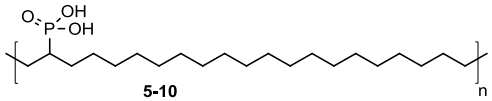 **5-10**
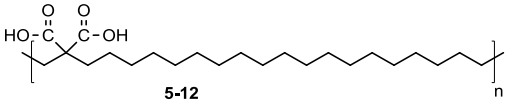 **5-12**	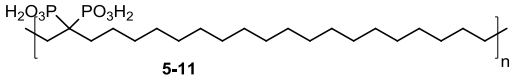 **5-11**
Random:	
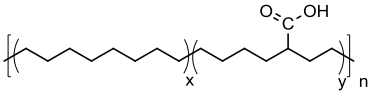 **5-4** 22 mol% AA **5-5** 13 mol% AA **5-6** 9.5 mol% AA	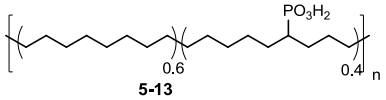 **5-13** 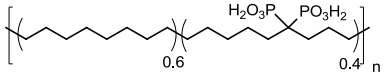 **5-14**

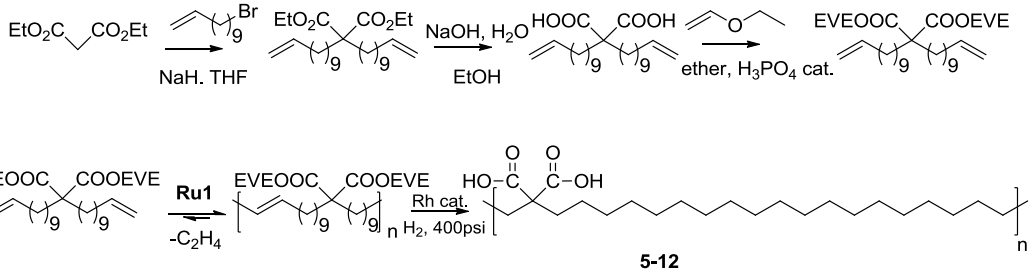

Figure 5-1. Synthesis of a precision geminal carboxylic acid copolymer

Once isolated the dialkylated product is saponified and then purified by column chromatography. Ethyl vinyl ether served as the protecting group for polymerization and was subsequently removed during saturation of the polymer backbone.

Next to understand the effect of the precision highly hydrogen bonded structures in comparison to random structures, random phosphonic acid copolymers were synthesized via copolymerization. Again in targeting semicrystalline materials, the same mol% functionality as those precisely functionalized with single or geminal acids with 20 intervening methylenes were obtained (Figure 5-2).

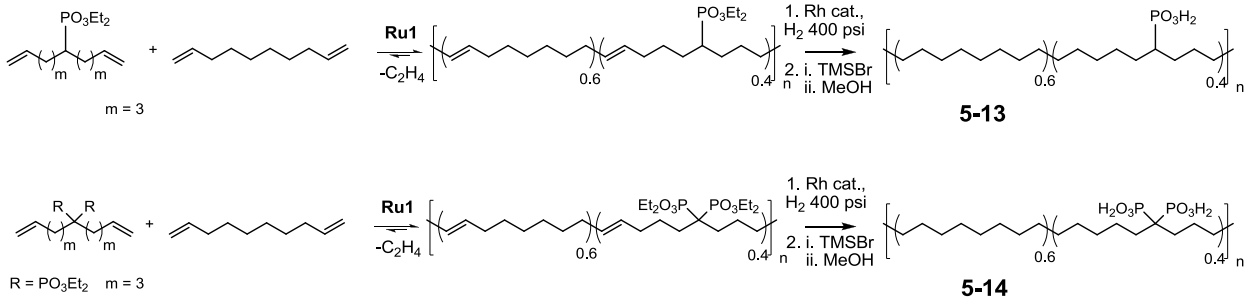

Figure 5-2. Synthesis of random phosphonic acid structures containing equal mol% as previously found semicrystalline precise phosphonic acid copolymers

Thermal Behavior of Acid Analogues

By fixing the composition with equal functional group frequency and increasing the polarity and hydrogen bonding capabilities compared to single carboxylic acid copolymers, interesting questions arise. Previously observed by DSC, increasing polarity and hydrogen bonding compared to single carboxylic acid copolymers introduced a requisite long annealing period at room temperature, a bimodal melt in the case of a single phosphonic acid and a broad melt in the case of geminal phosphonic acids. The nature of these interactions is further probed and compared to a geminal carboxylic copolymer and random phosphonic acid copolymers in order to determine

the functional group identities' role (carboxylic versus phosphonic), the structure (single versus geminal), and added features of precision polymers (precise versus random) using DSC. X-ray scattering was then utilized to visually compare the increased polar and increased hydrogen bonding single and geminal carboxylic and phosphonic acid functional groups to the layered single carboxylic acid structure previously reported.

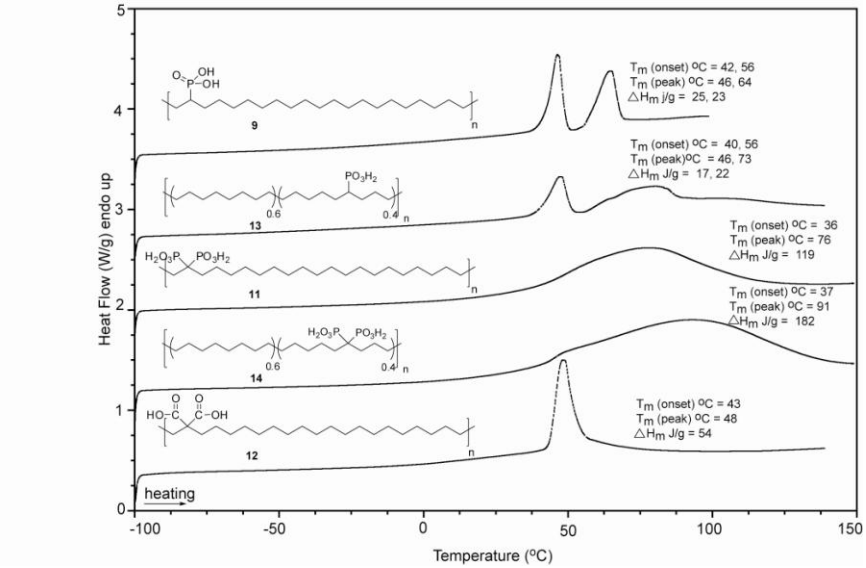

Figure 5-3. DSC overlay of first heating scans after annealing for 72 hours at room temperature (arbitrary vertical offsets for clarity)

Compared to the semicrystalline single phosphonic acid copolymer with increased hydrogen bonding donating capabilities, copolymer **5-12** also displayed melting behavior dependent on an aging period of 72 hours at room temperature (Figure 5-3). The first heating cycle of this polymer erases the thermal history, which includes any precipitation thermal history. Upon cooling at 10°C/min, no recrystallization is observed. After annealing at room temperature for a minimum of 72 hours, reproducible endotherms are obtained with a peak T_m at 48°C, onset of T_m at 42°C and ΔH_m of 60 J/g. *Increasing the hydrogen bonding with geminal carboxylic acid substitution shows that a slower crystallization timescale is not unique to phosphonic acids.* The thermal

behavior dependent on a 72 hour annealing period at room temperature also extends to the random phosphonic acid copolymers along with the feature of a bimodal endotherm preserved upon randomization.

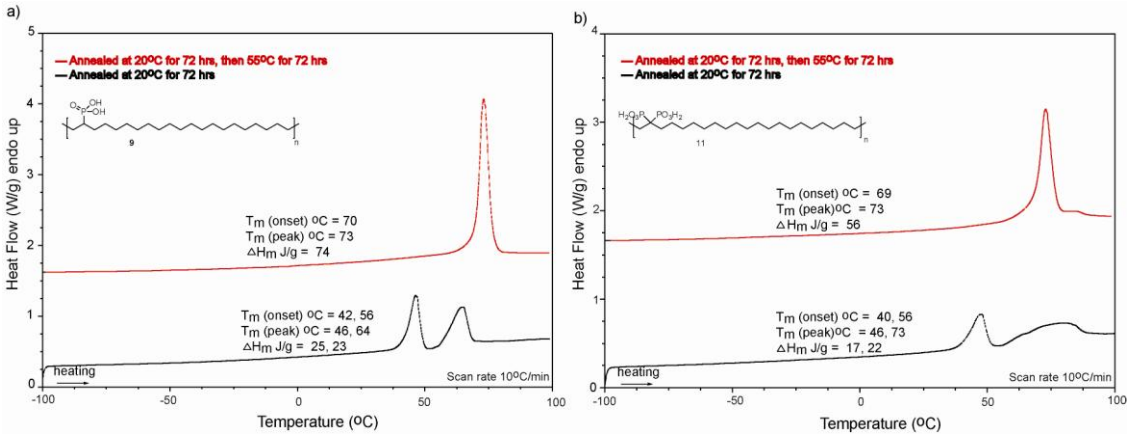

Figure 5-4. DSC overlay of a) precise and b) random first heating scans after annealing for 72 hours at room temperature (shown in black) then annealed for 72 hours at room temperature, then 55°C for 72 hours (shown in red) (arbitrary vertical offsets for clarity)

For both precise and random single phosphonic acids and annealing at room temperature, two crystalline regions are observed. By annealing in between the endotherms, the first is given enough energy to perfect into the higher melting endotherm. Thus a sample of precise **5-10** and random **5-13** were annealed for 72 hours at room temperature and then annealed for 72 hours at 55°C. The samples were sealed in aluminum pans and annealed under nitrogen atmosphere submerged in an oil bath and then first heating scans taken and shown (Figure 5-4). Indeed the higher melting regime shows the increase in enthalpy expected with perfection of PE crystallites.

Preliminary X-ray Analysis of Acid Analogues

Despite the annealing required for reproducible endotherms and crystallites, preliminary X-ray scattering shows similar characteristics in precise semicrystalline

single and geminal carboxylic and phosphonic acid samples to previously reported single carboxylic acid copolymers. Direct comparisons between the more highly polar precise acid containing copolymers presented here have been made in reference to the previously reported precise poly(ethylene-co-acrylic acid) (EAA) copolymers.[84] Using well defined thermal histories, SAXS and WAXS plots have been obtained in an ongoing collaboration with Professor Karen Winey at the University of Pennsylvania.

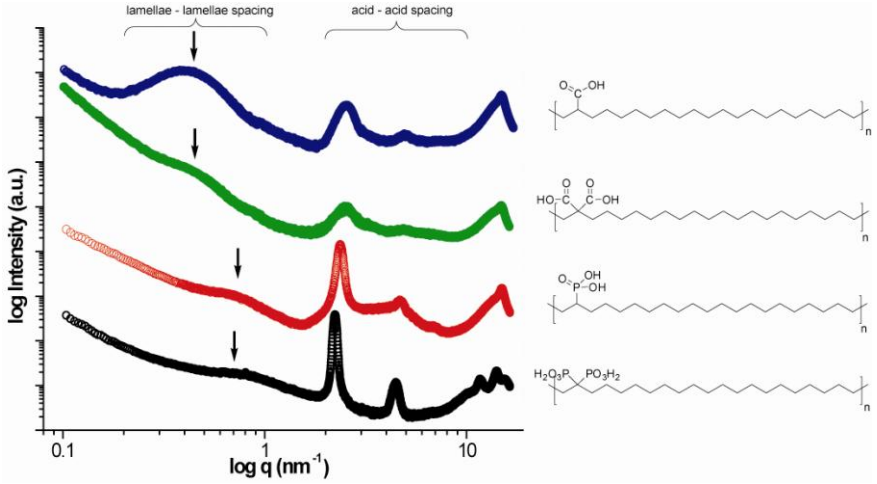

Figure 5-5. SAXS images on pressed isotropic samples of the precision semicrystalline acid copolymers shown at right

As previously observed the precision semicrystalline copolymers presented here display SAXS profiles that indicate both the lamellae – lamellae spacing (includes the portion of intervening amorphous) and acid – acid spacing in isotropic films prepared by melting on a Carver hotpress at 130°C to melt the samples completely. After the requisite 72 hour period at room temperature, SAXS images of the isotropic precision semicrystalline acid materials were obtained (Figure 5-5).

According to the previous report detailing the single carboxylic acid series and specifically the copolymer containing a precisely placed acid on every 21st carbon (**5-3**), the acid – acid distance was found to be 2.53nm, corresponding to the distance in an all

trans conformation between two acids. All copolymers studied here also show the same acid – acid spacing. However lamellae – lamellae spacing depends on the acid. From the scattering peaks and through Bragg's law, the carboxylic acid copolymers have a lamellae – lamellae spacing of 14nm. Using a calculated percent crystallinity, previous estimates of the 2.6-4.2nm lamellae thickness indicated each lamellae consisted of 2-3 acid rich layers. The phosphonic acid copolymers have much smaller lamellae – lamellae spacings of 8nm. This could mean fewer acid groups within the lamellae but the percent crystallinity would be a factor.

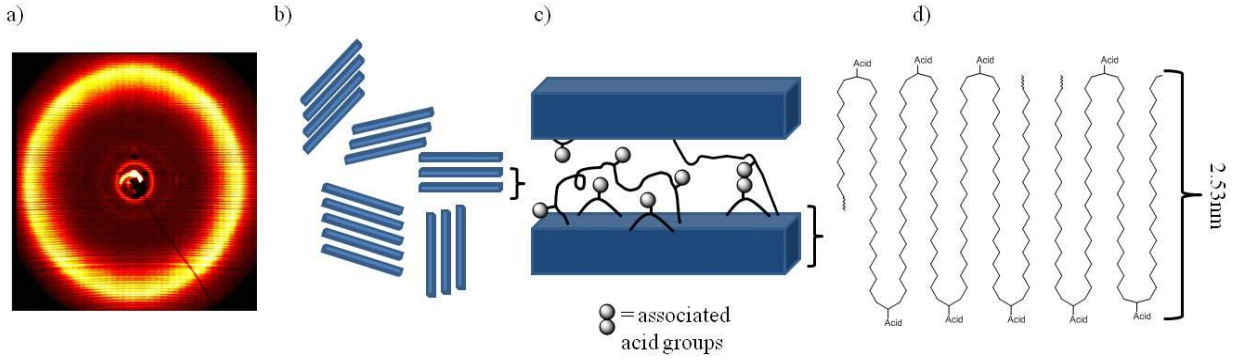

Figure 5-6. Isotropic progression describing the origin of the intense inner halo detailing the a) WAXS intense inner halo corresponding to a 2.53nm scattering feature b) isotropic lamellae within an amorphous matrix c) free amorphous chains between lamellae and d) the crystalline lamella detailed (ordering of crystalline domain is exaggerated and should not be assumed as orthorhombic PE)

A schematic of an undrawn carboxylic acid polymer is shown in comparison to a WAXS image (Figure 5-6). Of particular interest is the origin of the intense inner halo at low q. the inner halo of the WAXS image correlates to the acid – acid spacing shown through the detail progression in Figure 5-6.

To support the acid – acid assignments, the films were stretched after softening with a heat gun to induce anisotropic behavior. As mentioned this has been described previously in precision PE copolymers containing precise and random carboxylic acids

with one explanation proposed.[84] Similar to the layering mode previously illustrated, alignment of the amorphous chains between lamellae may be possible (Figure 5-7) and help explain the appearance of two melting endotherms previously observed upon stretching.[84]

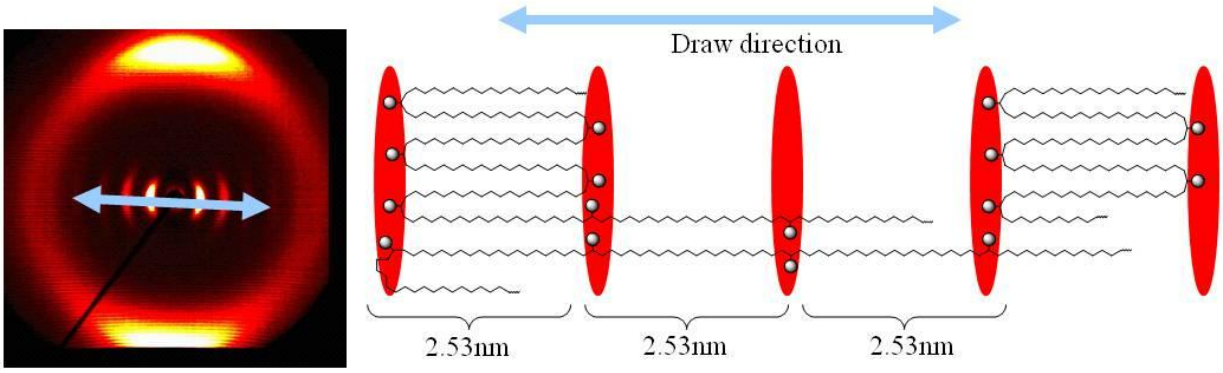

Figure 5-7. WAXS anisotropic representation leading to enhancement of acid spacing from alignment of lamellae and amorphous polymer chains

As mentioned to further support the assignments in Figure 5-5, these films were stretched after softening with a heat gun. While multiple 2.53 nm acid – acid reflections were observed in single carboxylic and phosphonic acid copolymers, heat treatment of the geminal copolymers did not increase the correlation ring intensity, possibly due to physical crosslinking restricting the alignment or uniform electron density from a network higher order morhphology. The carboxylic acid copolymers with the same lamellae – lamellae distance, behave differently upon stretching as do the phosphonic acids. From the anisotropic plots, the carboxylic acid copolymers would be expected to display similar behavior, but stretching results in single acids regardless of identity being more amenable to alignment.

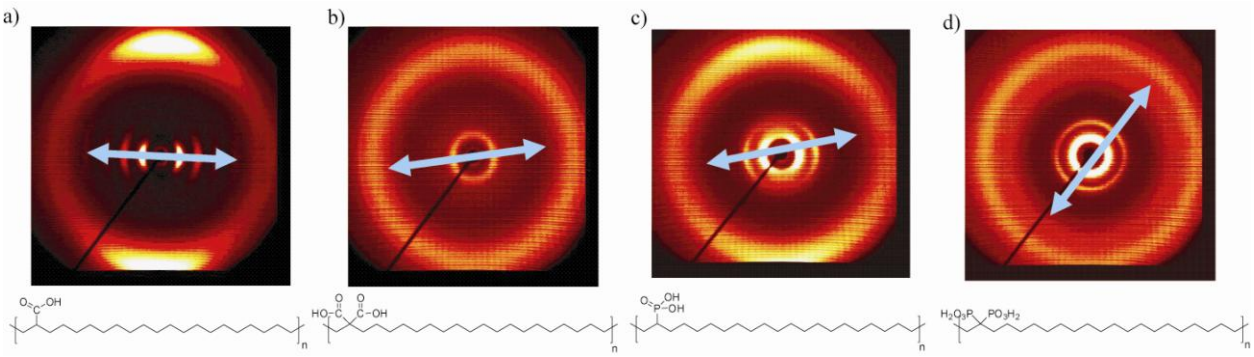

Figure 5-8. Anisotropic WAXS patterns with the draw direction shown with an arrow

WAXS also gives a good picture of even smaller features such as the crystallinity, a key point of interest. While large bulky aliphatic groups reach a limit and revert to branch exclusion and an orthorhombic unit cell of the PE crystallites,[65] the fate of the interactive groups is investigated here. For example, to accommodate an ethyl defect a shift in crystal structure from pure orthorhombic PE was observed. To further explore this phenomenon in polymers containing acids of various size and attachment, WAXS plots were obtained on pressed films (Figure 5-9).

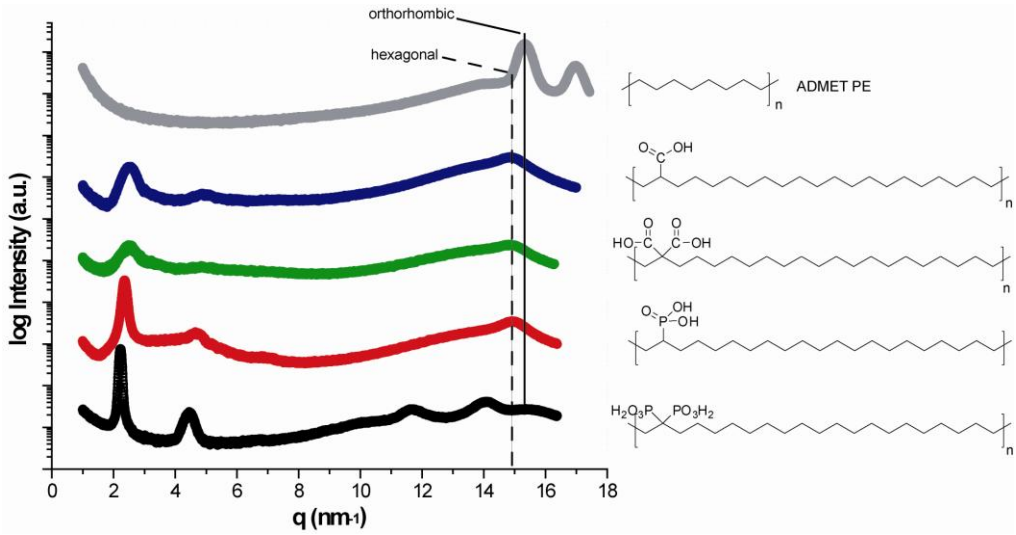

Figure 5-9. WAXS images on pressed isotropic samples of the precision semicrystalline acid copolymers shown at right as compared to orthorhombic PE synthesized by ADMET

While previously reported as orthorhombic, the precision carboxylic acid copolymer more likely adopts a hexagonal unit cell structure. As SAXS suggested 2 -3 acid groups within the lamellae, possibly a hexagonal structure more likely is adopted excluding the acids forcing the PE into a less perfect arrangement than pure orthorhombic PE. The 14.8nm^{-1} peak also found in the previous work on this exact polymer[84] and highlighted in Figure 5-9, more closely correlates to the hexagonal (100) Miller index than to orthorhombic (110) and (200) Miller indices.

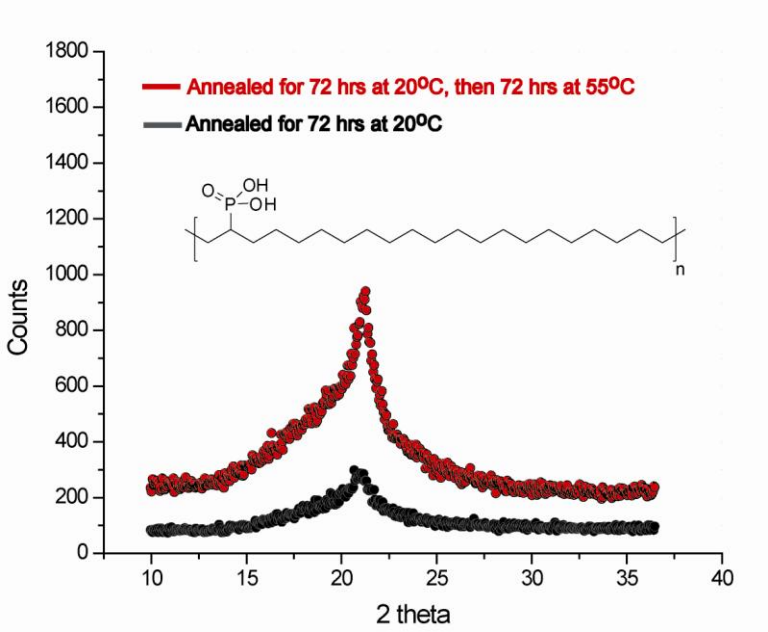

Figure 5-10. X-ray diffraction on annealed phosphonic acid copolymer perfecting the diffraction at 21.1° (λ = 0.154nm)

With the percent crystallinity in these pressed samples quite low, improving the resolution of the crystalline peak in the phosphonic acid copolymers was accomplished by annealing at 55°C. This annealing temperature was shown to improve the subsequent PE melting by DSC and hence was used in the preparation of a sample for X-ray diffraction (Figure 5-10). There is no change in crystal structure but a definite increase in crystallinity upon higher temperature annealing as expected. Additionally,

the peak at 21.2° is a bit higher than the reflection observed for hexagonal PE at 20.5°. However this assignment confirms the earlier DSC assignments of melting less perfect PE crystals and giving enough energy to perfect with a higher enthalpy.

Another interesting question lies in the small-angle region containing acid – acid distances (scattering vector q of ~2-5 nm^{-1}) but at higher temperatures. Upon holding the polymer at 130°C, the acid – acid correlation is still apparent yet shifting to higher q (Figure 5-9). At 130°C, the polymer is completely melted allowing association of the acid groups in a random coil still generating the regions of higher electron density. The crystalline peak at a q of 14.8nm^{-1} also broadens at 130°C due to melting. But, a scattering feature remains at low q, perhaps a remnant of aggregation, which is being further investigated by fitting to models more recognizable in the ionomer field. The shifting peak of this low q peak to higher q (a smaller feature size) further indicates the melting of trans crystalline PE to a random coil.

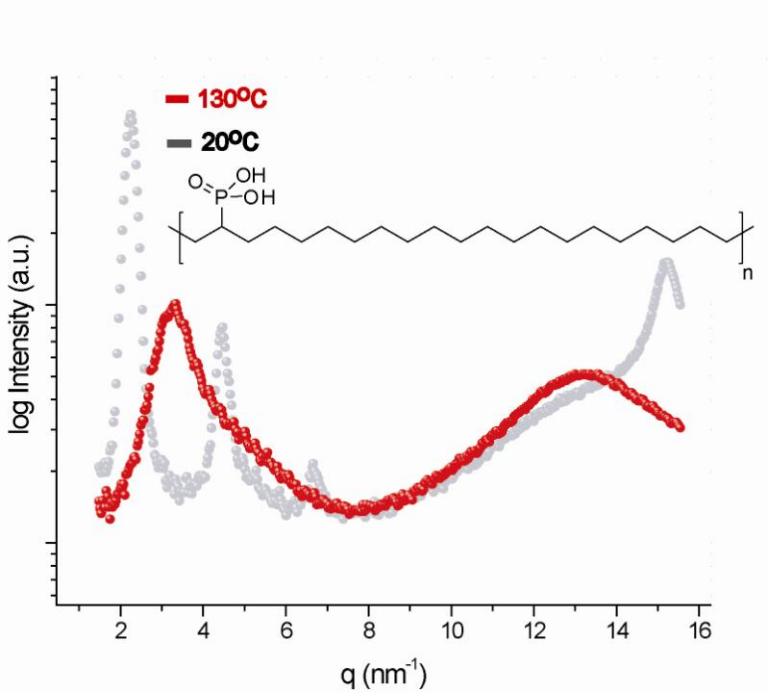

Figure 5-11. SAXS of melted phosphonic acid copolymer

Throughout this discussion, semicrystalline polymers have been examined beginning with the observation of slow crystallization, followed by solving the bimodal melt origin, while supporting higher level morphological assignments. Critical to polymer properties are direct crystallization and hydrogen bonding effects – this behavior and their morphology have been thoroughly covered in precise materials with randomization effects on morphology in progress.

Conclusions

Throughout the preceeding chapters, the polarity of the functional group has increased and has been modified further here. The implications of multiple hydrogen bonding groups have been studied by DSC and shown that the 72 hour annealing time is not unique to phosphonic acid materials but also was a property of the semicrystalline geminal carboxylic acid copolymer. Preliminary X-ray analysis presented thus far gives an indication of the behavior of interactive groups as compared to the crystalline structure. The insolubility and small scale size precludes the phosphonic acid polymers from neutralization either in solution or by extrusion but the remaining amorphous carboxylic acid copolymers offer a simple structure to further study in even more polar materials, ionomers, in the concluding chapter.

CHAPTER 6
AMORPHOUS IONOMER MORPHOLOGY

Introduction

The focus of the preceeding chapter on semicrystalline materials brought out interesting implications of crystallinity on precision structure in strongly associating polymers. Increasing the polarity even further in precision *ionomers* has shown ordering in the crystalline region, as well as in completely amorphous precision ionomers. Acid materials have already been well studied[84] as well as ionomers synthesized upon neutralization with Zn^{2+}.[220] The combination of features, both acid correlations and the ionomer peak, were recently reported as a function of precision, branching, crystallinity, acid content, and Zn^{2+} neutralization level in EAA copolymers and commercial Nucrel® materials.[220] Linear random ionomers showed a much less intense ionomer peak as did branched materials. In semicrystalline precision ionomers, partial deconvolution of scattering contributions from precision acid dimers and interaggregate scattering was achieved by drawing. The Kinning Thomas (KT) model was used to model the interaggregate scattering, aided in success from the precision structure resulting in reduced dispersity of correlation lengths. With an increase in acid content, an increased temperature resulted in higher order structure of aggregates self-assembling into a BCC lattice. In the completely amorphous EAA copolymer containing a carboxylic acid on every 9^{th} carbon neutralized with Zn^{2+}, a higher ordered BCC lattice structure was observed. At the higher temperatures, the precision ionomer adopts this structure similar to the observations in block copolymers, which are well known to microphase separate into spheres, cylinders or lamellae. In an amorphous precise ionomer the same higher ordered phenomenon was observed except in the nanophase.

To further investigate the effects of precision, acid content, and, *metal ion size*, yet devoid of crystallinity, amorphous materials **6-1**, **6-2**, **6-3** and **6-4** were neutralized with various metal salts yielding the ionomer family, **6-5** – **6-8**, depicted in Figure 6-1. With the local environment within the aggregate of interest in this study, there are no wide-angle contributions from crystallites in these amorphous parent acid copolymers.

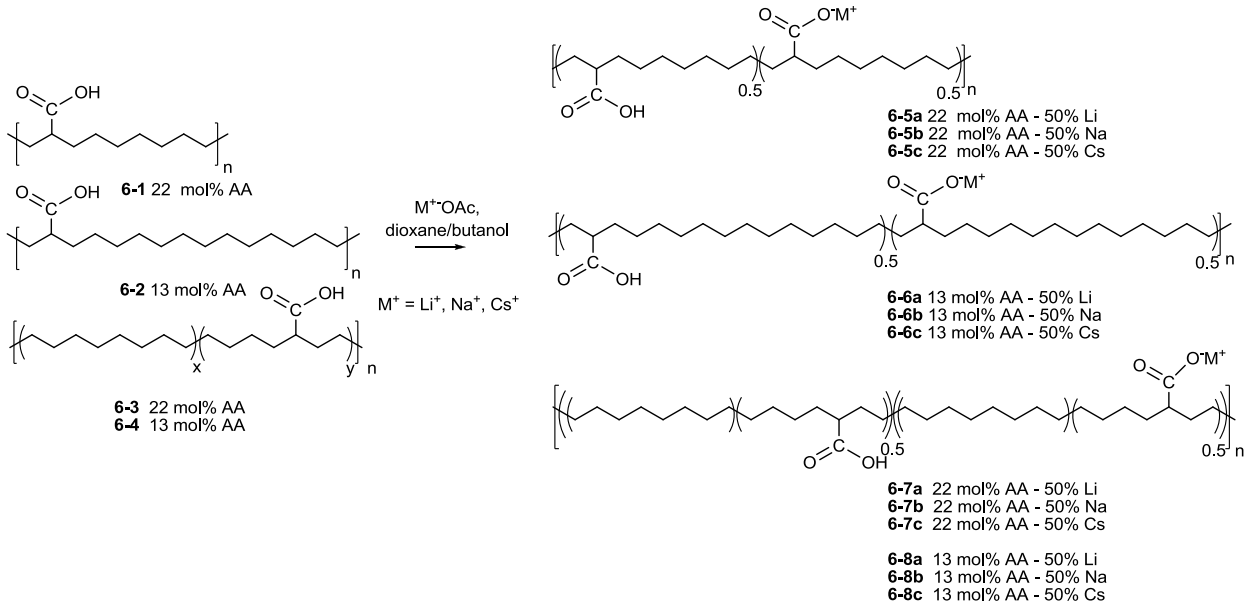

Figure 6-1. Synthetic comparison of amorphous carboxylic acid copolymers to ionomers with varying monovalent cations

Experimental

Materials

All chemicals were purchased from Sigma-Aldrich and used as received unless noted otherwise. Ethyl vinyl ether was distilled prior to use. Metal acetate salts were received as 99.95%+ trace metals basis, measured under a dry, inert atmosphere, and dissolved into reagent grade solvents. The synthesis of polymers **6-1** – **6-4** were previously reported[84] while the synthesis of the remaining polymers is described here.

Synthesis

General neutralization procedure to yield ionomers (6-5 – 6-8). In a dry single neck round bottom flask polymer **1** was weighed (150mg, 0.88mmol), sealed with a septa, and dissolved with a 1:4 mixture of 1,4-dioxane and 1-butanol (30mL) under nitrogen. A magnetic stir bar was added and complete dissolution was obtained upon heating at 90°C for 3 hours. During that time, (29mg, 0.44mmol) of the lithium salt was weighed under a dry and inert atmosphere. Lithium and sodium acetate salts were soluble in 1:2 mixtures of 1,4-dioxane and 1-butanol while cesium acetate was soluble in 1:1 mixtures of 1,4-dioxane and 1-butanol. The 1:2 mixture was added to the lithium salt in a glass vial (18mL). For complete dissolution, a small stir bar was added, the vial closed and heated to 90°C for 30 minutes. The round bottom flask was then outfitted with an addition funnel. The salt solution was added to the addition funnel and was allowed to drip dropwise into the vigorously stirring polymer solution at 90°C. Cloudiness was observed upon partial addition. After stirring for 3 hours at 90°C and cooling to room temperature, the fine precipitate coagulated into larger pieces. No further changes or additions in solvent were necessary. Lithium and sodium precipitate were free while cesium precipitate adhered to the bottom of the flask. The precipitate was filtered and dried at 80°C overnight.

Ethyl 2-(diethoxyphosphoryl)-2-(undec-10-enyl)tridec-12-enoate (6-9). In a flame dried 3-necked flask equipped with a magnetic stir bar, 100 mL of DMF was stirred at 0ºC under a constant argon flow. Using a powder funnel under continued constant argon flow, 2.4g of 60% NaH powder (100 mmol, 3 eq) was added to the flask. Upon resealing the flask, 4 mL (20 mmol, 1 eq) ethyl 2-(diethoxyphosphoryl)acetatewas added dropwise over 30 minutes. After an additional hour stirring at 0ºC, 9.7mL

(44.4mmol, 2.2 eq) of 11-bromoundecene was added dropwise over 30 minutes. The reaction was allowed to warm to room temperature over 4 hours and then allowed to stir at room temperature overnight. Reaction progress was monitored by TLC noting the disappearance of starting materials. The flask was charged with additional 1g of NaH and 1eq of alkenyl bromide. After stirring overnight, the reaction was quenched at 0ºC by first diluting the mixture with 75mL of hexane and then adding 750 mL of deionized water. The reaction mixture was then extracted (3 x 75 mL) hexane. After washing the hexane with water, the crude mixture was concentrated to a light tan oil. Upon column chromatography with 1:1 hexane:ethyl acetate, 3.16g or 30% purified unoptimized yield was obtained. ^{1}H NMR ($CDCl_3$): δ (ppm) 1.26-1.36 (br, 30H), 1.87 (m, 4H), 1.98-2.06 (m, 4H), 4137 (br, 6H), 4.89-5.00 (m, 4H), 5.73-5.86 (m, 2H). ^{31}P NMR ($CDCl_3$, PPh_3 reference): δ (ppm) 26.02; HRMS Calcd for $C_{30}H_{57}O_5P$ [$(M+H)^+$] (*m/z*), 529.4016; found, 529.4024

Discussion

Preliminary X-ray Analysis of Ionomers

In the preceeding chapter SAXS and WAXS were utilized in looking at the larger features including the acid – acid spacing as well as lamellae – lamellae spacing and smaller crystalline structure features respectively. These particular tools are also useful for investigating other nanoscale features such as ionic aggregates in ionomers, particularly interaggregate scattering and local arrangement within the aggregate.

To further examine the effects of precision, acid content, and cation size, several amorphous ionomers were prepared using solution techniques. Noteworthy to mention, cation size was one of the first criteria to validate particular models. The postulate by Longworth and Vaughan arguing for polymer chain ordering between aggregates was

discounted since it could not account for the more intense ionomer peak for Cs^+ as compared to Li^+ salts.[139] The reason for a more intense ionomer peak in cesium materials is of course the higher electron density of Cs^+. Around the same time, Bonotto and Bonner released a report on the effects of ion valency on the physical properties.[138] They found that at similar ionization levels, valency should not be considered analogous to crosslinking functionality since there were many similarities in physical properties such as moduli and tensile strengths.

Since then there have been multiple recent reports in varying the cation in EAA and EMAA copolymers studied by a multitude of techniques including FT-IR,[221,222] mechanical measurements,[223] and SAXS.[224,225] Combining physical property measurement with scattering techniques is complex and has been most successfully attempted by Eisenberg.[145] Eisenberg was able to account for threshold size of independent phase behavior (5-10nm) with multiple glass transitions through the concept of introducing the isolated multiplet and clusters. The isolated multiplet (a few ion pairs and ~0.5nm) although reduced in mobility, is not large enough to exhibit a T_g. As the ion content is increased, there is an overlap in multiplet density ultimately reaching a size capable of exhibiting a T_g and termed a cluster. Thus the two glass transitions are observed from 1) the polymer matrix 2) the reduced chain mobility within a cluster from the additive effect of the many multiplets reduced mobility.

Here the effects of monovalent cation size in linear precision and random ionomers with increased acid content are best summarized as visualized by WAXS. Preliminary scattering at room temperature comparing precise and random linear

ionomers have been obtained with qualitative arguments following (Figure 6-2 and Figure 6-3).

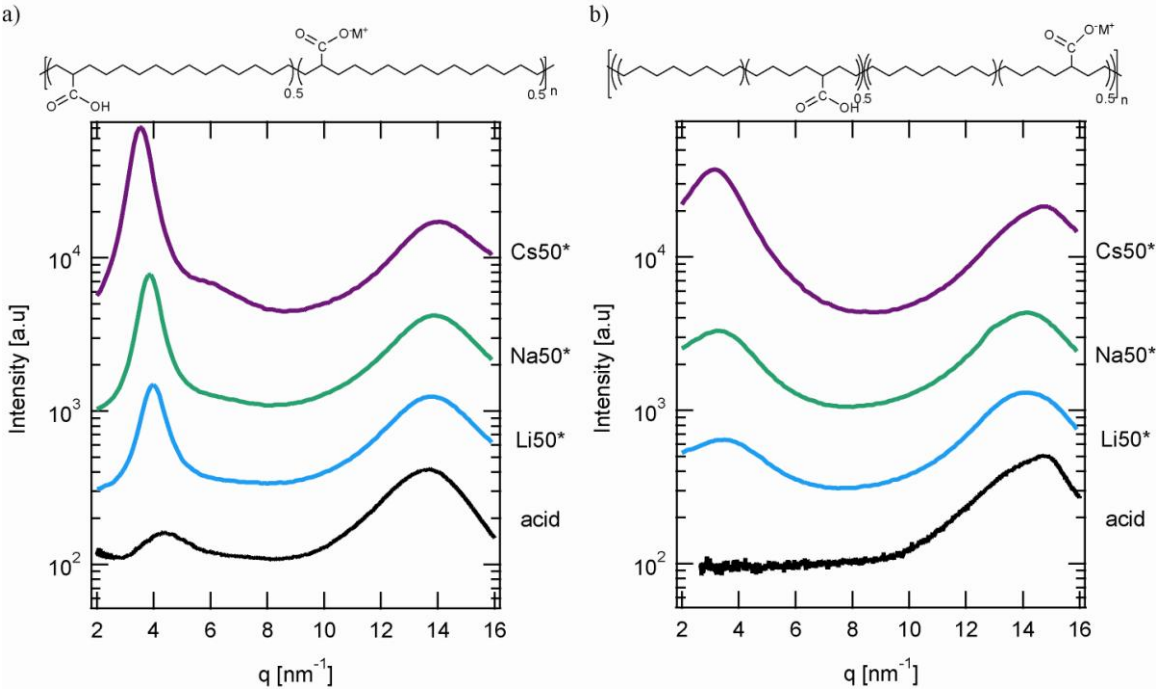

Figure 6-2. A comparison of a) precision and b) random linear ionomers with varied metal ions at equal metal ion content

The common ionomer WAXS feature are apparent in these plots — the ionomer peak (scattering vector of q ~3-5nm^{-1}). After normalization to the amorphous peak at ~14nm^{-1}, each cation scattering plot is offset. In the precision series shown in Figure 6-2a, the precision acid polymer **6-2** shows the periodicity of acid groups at ~4nm^{-1}. As cations are introduced, the ionomer peak becomes apparent although convoluted by acid periodicity (most easily seen as a shoulder in the Cs^+ neutralized ionomer). As the cation size and electron density are increased, the peak is enhanced. Also as cation size is increased the peak shifts to smaller q implicating a larger scattering feature as expected. In the random series shown in Figure 6-2b, the random acid polymer shows no acid periodicity in the low q region owing to the random structure. However, the

trends in ionomer cation size are apparent. The main difference between precise and random is the sharpness of scattering peaks. The broader peaks in Figure 6-2b indicate the more polydisperse correlation lengths in random ionomers. The local aggregate environment is also convoluted by the amorphous scattering but efforts at examining this feature are underway.

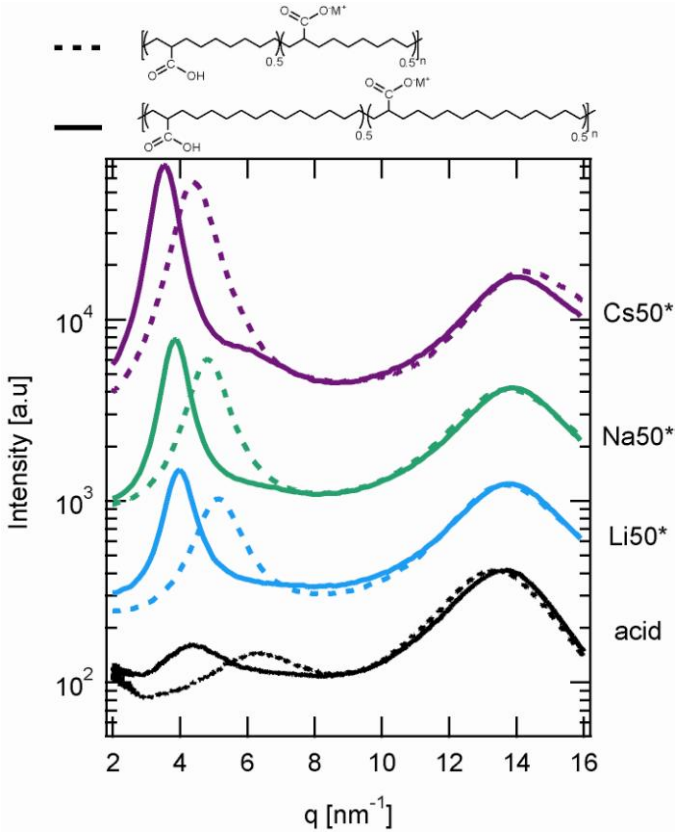

Figure 6-3. A comparision of precision ionomers with different parent acid frequency maintaining metal ion content

In precise copolymers increasing the acid frequency (parent acid copolymers **6-1** and **6-2**) and subsequent neutralization results in some interesting comparisons (Figure 6-3). Again the acid periodicity is apparent with the more frequent acid at higher q as compared to less frequent acid previously described at ~4nm^{-1}. The ionomer peak of the more frequent acid again shifts to lower q in reference to the parent acid (dashed lines)

owing to formation of ionomer along with larger aggregates with increasing cation size. Within the cesium ionomers shown, the more frequent parent acid yields in an ionomer with shorter aggregate correlations.

This trend is followed in each Li^+, Na^+, and Cs^+ ionomer and awaits a quantitative model fit in determining the radius of the aggregate, radius of closest approach and number density of the aggregates. Also once subtracted from the amorphous scattering, the local environment of the aggregate in the scattering vector region with q ~14nm^{-1} will be interesting in examining the coordination environment.

ADMET Perspective

From this current X-ray study and past X-ray studies on precision acid polymers and ionomers, [220,226,84] the simplest cases are not trivial. Since α-ω diene monomer synthesis is also not trivial, new materials based on the available polymer library were worth investigating.

The next simplest extension of the work is on ionomerization of phosphonic acids on a larger scale. Indeed a report on phosphonylated ethylene/propylene (EP) copolymer ionomers resurfaced in 1980 by Richard A. Weiss of Dow[227] as a follow-up to carboxylation of EP and ethylene/propylene/diene terpolymers (EPDM)[228] and also to phosphonylation by elastomer researchers at Union Carbide in the 1960s.[229,230] In the 1980 report, the phosphonylated copolymers were neutralized using solution techniques whereas the 1961 report uses metal oxide extrusion. More recently Weiss reported the synthesis of styrene/vinyl phosphonic acid ionomers but little incite was offered on ionomer morphology[231,232]. As mentioned earlier, the solution techniques were unfeasible from lack of solubility. Solvent mixtures typical of solubilizing aramid fibers

with lithium chloride salts also did not result in solubilized precision phosphonic acid polymers.

Beyond the phosphonic acid ionomer, is the geminal carboxylic acid ionomer. Ionomers of this type have never been reported but preliminary synthetic ventures were positive. The polarity of the beginning polymer compared to the ionomer solution was not optimized and only a fine haze was observed in a Zn^{2+} neutralization. Manipulation of the solvent system to encourage solubility of parent polymer and ionic salt while then also resulting in an insoluble ionomer is required for realization of geminal carboxylic acid ionomers.

Perhaps a hybrid geminal acid will also be of interest in the future. The monomer synthesis was simple and resulted in an ethyl protected carboxylic acid and a diethyl protected phosphonic acid attached on the same central carbon of the α-ω diene monomer (Figure 6-4).

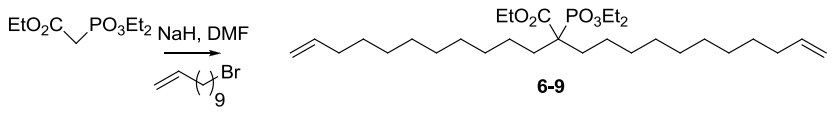

Figure 6-4. Synthesis of hybrid acid precursor

However the preferential carboxylic acid protecting group, the hemi-acetal, is required for easiest removal after polymerization. Optimization of selective hydrolysis and reprotection using ethyl vinyl ether is required for realization of a hybrid polymer. Efforts at selective hydrolysis were successful in isolating starting material. The steps outlining the remaining slightly non-trivial monomer manipulations, polymerization, hydrogenation, and phosphonic acid deprotection are outlined in Figure 6-5.

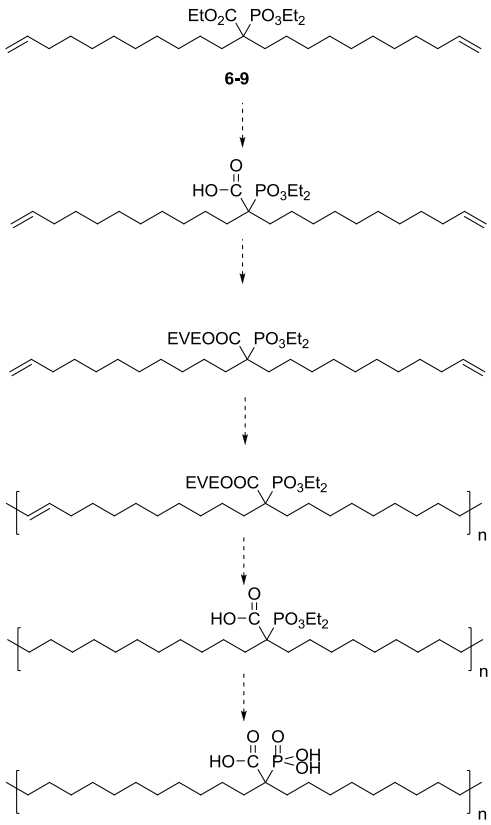

Figure 6-5. Hybrid acid scheme

The final atactic polymer structure offered here would combine the carboxylic acid ability to perfectly dimerize and the phosphonic acid ability to strongly associate. The solubility of the precursor polymers and the final polymer however is unpredictable.

A progression detailing the ongoing utility of ADMET in producing polyethylene copolymers has been described. The highly ordered macromolecular structures presented in this concluding chapter are a prime example in the higher level of control offered from metathesis polymerzation. Throughout this dissertation a progression in primary structure and polar functionality were followed leading to interesting secondary structure behavior and finally in these last two chapters, showing the utility of well-defined structure in understanding morphology. With the dispute in ionomer structure stemming from 50 years ago when particular synthetic advances were not yet

discovered, resolutions are now possible from systematic precision studies. The future of ADMET chemistry lies in systematic simple structure control, catalysis, and even more functional polymers for forthcoming applications.

LIST OF REFERENCES

(1) Ivin, K. J.; Mol, J. C. *Olefin Metathesis and Metathesis Polymerization*, 2nd ed.; Academic Press, Inc.: San Diego, CA, 1997.

(2) Hoveyeda, A. H.; Zhugralin, A. R. *Nature* **2007**, *450*, 243-251.

(3) Nobelprize.org "The Nobel prize in Chemistry 2005", 2010, http://nobelprize.org/nobel_prizes/chemistry/laureates/2005/. Date last accessed: June 1, 2010.

(4) Grubbs, R. H., Ed. *Handbook of Metathesis*; Wiley VCH, 2003; Vol. 1-3.

(5) Basset, J.-M.; Coperet, C.; Soulivong, D.; Taoufik, M.; Cazet, J. T. *Acc. Chem. Res.* **2009**, *43*, 323-334.

(6) Bielawski, C. W.; Grubbs, R. H. *Prog. Polym. Sci.* **2007**, *32*, 1-29.

(7) Dieters, A.; Martin, S. F. *Chem. Rev.* **2004**, *104*, 2199-2238.

(8) McReynolds, M. D.; Dougherty, J. M.; Hanson, P. R. *Chem. Rev.* **2004**, *104*, 2239-2258.

(9) Buchmeiser, M. R. *Chem. Rev.* **2000**, *100*, 1565-1604.

(10) Lindmark-Hamberg, M.; Wagener, K. B. *Macromolecules* **1987**, *20*, 2949-2951.

(11) Lehman, S. E.; Wagener, K. B.; Grubbs, R. H., Ed.; Wiley-VCH, 2003; Vol. 3, pp 283-353.

(12) Baughman, T. W.; K.B.Wagener. *Adv. Polym. Sci.* **2005**, 1-42.

(13) Ziegler, K.; Holzkamp, K.; Breil, H.; Martin, H. *Angew. Chem.* **1955**, *426*, 541.

(14) Natta, G.; Pino, P.; Corradini, P.; Danusso, F.; Mantica, E.; Mazzanti, G.; Moraglio, G. *J. Am. Chem. Soc.* **1955**, *77*, 1708-1710.

(15) Nobelprize.org "The Nobel prize in Chemistry 1963", 2010, http://nobelprize.org/nobel_prizes/chemistry/laureates/1963/, Date last accessed: June 1, 2010.

(16) Eleuterio, H.; 3074918: U.S., 1957.

(17) Truett, W. L.; Johnson, D. R.; Robinson, I. M.; Montague, B. A. *J. Am. Chem. Soc.* **1960**, *82*, 2337-2340.

(18) Banks, R. L.; Bailey, B. C. *Ind. Eng. Chem. Prod. Res. Dev.* **1964**, *3*, 170-173.

(19) Calderon, N.; Morris, M. C. *J. Polym. Sci., Part A: Polym. Chem.* **1967**, *5*, 2209-2217.

(20) Calderon, N.; Chen, H. Y.; Scott, K. W. *34* **1967**, 3327-3329.

(21) Calderon, N.; Ofstead, E. A.; Ward, J. P.; Judy, W. A.; Scott, K. W. *J. Am. Chem. Soc.* **1968**, *90*, 4133-4140.

(22) Calderon, N.; Scott, K. W.; Ofstead, E. A. *Chim. Ind. (Milan)* **1970**, *52*, 1169.

(23) Herrison, J. L.; Chauvin, Y. N. *Makromol. Chem.* **1971**, *141*, 161.

(24) Chauvin, Y. *Angew. Chem.* **2006**, *23*, 3741-3747.

(25) Katz, T. J.; McGinnis, J. *J. Am. Chem. Soc.* **1975**, *97*, 1592-1594.

(26) Rothchild, R.; Katz, T. J. *J. Am. Chem. Soc.* **1976**, *98*, 2519-2526.

(27) McGinnis, J.; Katz, T. J. *J. Am. Chem. Soc.* **1977**, *99*, 1903-1912.

(28) Grubbs, R. H.; Hoppin, C. R. *J. Am. Chem. Soc.* **1979**, *101*, 1499-1508.

(29) Schrock, R. R. *J. Am. Chem. Soc.* **1974**, *96*, 6796-6797.

(30) Schaverien, C. J.; Dewan, J. C.; Schrock, R. R. *J. Am. Chem. Soc.* **1986**, *108*, 2771-2773.

(31) Schrock, R. R.; DePue, R. T.; Feldman, J.; Schaverien, C. J.; Dewan, J. C.; Liu, A. H. *J. Am. Chem. Soc.* **1988**, *110*, 1423-1435.

(32) Schrock, R. R.; Murdzek, J. S.; Bazan, G. C.; Robbins, J.; DiMarie, M.; O'Regan, M. *J. Am. Chem. Soc.* **1990**, *112*, 3875-3886.

(33) Oskam, J. H.; Fox, H. H.; Yap, K. B.; McConville, D. H.; O'Dell, R.; Lichtenstein, B. J.; Schrock, R. R. *J. Organomet. Chem.* **1993**, *459*, 185-198.

(34) Schrock, R. R.; Toreki, R. *J. Am. Chem. Soc.* **1990**, *112*, 2448-2449.

(35) Howard, T. R.; Lee, J. B.; Grubbs, R. H. *J. Am. Chem. Soc.* **1980**, 6876-6878.

(36) Lee, J. B.; Ott, K. C.; Grubbs, R. H. *J. Am. Chem. Soc.* **1982**, *104*, 7491-7496.

(37) Gilliom, L. R.; Grubbs, R. H. *J. Am. Chem. Soc.* **1986**, *108*, 733-742.

(38) Nguyen, S. T.; Johnson, L. K.; Grubbs, R. H.; Ziller, J. W. *J. Am. Chem. Soc.* **1992**, *114*, 3974-3975.

(39) Nguyen, S. T.; Grubbs, R. H. *J. Am. Chem. Soc.* **1993**, *115*, 9858-9859.

(40) Schwab, P.; Grubbs, R. H.; Ziller, J. W. *J. Am. Chem. Soc.* **1995**, *117*, 5503-5511.

(41) Odian, G. *Principles of Polymerization*, 4th ed.; Wiley Interscience, 2004.

(42) Wagener, K. B.; Nel, J. G.; Konzelman, J.; Boncella, J. M. *Macromolecules* **1990**, *23*, 5155-5157.

(43) Wagener, K. B.; Boncella, J. M.; Nell, J. G.; Duttweiler, R. P.; Hillmyer, M. A. *Makromol. Chem.* **1990**, *191*, 365-374.

(44) Wagener, K. B.; Boncella, J. M.; Nell, J. G. *Macromolecules* **1991**, *24*, 2649-2657.

(45) Wagener, K. B.; Nel, J. G.; Duttweiler, R. P.; Hillmyer, M. A.; Boncella, J. M.; Konzelman, J.; D.W. Smith, J.; Puts, R.; Willoughby, L. *Rubber Chem. Technol.* **1991**, *64*, 83-95.

(46) Konzelman, J. *Ph.D. dissertation*; University of Florida, 1993.

(47) Wagener, K. B.; D.W. Smith, J. *Macromolecules* **1991**, *24*, 6073-6078.

(48) Bielwaski, C. W.; Benitez, D.; Grubbs, R. H. *Science* **2002**, *297*, 2041-2044.

(49) Furstner, A.; Thiel, O. R.; Ackermann, L.; Schanz, H. J.; Nolan, S. P. *J. Org. Chem.* **2000**, *65*, 2204-2207.

(50) Wagener, K. B.; Puts, R. D.; D.W. Smith, J. *Makromol. Chem. Rapid Commun.* **1991**, *12*, 419-425.

(51) Watson, M. D.; Wagener, K. B. *Macromolecules* **2000**, *33*, 1494-1496.

(52) Louie, J.; Grubbs, R. H. *Organometallics* **2002**, *21*, 2153-2164.

(53) Sanford, M. S.; Ulman, M.; Grubbs, R. H. *J. Am. Chem. Soc.* **2001**, *123*, 749-750.

(54) Peacock, A. J. *J. Macromol. Sci: Polymer Reviews* **2001**, *C41*, 285-323.

(55) Peacock, A. *Handbook of Polyethylene: Structures, Properties, and Applications*, 1 ed.; CRC Press, 2000.

(56) Berda, E. B.; Baughman, T. W.; Wagener, K. B. *J. Polym. Sci., Part A: Polym. Chem.* **2006**, *44*, 4981-4989.

(57) Qui, W.; Pyda, M.; Nowak-Pyda, E.; Habenschuss, A.; Wagener, K. B.; Wunderlich, B. *J. Polym. Sci., Part B: Polym. Phys.* **2006**, *44*, 3461-3474.

(58) Qui, W.; Sworen, J. C.; Pyda, M.; Nowak-Pyda, E.; Habenschuss, A.; Wagener, K. B.; Wunderlich, B. *Macromolecules* **2006**, *39*, 204-217.

(59) Rojas, G.; Berda, E. B.; Wagener, K. B. *Polymer* **2008**, *49*, 2985-2995.

(60) Hosada, S.; Nozue, Y.; Kawashima, Y.; Utsumi, S.; Nagamatsu, T.; Wagener, K. B.; Berda, E. B.; Rojas, G.; Baughman, T. W.; Leonard, J. K. *Macromol. Symp.* **2009**, *282*, 50-64.

(61) Sworen, J. C.; Wagener, K. B. *Macromolecules* **2007**, *40*, 4414-4423.

(62) Rojas, G.; Wagener, K. B. *Macromolecules* **2009**, *43*, 1934-1947.

(63) Lieser, G.; Wegner, G.; Smith, J. A.; Wagener, K. B. *Colloid Polym. Sci.* **2004**, *282*, 773-781.

(64) Baughman, T. W.; Sworen, J. C.; Wagener, K. B. *Macromolecules* **2006**, *39*, 5028-5036.

(65) Rojas, G.; Inci, B.; Wei, Y.; Wagener, K. B. *J. Am. Chem. Soc.* **2009**, *131*, 17376-17386.

(66) Karabulut, S.; Aydogdu, C.; Duz, B.; Imamoglu, Y. *J. Inorg. Organomet. Polym.* **2006**, *16*, 115-122.

(67) Schultz, G. V.; Zakharov, L. N.; Tyler, D. R. *Macromolecules* **2008**, *41*, 5555-5558.

(68) Schultz, G. V.; Tyler, D. R. *J. Inorg. Organomet. Polym.* **2009**, *19*, 423-435.

(69) Schultz, G. V.; Zemke, J. M.; Tyler, D. R. *Macromolecules* **2009**, *42*, 7644-7649.

(70) Boz, E.; K.B.Wagener; Ghosal, A.; Fu, R.; Alamo, R. G. *Macromolecules* **2006**, *39*, 4437-4447.

(71) Boz, E.; Nemith, A.; Ghiviriga, I.; Jeon, K.; Alamo, R.; Wagener, K. B. *Macromolecules* **2007**, *40*, 6545-6551.

(72) Boz, E.; Nemith, A.; Ghiviriga, I.; Jeon, K.; Alamo, R.; Wagener, K. B. *Macromolecules* **2008**, *41*, 25-30.

(73) Baughman, T. W.; Aa, E. v. d.; Lehman, S. E.; Wagener, K. B. *Macromolecules* **2006**, *38*, 2550-2551.

(74) Baughman, T. W.; Aa, E. v. d. *Macromolecules* **2006**, *39*, 7015-7021.

(75) Berda, E. B.; Lande, R. E.; Wagener, K. B. *Macromolecules* **2007**, *40*, 8547-8552.

(76) Berda, E. B.; Wagener, K. B. *Macromolecules* **2008**, *41*, 5116-5122.

(77) Berda, E. B.; Wagener, K. B. *Macromol. Chem. Phys.* **2008**, *209*, 1601-1611.

(78) Lehman, S. E.; Wagener, K. B.; Baugh, L. S.; Rucker, S. P.; Schultz, D. N.; Varma-Nair, M.; Berluche, E. *Macromolecules* **2007**, *40*, 2643-2656.

(79) Rybak, A.; Meier, M. A. R. *Chem. Sus. Chem.* **2008**, *1*, 542-547.

(80) Espinosa, L. M. d.; Meier, M. A. R.; Ronda, J. C.; Galia, M.; Cadiz, V. *J. Polym. Sci., Part A: Polym. Chem.* **2009**, *48*, 1649-1660.

(81) Espinosa, L. M. d.; Ronda, J. C.; Galia, M.; Cadiz, V.; Meier, M. A. R. *J. Polym. Sci., Part A: Polym. Chem.* **2009**, *47*, 5760-5771.

(82) Mutlu, H.; Meier, M. A. R. *Macromol. Chem. Phys.* **2009**, *210*, 1019-1025.

(83) Opper, K. L.; Wagener, K. B. *Macromol. Rapid Commun.* **2009**, *30*, 915-919.

(84) Baughman, T. W.; Chan, C. D.; Winey, K. I.; Wagener, K. B. *Macromolecules* **2007**, *40*, 6565-6571.

(85) Opper, K. L.; Fassbender, B.; Brunklaus, G.; Spiess, H. W.; Wagener, K. B. *Macromolecules* **2009**, *42*, 4407-4409.

(86) Opper, K. L.; Markova, D. M.; Klapper, M.; Muellen, K.; Wagener, K. B. *Macromolecules* **2010**, *43*, 3690-3698.

(87) Aitken, B.; Lee, M.; Hunley, M. T.; Gibson, H. W.; Wagener, K. B. *Macromolecules* **2010**, *43*, 1699-1701.

(88) Guidry, E. N.; Li, J.; Stoddart, F.; Grubbs, R. H. *J. Am. Chem. Soc.* **2007**, *129*, 8944-8945.

(89) Seitz, M. E.; Chan, C. D.; Opper, K. L.; Baughman, T. W.; Wagener, K. B.; Winey, K. I. *J. Am. Chem. Soc.* **2010**, *ASAP*.

(90) Schwendeman, J. E.; Wagener, K. B. *Macromol. Chem. Phys.* **2009**, *210*, 1818-1833.

(91) Matloka, P. M.; Kean, Z.; Greenfield, M.; Wagener, K. B. *J. Polym. Sci., Part A: Polym. Chem.* **2008**, *46*, 3992-4011.

(92) Matloka, P. M.; Wagener, K. B. *Journal of Molecular Catalysis A: Chemical* **2006**, *257*, 89-98.

(93) Pietraszuk, C.; Rogalski, S.; Majchrzak, M.; Marciniec, B. *J. Organomet. Chem.* **2006**, *691*, 5476-5481.

(94) Rathore, J. S.; Interrante, L. V. *Macromolecules* **2009**, *42*, 4614-4621.

(95) Delgado, P. A.; Zuluaga, F.; Matloka, P.; Wagener, K. B. *J. Polym. Sci., Part A: Polym. Chem.* **2009**, *47*, 5180-5183.

(96) Matloka, P. M.; Sworen, J. C.; Zuluaga, F.; Wagener, K. B. *Macromol. Chem. Phys.* **2005**, *206*, 218-226.

(97) Ding, L.; Zhang, L.; Han, H.; Huang, W.; Song, C.; Xie, M.; Zhang, Y. *Macromolecules* **2009**, *42*, 5036-5042.

(98) Gorodetskaya, I. A.; Gorodetsky, A. A.; Vinogradova, E. V.; Grubbs, R. H. *J. Am. Chem. Soc.* **2009**, *42*, 2895-2898.

(99) Fokou, P. A.; Meier, M. A. R. *Macromol. Rapid Commun.* **2008**, *29*, 1620-1625.

(100) Gorodetskaya, I. A.; Choi, T.-L.; Grubbs, R. H. *J. Am. Chem. Soc.* **2007**, *129*, 12672-12673.

(101) Hou, H.; Leung, K. C.-F.; Lanari, D.; Nelson, A.; Stoddart, J. F.; Grubbs, R. H. *J. Am. Chem. Soc.* **2006**, *128*, 15358-15359.

(102) Enholm, E. J.; Mondal, K. *Syn. Lett.* **2009**, *15*, 2539-2541.

(103) Terada, K.; Berda, E. B.; Wagener, K. B.; Sanda, F.; Masuda, T. *Macromolecules* **2008**, *41*, 6041-6046.

(104) Gautrot, J. E.; Zhu, X. X. *Anal. Chim. Acta* **2006**, *581*, 281-286.

(105) Ohkawa, H.; Ligthart, G. B. W. L.; Sijbesma, R. P.; Meijer, E. W. *Macromolecules* **2007**, *40*, 1453-1459.

(106) Leonard, J. K.; Hopkins, T. E.; Chaffin, K.; Wagener, K. B. *Macromol. Chem. Phys.* **2008**, *209*, 1485-1494.

(107) Leonard, J. K.; Turek, D.; Sloan, K. B.; Wagener, K. B. *Macromol. Chem. Phys.* **2010**, *211*, 154-165.

(108) Khaja, S. D.; Lee, S.; Murthy, N. *Biomacromolecules* **2007**, *8*, 1391-1395.

(109) Trimmel, G.; Riegler, S.; Fuchs, G.; Slugovc, C.; Stelzer, F. *Adv. Polym. Sci.* **2005**, *176*, 43-87.

(110) Walba, D. M.; Yang, H.; Shoemaker, R. K.; Keller, P.; Shao, R.; Coleman, D. A.; Jones, C. D.; Nakata, M.; Clark, N. A. *Macromolecules* **2006**, *18*, 4576-4584.

(111) Walba, D. M.; Yang, H.; Keller, P.; Zhu, C.; Shao, R.; Coleman, D. A.; Jones, C. D.; Clark, N. A. *Macromol. Rapid Commun.* **2009**, *30*, 1894-1899.

(112) Sovic, T.; Kappaun, S.; Koppitz, A.; Zojer, E.; Saf, R.; Bartl, K.; Fodor-Csorba, K.; Vajda, A.; Diele, S.; Pelzl, G.; Slugovc, C.; Stelzer, F. *Macromol. Chem. Phys.* **2007**, *208*, 1458-1468.

(113) Galli, G.; Demel, S.; Slugovc, C.; Stelzer, F.; Diele, S.; Fodor-Csorba, K. *Mol. Cryst. Liq. Cryst.* **2005**, *439*, 1909-1919.

(114) Kim, J. Y.; Qin, Y.; Stevens, D. M.; O.Ugurlu; Kalihar, V.; Hillmyer, M. A.; Frisbie, C. *J. Phys. Chem. C.* **2009**, *113*, 10790-10797.

(115) Weychardt, H.; Plenio, H. *Organometallics* **2008**, *27*, 1479-1485.

(116) Nomura, K.; Miyamoto, Y.; Morimoto, H.; Geerts, Y. *J. Polym. Sci., Part A: Polym. Chem.* **2005**, *43*, 6166-6177.

(117) Nomura, K.; Yamamoto, N.; Ito, R.; Fujiki, M.; Geerts, Y. *Macromolecules* **2008**, *41*, 4245-4249.

(118) Strachota, A.; Cimrova, V.; Thorn-Csanyi, E. *Macromol. Symp.* **2008**, *268*, 66-71.

(119) Yamamoto, N.; Ito, R.; Geerts, Y.; Nomura, K. *Macromolecules* **2009**, *42*, 5104-5111.

(120) Qin, Y.; Hillmeyer, M. A. *Macromolecules* **2009**, *42*, 6429-6432.

(121) Oakley, G. W.; Wagener, K. B. *Macromol. Chem. Phys.* **2005**, *206*, 15-24.

(122) Muellen, K.; Scherf, U. *Organic Light Emitting Devices*; Wiley VCH: Weinheim, 2005.

(123) Peetz, R. M.; Sinnwell, V.; Thorn-Csanyi, E. *J. Mol. Catal. A: Chem.* **2006**, *254*, 165-173.

(124) Pecher, J.; Mecking, S. *Macromolecules* **2007**, *40*, 7733-7735.

(125) Copenhafer, J. E.; Walters, R. W.; Meyer, T. Y. *Macromolecules* **2008**, *41*, 31-35.

(126) Mukherjee, N.; Peetz, R. M. *Macromolecules* **2008**, *41*, 6677-6685.

(127) Tant, M. R.; Mauritz, K. A.; Wilkes, G. L., Eds. *Ionomers*; Chapman & Hall: New York, NY, 1997.

(128) Eisenberg, A.; Kim, J. *Introduction to Ionomers*; John Wiley & Sons: New York, NY, 1998.

(129) Williams, S. R.; Long, T. E. *Prog. Polym. Sci.* **2009**, *34*, 762-782.

(130) A.G., I. G. F. I.; 701102: France, 1933.

(131) Rees, R. W. In *Thermoplastic Elastomers*, 3 ed.; Holden, G.; Kricheldorf, H. R.; Quirk, R. P., Eds.; Hanser: Munich, 2004; pp 247-259.

(132) Rees, R. W.; Vaughan, D. J. *Polym. Prepr.* **1965**, *6*, 287-295.

(133) Rees, R. W.; 3264272: U.S., 1966.

(134) Grady, B. P. *Polym. Eng. Sci.* **2008**, 1029-1051.

(135) Tobolsky, A. V.; Lyons, P. F.; Hata, N. *Macromolecules* **1968**, *1*, 515-519.

(136) MacKnight, W. J.; McKenna, L. W.; Read, B. E.; Stein, R. S. *J. Phys. Chem.* **1967**, *72*, 1122-1126.

(137) MacKnight, W. J.; McKenna, L. W.; Read, B. E. *J. Appl. Phys.* **1967**, *38*, 4208-4212.

(138) Bonotto, S.; Bonner, E. F. *Macromolecules* **1968**, *1*, 510-515.

(139) Longworth, R.; Vaughan, D. J. *Nature* **1968**, *218*, 85-87.

(140) Eisenberg, A. *Macromolecules* **1970**, *3*, 147-154.

(141) Longworth, R.; Vaughan, D. J. *Polym. Prepr.* **1968**, *9*, 525.

(142) MacKnight, W. J.; Taggart, W. P.; Stein, R. S. *J. Polym. Sci.: Symposium* **1974**, *45*, 113-118.

(143) Yarusso, D. J.; Cooper, S. L. *Macromolecules* **1983**, *16*, 1871-1880.

(144) Kinning, D. J.; Thomas, E. L. *Macromolecules* **1984**, *17*, 1712-1718.

(145) Eisenberg, A.; Hird, B.; Moore, R. B. *Macromolecules* **1990**, *23*, 4098-4107.

(146) Benetatos, N. M.; Smith, B. W.; Heiney, P. A.; Winey, K. I. *Macromolecules* **2005**, *38*, 9251-9257.

(147) Benetatos, N. M.; Heiney, P. A.; Winey, K. I. *Macromolecules* **2006**, *39*, 5174-5176.

(148) Benetatos, N. M.; Chan, C. D.; Winey, K. I. *Macromolecules* **2007**, *40*, 1081-1088.

(149) Zhou, N. C.; Chan, C. D.; Winey, K. I. *Macromolecules* **2008**, *41*, 6134-6140.

(150) Doak, K. W. In *Encyclopedia of Polymer Science and Engineering*; Mark, H. F.; Bikales, N. M.; Overberger, C. G.; Menges, G.; Kroschwitz, J. I., Eds.; John Wiley & Sons: New York, 1986; Vol. 6, pp 386-429.

(151) Boffa, L. S.; Novak, B. M. *Chem. Rev.* **2000**, *100*, 1479-1493.

(152) Lehman, S. E.; Wagener, K. B.; Baugh, L. S.; Rucker, S. P.; Schulz, D. N.; Varma-Nair, M.; Berluche, E. *Macromolecules* **2007**, *40*, 2643-2656.

(153) Baughman, T. W.; Chan, C. D.; Winey, K. I. *Macromolecules* **2007**, *40*, 6564-6571.

(154) Berda, E. B.; Lande, R. E.; Wagener, K. B. *Macromolecules* **2007**, *40*, 8547-8552.

(155) Boz, E.; Wagener, K. B. *Polymer Reviews* **2007**, *47*, 511-541.

(156) Breslow, D. S. In *Encyclopedia of Polymer Science and Engineering*; Mark, H. F.; Bikales, N. M.; Overberger, C. G.; Menges, G.; Kroschwitz, J. I., Eds.; John Wiley & Sons: New York,, 1986; Vol. 6, p 362.

(157) Breslow, D. S.; Hulse, G. E. *J. Am. Chem. Soc.* **1954**, *76*, 6399-6401.

(158) Breslow, D. S.; Hough, R. R. *J. Am. Chem. Soc.* **1957**, *79*, 5000-5002.

(159) Schwendemen, J. E.; Wagener, K. B. *Macromolecules* **2004**, *37*, 4031-4037.

(160) Truce, W. E.; Vrencur, D. J. *Journal of Organic Chemistry* **1970**, *35*, 1226-1227.

(161) Musicki, B.; Widlanski, T. S. *J. Org. Chem.* **1990**, *55*, 4231-4233.

(162) Musicki, B.; Widlanski, T. S. *Tetrahedron Letters* **1991**, *32*, 1267-1270.

(163) Wuts, P. G. M.; Greene, T. W. *Protective Groups in Organic Synthesis*, 3 ed.; Wiley-Interscience: New York, 1999.

(164) Patch, R. J.; Kongsjahju, A.; Gopalsamy, A.; Gao, H.; Roberts, J. C. *Tetrahedron Lett.* **1997**, *38*, 355-358.

(165) Watson, M. D.; Wagener, K. B. Macromolecules 2000, 32, 8963-8970.

(166) Boffa, L. S.; Novak, B. M. *Chem. Rev.* **2000**, *100*, 1479-1493.

(167) Doak, K. W. In *Encyclopedia of Polymer Science and Engineering*; Mark, H. F.; Bikales, N. M.; Overberger, C. G.; Menges, G.; Kroschwitz, J. I., Eds.; John Wiley & Sons: New York, 1986; Vol. 6, pp 386-429.

(168) Popa, A.; Davidescu, C.-M.; Negrea, P.; Ilia, G.; Katsaros, A.; Demadis, K. D. *Ind. Eng. Chem. Res.* **2008**, *47*, 2010-2017.

(169) Steininger, H.; Schuster, M.; Kreuer, K. D.; Kaltbeitzel, A.; Bingol, B.; Meyer, W. H.; Schauff, S.; Brunklaus, G.; Maier, J.; Spiess, H. W. *Phys. Chem. Chem. Phys.* **2007**, *9*, 1764-1773.

(170) Jiang, D. D.; Yao, Q.; McKinney, M. A.; Wilkie, C. A. *Polym. Degrad. Stab.* **1999**, *63*, 423-434.

(171) Tana, J.; Gemeinharta, R. A.; Maa, M.; Saltzman, W. M. *Biomaterials* **2005**, *26*, 3663-3671.

(172) Chirila, T. V. *Reactive and Functional Polymers* **2007**, *67*, 165-172.

(173) Greish, Y. E.; Brown, P. W. *J. Am. Ceram. Soc.* **2002**, *85*, 1738-1744.

(174) Adusei, G. O.; Deb, S.; Nicholson, J. W. *Dental Materials* **2005**, *21*, 491-497.

(175) Bingol, B.; Meyer, W. H.; Wagner, M.; Wegner, G. *Macromol. Rapid Comm.* **2006**, *27*, 1719-1724.

(176) Komber, H.; Steinert, V.; Voit, B. *Macromolecules* **2008**, *41*, 2119-2125.

(177) Lehman, S. E.; Wagener, K. B. In *Handbook of Metathesis*; Grubbs, R. H., Ed.; Wiley-VCH, 2003; Vol. 3, pp 283-353.

(178) Berda, E. B.; Baughman, T. W.; Wagener, K. B. *Journal of Polymer Science, Part A: Polymer Chemistry* **2006**, *44*, 4981-4989.

(179) Baughman, T. W.; Chan, C. D.; Winey, K. I.; Wagener, K. B. *Macromolecules* **2007**, *40*, 6565-6571.

(180) Clayton, J. O.; Jensen, W. L. *JACS* **1948**, *70*, 3880-3882.

(181) Allan, J. M.; Dooley, R. L.; Shalaby, S. W. *J. Appl. Polym. Sci.* **2000**, *76*, 1870-1875.

(182) Opper, K. L.; Wagener, K. B. *Macromol. Rapid Comm.* **2009**, accepted.

(183) Wuts, P. G. M.; Greene, T. W. *Protective Groups in Organic Synthesis*, 3 ed.; Wiley-Interscience: New York, 1999.

(184) Vanderhart, D. L. *J. Magn. Reson.* **1981**, 117-125.

(185) Wei, Y.; Graf, R.; C., S. J.; Y., C. C.; Bowers, C. R.; Wagener, K. B.; Spiess, H. W. *Angew. Chem. Int. Ed.* **2009**, in press.

(186) Peacock, A. J. *Handbook of polyethylene: Structures, properties, and applications*; Marcel Dekker: New York, 2000; Vol. 57.

(187) Novak, B. M.; Boffa, L. S. *Chem. Rev.* **2000**, *100*, 1479-1493.

(188) Domski, G. J.; Rose, J. M.; Coates, G. W.; Bolig, A. D.; Brookhart, M. *Prog. Polym. Sci.* **2007**, *32*, 30-92.

(189) Berkefeld, A.; Mecking, S. *Angew. Chem. Int. Ed.* **2008**, *47*, 2538-2542.

(190) Chen, E. *Chem. Rev.* **2009**, *109*, 5157-5214.

(191) Boaen, N. K.; Hillmyer, M. A. *Chem. Soc. Rev.* **2005**, *34*, 267-275.

(192) Hu, Y.; Dong, J. Y. *Coord. Chem. Rev.* **2006**, *250*, 47-65.

(193) Amin, S. B.; Marks, T. J. *Angew. Chem. Int. Ed.* **2008**, *47*, 2006-2025.

(194) Lehman, S. E.; Wagener, K. B. In *Handbook of Metathesis*; Grubbs, R. H., Ed.; Wiley-VCH, 2003; Vol. 3, pp 283-353.

(195) Baughman, T. W.; K.B.Wagener. *Adv. Polym. Sci.* **2005**, 1-42.

(196) Berda, E. B.; Baughman, T. W.; Wagener, K. B. *Journal of Polymer Science, Part A: Polymer Chemistry* **2006**, *44*, 4981-4989.

(197) Baughman, T. W.; Chan, C. D.; Winey, K. I.; Wagener, K. B. *Macromolecules* **2007**, *40*.

(198) Rojas, G.; Inci, I.; Wei, Y.; Wagener, K. B. *JACS* **2009**, *131*, 17376-17386.

(199) Phillips, P. J.; Emerson, F. A.; MacKnight, W. J. *Macromolecules* **1970**, *3*, 767-771.

(200) Schroeder, J. P.; Sopchak, W. P. *Journal of Polymer Science* **1960**, *XLVII*, 417-433.

(201) Kang, N.; Xu, Y.-Z.; Wu, J.-G.; Feng, W.; Xu, D.-F. *Phys. Chem. Chem. Phys.* **2000**, *2*, 3627-3630.

(202) Steininger, H.; Schuster, M.; Kreuer, K. D.; Kaltbeitzel, A.; Bingol, B.; Meyer, W. H.; Schauff, S.; Brunklaus, G.; Maier, J.; Spiess, H. W. *Phys. Chem. Chem. Phys.* **2007**, *9*, 1764-1773.

(203) Sata, T.; Sata, T.; Yang, W. *Journal of Membrane Science* **2002**, *206*, 31-60.

(204) Lu, S. Y.; Hamerton, I. *Prog. Polym. Sci.* **2002**, *27*, 1661-1712.

(205) Markova, D.; Avneesh, K.; Klapper, M.; Muellen, K. *Polymer* **2009**, *50*, 3411-3421.

(206) Sudip, R.; Markova, D.; Kumar, A.; Klapper, M.; Mueller-Plathe, F. *Macromolecules* **2009**, *42*, 841-848.

(207) Francis, M. D.; Centner, R. L. *J. Chem. Ed.* **1978**, *55*, 760-766.

(208) Wang, D.; Miller, S. C.; Kopeckova, P.; Kopecek, J. *Advanced Drug Delivery Reviews* **2005**, *57*, 1049-1076.

(209) Chirila, T. V. *React. Funct. Polym.* **2007**, *67*, 165-172.

(210) Hawker, C. J.; Wooley, K. L. *Science* **2005**, *309*, 1200-1205.

(211) Jimenez-Garcia, L.; Kaltbeitzel, A.; Pisula, W.; Gutmann, J. S.; Klapper, M.; Muellen, K. *Angew. Chem. Int. Ed.* **2009**, DOI: 10.1002/anie.200902116.

(212) Opper, K. L.; Fassbender, B.; Brunklaus, G.; Spiess, H. W.; Wagener, K. B. *Macromolecules* **2009**, *42*, 4407-4409.

(213) Wuts, P. G. M.; Greene, T. W. *Protective Groups in Organic Synthesis*, 4 ed.; Wiley-Interscience: New York, 2006.

(214) O' Gara, J. E.; Wagener, K. B.; Hahn, S. F. *Makromol. Chem., Rapid Commun.* **1993**, *14*, 657-662.

(215) Kotov, S. V.; Pedersen, S. D.; Qiu, W.; Qiu, Z.-M.; Burton, D. J. *J. Fluorine Chem.* **1997**, *82*, 13-19.

(216) Boz, E.; Wagener, K. B.; Ghosal, A.; Fu, R.; Alamo, R. G. *Macromolecules* **2006**, *39*, 4437-4447.

(217) Snyder, R. G. *J. Mol. Spec.* **1961**, *7*, 116-144.

(218) Ungar, G.; Zeng, X. B. *Chem. Rev.* **2001**, *101*, 4157-4188.

(219) Tashiro, K.; Sasaki, K.; Kobayashi, M. *Macromolecules* **1996**, *29*, 7460-7469.

(220) Seitz, M. E.; Chan, C. D.; Opper, K. L.; Baughman, T. W.; Wagener, K. B.; Winey, K. I. *J. Am. Chem. Soc.* **2010**, *ASAP*.

(221) Painter, P. C.; Brozoski, B. A.; Coleman, M. M. *J. Polym. Sci., Part B: Polym. Phys.* **1982**, *20*, 1069-1080.

(222) Brozoski, B. A.; Coleman, M. M.; Painter, P. C. *Macromolecules* **1984**, *17*, 230-234.

(223) Hirasawa, E.; Yamamoto, Y.; Tanado, K.; Yano, S. *J. Appl. Polym. Sci.* **1991**, *42*, 351-362.

(224) Tsujita, Y.; Yasuda, M.; Takei, M.; Kinoshita, T.; Takizawa, A.; Yoshimizu, H. *Macrmolecules* **2001**, *34*, 2220-2224.

(225) Capek, I. *Adv. Colloid Interface Sci.* **2005**, *118*, 73-112.

(226) *Ibid.*, Ch. 5.

(227) Weiss, R. A. *J. Polym. Sci. Polym. Chem.* **1980**, *18*.

(228) Crugnola, A.; Pegoraro, M.; Severine, F. *J. Polym. Sci., C* **1969**, *16*, 4547-4557.

(229) Leonard, E.; Loeb, W.; Mason, J.; Stenstrom, J. *J. Polym. Sci.* **1961**, *55*, 799-808.

(230) Leonard, E. C.; Loeb, W. E.; J.H. Mason, J. H.; Wheelwright., W. L. *J. Appl. Polym. Sci.* **1961**, *5*, 157-162.

(231) Wu, Q.; Weiss, R. A. *J. Polym. Sci., Part B: Polym. Phys.* **2004**, *42*, 3628-3641.

(232) Wu, Q.; Weiss, R. A. *Polymer* **2007**, *48*, 7558-7566.

BIOGRAPHICAL SKETCH

Kathleen Louise Opper was born in Pittsfield, MA and grew up in New Lebanon, NY where parents Norreen and Patrick Opper still reside. After receiving the Rensselaer Medal, she moved to Troy, NY in 2001 to study biology at Rensselaer Polytechnic Institute (RPI). During her time there, she began undergraduate research under Professor Brian Benicewicz and added chemistry for a B.S. degree with a dual major. Upon graduating with her B.S. in 2005, she began graduate studies in Polymer and Organic Chemistry later that year at the University of Florida under Professor Ken Wagener's guidance. In the winter months of 2008 she completed collaborative research at the Max Planck Institute for Polymer Research under the direction Professor Dr. Klaus Müllen and Dr. Markus Klapper. Ending a successful graduate career, she then completed the requirements for the degree of Doctor of Philosophy in August of 2010.